AD NUMBER: AD0417093
CLASSIFICATION CHANGES
TO: Unclassified
FROM: Secret
AUTHORITY
S to U/DASA Ltr., 23 Mar 1964

eration
SHOT-KNOTHOLE
A PROVING GROUNDS
1953

1

DISTRIBUTION AND CHARACTERISTICS OF FALL-OUT AT DISTANCES GREATER THAN 10 MILES FROM GROUND ZERO, MARCH AND APRIL 1953

(4) NA (5) 161600 UNCLASSIFIED 56-9428 C-1

[redacted]

WT-811

This document consists of 98 pages
No. 288 of 290 copies, Series A

(7) NA

Report to the Test Director

(6)

DISTRIBUTION AND CHARACTERISTICS OF FALL-OUT AT DISTANCES GREATER THAN 10 MILES FROM GROUND ZERO, MARCH AND APRIL 1953

(10)

By

Charles T. Rainey, James W. Neel,
Harold M. Mork, and Kermit H. Larson

(9) NA (8) NA

(11) Feb 54,
(12) 98p.

Approved by: KERMIT H. LARSON
Director, Program 27

Approved by: ROBERT L. CORSBIE
Director
Civil Effects Test Group

(13-17) NA

(18) DASA

University of California at Los Angeles
School of Medicine
Atomic Energy Project
Los Angeles, California
February 1954

"This document contains information affecting the National Defense of the United States within the meaning of the Espionage Laws, Title 50 U. S. C., Sections 793 and 794. Its transmission or the revelation of its contents in any manner to an unauthorized person is prohibited by law."

[redacted]

(50) U

(19) Rept. No. WT-811

This document contains restricted data as defined in the Atomic Energy Act of 1946. Its transmittal or the disclosure of its contents in any manner to an unauthorized person is prohibited.

file

(21) Report and Operation Upshot-Knothole, Proj. 27.1

[redacted]

UNCLASSIFIED

1-2

[redacted]

WD-54-1589

[redacted]

UNCLASSIFIED [redacted]

ABSTRACT

Project 27.1 of the Civil Effects Test Group performed detailed studies of the physical phenomenon of fall-out to provide information basic to the proper evaluation of the possible hazards associated with fall-out. The project functioned during Shots 2, 3, 4, 5, and 7 of Operation Upshot-Knothole; samples and measurements were taken along existing trails and roads which crossed the various fall-out patterns at distances greater than 10 miles from Ground Zero.

Shots 2, 3, and 7 resulted in downwind areas of moderate to high-level contamination. The maximum sample station contamination was detected following Shot 7 at approximately 15 miles from Ground Zero (sampling station Nye 1). Field measurements at this location indicated a dose rate at H + 12 hr of 1630 mr/hr. The surface contamination as determined by laboratory assays was 18,580 $\mu c/ft^2$. Eighty-five per cent of the activity was found to be associated with the 175- to 350-μ size fraction of soil at this location. The resulting integrated dose from measured fall-out time to infinity would be 176 r. The calculated Sr^{89-90} component would approximate 20 $\mu c/ft^2$ in this area.

Detailed sampling of airborne material was successful for Shot 7 only. A maximum 2-hr concentration of 9.9 $\mu c/m^3$ was detected at the above location, with the 24-hr average concentration being 1.1 $\mu c/m^3$. No relation between airborne and surface concentrations was found.

Particle-size studies of the settled material indicated an inverse relation between median diameter and distance. Following Shot 5, the median diameters of the radioactive particles were 450 and 225 μ along arcs 17 and 51 miles, respectively, from Ground Zero. A significant variation in particle-size distribution occurred at individual locations along each arc. The radioactivity per particle was determined to be approximately proportional to the surface area of particles greater than 150 μ and more nearly proportional to the volume for particles less than 150 μ. The solubility of collected radioactive particles approximated 1 per cent in H_2O and 2 per cent in 0.1N HCl. Particle-size studies of airborne material yielded inconclusive results.

The decay rate of the collected samples generally varied as $t^{-1.2}$, with variations attributable to sample thickness and instrument sensitivity. The effective energy of beta radiation varied between 0.4 and 0.6 Mev during the four months following the detonation.

An empirical treatment of the data obtained yielded the following relations during the first 5 hr following a detonation: the total primary material falling out is approximately proportional to the kt yield; along any arc crossing the fall-out pattern, the average dose in milliroentgens per hour (mr/hr) is one-third of the maximum dose; correlation of field and laboratory measurements indicates that 1 mr/hr corresponds to 10 $\mu c/ft^2$ beta radiation; the total material falling out at any distance from Ground Zero is inversely proportional to the time of fall-out at that distance. These empirical relations describing the distribution and rate of deposition of primary fall-out material are formulated as $F = F_0 t^{-1}$ within the limits from 0.5 to 5.0 hr after detonation. In the case of Shot 7 approximately 4 per cent of the estimated total fission product produced is thereby accounted for in fall-out between 12 and 120 miles.

[redacted]

UNCLASSIFIED [redacted]

It is concluded that the foregoing relations may be used to predict the fall-out pattern originating from a detonation at 300 ft above the soil surface at Nevada Proving Grounds. By selecting proper conditions of wind, height of burst, and kt yield, contamination in a given area could be controlled.

It is recommended, therefore, that the empirical treatment be expanded by theoretical analysis and confirmatory studies performed in subsequent test series, particularly to determine the time interval over which the observed relations are valid.

ACKNOWLEDGMENTS

The successful execution of Project 27.1 was dependent upon the cooperation and assistance of numerous organizations and individuals. The authors and this laboratory wish to express their sincere appreciation for the wholehearted cooperation and support given the project.

In particular, the contributions of the following are gratefully acknowledged: Dr. John C. Bugher, Division of Biology and Medicine, Atomic Energy Commission (AEC), who initiated the arrangements for the temporary assignment of personnel from the various AEC contractors and the Navy Department. Dr. A. W. Bellamy, Division of Radiological Services, State of California Office of Civil Defense, for supplying the field-monitoring instruments. W. S. Johnson of the Rad-Safe Organization for providing part of the equipment necessary for the field operation. The meteorological group of the Test Organization for sharing meteorological data and James Fuquay, Hanford Engineer Works (HEW), for meteorological analysis and preparation of Appendix B while temporarily assigned to Project 27.1. Leonard Baurmash, Dust and Fume Measuring Section, Industrial Hygiene Division, Atomic Energy Project (AEP), University of California at Los Angeles (UCLA), for his assistance and many helpful suggestions in designing the program and for development of various techniques and equipment. Louis B. Silverman and staff, Health Physics Section, Industrial Hygiene Division, AEP, UCLA, for evaluation of the film-badge exposures. Dr. Robert G. Lindberg, Project Officer, and other personnel of Project 27.2 for cooperation in field operations.

The civilian personnel who participated in Project 27.1, without whose efforts this program would not have been possible, were Gerald I. Daly, Ames Laboratory; James J. Fuquay, John F. Honstead, and Herman G. Ruppert, HEW; Earl D. Graham, Idaho Operations Office; Ross A. Guillet and Harold E. Smith, Mound Laboratory; Karl E. Herde, Savannah River Operations Office; Dr. Frederick B. Oleson, Brookhaven National Laboratory; Philip S. Chen, Charles J. Spiegl, and Robert E. Vosteen, AEP, University of Rochester; Jack Bailey, Oak Ridge National Laboratory (ORNL), K-25 Plant; William T. Martin, ORNL, Y-12 Plant; and Everett L. Sharpe, ORNL, X-10 Plant.

Appreciation is further extended to the 32 enlisted men temporarily assigned to Project 27.1 by the Navy Department and to the following personnel from other divisions of AEP, UCLA: Philip I. Gill, William C. Burke, J. D. Nelson, Dr. Hideo Nishita, Ora L. Smith, Gunther Steinberg, and Marcus Vogel.

[redacted]

CONTENTS

CONTENTS (Continued)

CONTENTS (Continued)

ILLUSTRATIONS

CHAPTER 2 METHODS AND MATERIALS

CHAPTER 3 RESULTS

CHAPTER 4 DISCUSSION AND ANALYSIS OF RESULTS

[redacted]

ILLUSTRATIONS (Continued)

TABLES

TABLES (Continued)

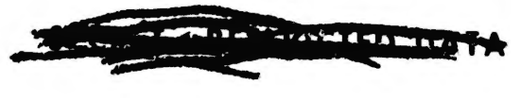

CHAPTER 1

INTRODUCTION

1.1 SCOPE OF THE PROGRAM

The proper evaluation of the possible hazards due to fall-out from an atomic detonation must include an understanding of the physical phenomenon of fall-out itself. As an aid in determining the various types of information which would promote such an understanding, conferences were held during the year prior to Operation Upshot-Knothole with representatives of the Atomic Energy Commission (AEC), Los Alamos Scientific Laboratory (LASL), U. S. Public Health Service, University of Rochester, and others who have been concerned with fall-out programs in the past. From such discussions and a review of the data obtained from Operation Tumbler-Snapper by the Atomic Energy Project, University of California at Los Angeles (AEP, UCLA), evolved the following specific objectives of Project 27.1:

1. The determination of the pattern of fall-out activity distribution in terms of dose rate and integrated dosage.
2. The determination of the distribution of residual settled fall-out material in terms of microcuries per unit area.
3. The determination of a residual mr/hr : μc/unit area relation.
4. The determination of the distribution and concentrations of airborne radioactive material.
5. The determination of the particle-size distribution of both airborne and settled radioactive particles.
6. The investigation of the radioactivity of the fall-out particles as a function of particle size.
7. The investigation of the physical and chemical properties of the fall-out particle.
8. The investigation of radiation decay rates and energy spectra of the collected material.
9. The development of a method of formulating the phenomenon of fall-out based upon meteorological observations and any empirical relations which might be indicated by the above investigations.
10. Techniques of collection and analysis of samples were to be studied in order to obtain more reliable and useful data.

1.2 OTHER FALL-OUT STUDIES

During Operation Upshot-Knothole, as in previous series, fall-out programs were conducted as a part of the Radiological Public Safety Program of the Weapon Test Organization. These programs were conducted under the auspices of the Rad-Safe Unit, which directed the

on-site and off-site monitoring in populated areas within 200 miles, and the New York Operations Office, which operated at distances of greater than 200 miles.

During Operation Tumbler-Snapper, a fall-out study similar to the present investigation was directed by the Radio-Ecology Division, AEP, UCLA, under the designation of Program 22 of the Test Director's organization. The results of this investigation have been reported.[1]

Results of related investigations by other groups during previous test series, which primarily concern the test-site area, have been presented in the Weapon Test Report Series.

1.3 CONCEPTS OF THE FALL-OUT PHENOMENON

The subject of this report is but one of the many physical phenomena associated with an atomic detonation. As such, it is related to, and is a function of, many factors. Therefore the inclusion of a brief discussion of those factors which are presently considered by this group to play a major role in the determination of the mechanics and the characteristics of fall-out is necessary. For other interpretations and a more detailed account, the reader is referred to any one of the numerous reports on the subject (see references 2 and 3).

1.3.1 Mechanics of Formation of Fall-out Material

At the time of detonation, enormous amounts of energy are released in the form of heat and ionizing radiation. Within a few microseconds, an intensely hot, luminous sphere of compressed gases, called the "fireball," is formed. The fireball contains, in vapor form, the fission products as well as any of the remaining unfissioned primary materials. Also present are the vaporized bomb casing and any auxiliary equipment necessary for a particular test detonation. The fireball is extremely radioactive, due to both fission products and radioactivity induced in the bomb casing, tower, and auxiliary equipment.

The fireball rapidly expands, reaching a maximum diameter in less than 1 sec and at the same time begins to rise in the air and cool. As it rises, a toroidal system develops with strong internal revolving or circulating air currents. Coincidental to this development, the thermal energy emitted by the fireball strikes the surface of the ground, causing a disc-shaped cloud of dust and smoke to rise for considerable distances from Ground Zero. On striking the ground the blast wave, reinforced by its reflected wave, travels outward from Ground Zero. This is preceded by a wave of increased pressure. As the pressure fronts pass over the soil surface, dense clouds of dust arise showing strong turbulent motions with the forward dislocation of both dust and large objects (drag effects or secondary missiles). Shortly thereafter, violent and high-velocity updrafts are created in the wake of the rising fireball. Large volumes of dust from the region of Ground Zero and at considerable distances from it are drawn in and up toward the fireball. This forms a rapidly rising stem, containing tons of soil and debris, directly beneath the rising fireball. Much of the material in the stem may be circulated through and around the toroidal-shaped fireball or perhaps even sucked into the fireball itself. Depending upon the height of the burst from the ground surface, a portion of this lifted material will contain some neutron-induced radioactivity. This surface material may become either molten or vaporized, or, in the cooler regions of the cloud, it may remain unchanged. This phase reaction would be dependent upon the chemical properties of the soil, e.g., the melting point of silica is lowered by the presence of certain carbonates. The foreign material provides surfaces for the adsorption of vaporized fission products or nuclei for condensation. As the fireball cools, one may expect particle growth and solidification. The physical and chemical properties will be dependent upon the chemical content of the soil and the interrelation of the many reactions which take place during the process of radioactive particle formation, i.e., the transition from a vaporized and/or molten state to the final solidification of the fall-out material. The height of detonation influences the amount of material which, in addition to the fission fragments, is available for particle formation.

Ultimately the cloud rises to an elevation where the density of the gases is the same as that of the surrounding air, and the familiar mushroom-capped cloud with a long stem of debris is observed. Wind shearing may distort the symmetry of the cloud and stem at any level.

Thus we may group together all the phenomena of the detonation and the subsequent growth and rise of the fireball, cap, and stem, as being some of the more important factors which give rise to the initial distribution of radioactive particles in the air over Ground Zero.

1.3.2 Distribution of Fall-out Material

The subsequent dispersal and the ultimate pattern of fall-out from the initial particle distribution over and adjacent to Ground Zero is a very complex phenomenon depending, among other factors, upon the particle size, the particle density and shape, the distribution of particles as a function of height, and the various meteorological conditions following the detonation. Owing to the heights to which particles may rise and to the size spectrum, some particles may remain in the air for very long periods of time, their ultimate location being dependent upon various climatic influences. With even moderate winds opportunity is provided for large-scale movements with or without appreciable dilution due to turbulence. Thus large areas may be severely contaminated with probable local variations of large magnitude resulting from localized weather conditions and topography.

1.3.3 Definitions of Primary Fall-out and Airborne Material

Although all the radioactive material which settles out of the cloud may be described as fall-out, a practical distinction should be made between material which remains suspended for long periods of time and material which settles out within the "reasonable" time of the survey period and remains associated with the surfaces of soil, vegetation, etc. The distinction is primarily one of particle size. Throughout this report, settled fall-out material will be designated as "primary fall-out," or "fall-out," and material sampled while still airborne will be described as "airborne material." Some movement of fall-out material picked up from the ground and temporarily airborne by the local winds can be expected at any time, but, since this occurrence cannot be identified except on rare occasions, it will be mentioned only when directly observed.

REFERENCES

1. J. H. Olafson et al., Preliminary Study of Off-site Airborne Radioactive Materials, Nevada Proving Grounds. I. Fall-out Originating from Snapper 6, 7, and 8 at Distances of 10 to 50 Miles from Ground Zero, AEP-UCLA Report UCLA-243, February 1953.
2. Los Alamos Scientific Laboratory, "The Effects of Atomic Weapons," U. S. Government Printing Office, Washington, June 1950.
3. Armed Forces Special Weapons Project, "Radiological Defense," Vol. II, U. S. Government Printing Office, Washington, 1951.

CHAPTER 2

METHODS AND MATERIALS

2.1 OPERATIONS

2.1.1 Nevada Test Site and Area of Operations

The Nevada Proving Grounds (NPG) are located in a sparsely populated mountainous desert. The shots in which Project 27.1 participated occurred at or over test sites in Yucca Flat, which can be described as a "bowl," the floor of which is approximately 4500 ft above sea level, surrounded by mountain ranges which reach elevations of 7000 ft above sea level. The surrounding region of from 10 to 100 miles from Ground Zero was the primary area of routine operations for this project. This region consists of mountain ranges with elevations to 10,000 ft above sea level and over, which are oriented north and south and separated by wide, alluvial valleys. Within this area are very few improved roads. However, there are many trails in varying degrees of repair which have been established and used by miners and stockmen. See Fig. 4.1 for details of the area and terrain.

2.1.2 Organization

A total of no more than 55 men participated in Project 27.1 at any one time. Of these, 14 were temporarily assigned from other AEC contractors, 9 were full-time personnel from AEP, UCLA, and 32 were enlisted personnel from the U. S. Navy.

The personnel were divided into three operational units: (1) the Field Group, consisting of 13 teams directed by 3 squad leaders, was responsible for the placement of equipment, collection of samples, monitoring, and field observations, (2) the Laboratory Group was responsible for the preparation of samples and radiological assay of all collected samples, and (3) the Administrative Group was responsible for the direction and correlation of both laboratory and field efforts, including the necessary logistics and support.

2.1.3 Operational Plan

The dependence of the fall-out pattern upon meteorological conditions necessitated a mobile Field Group. In order to obtain as many data as possible, the Field Group remained at previously assigned rendezvous points until after the final weather meeting was held (2100 hours, D−1 day). At this time a prediction of the fall-out pattern was obtained from the Air Weather Service of the Test Director's organization. Instructions were relayed to the field via telephone or radio according to the prediction of the fall-out pattern. Stations were then established in a pattern which covered approximately 30° each side of the estimated midline of fall-out at that time. Approximately 4 hr was allowed for the establishment of stations and the safe return of personnel to the rendezvous points.

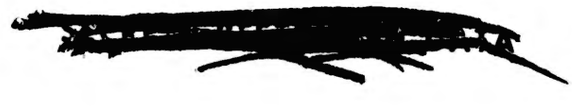

Maximum use was made of air samplers which changed samples automatically every 2 hr. This simplified comparison of data obtained from different locations, as well as greatly facilitating the mobile operation of the Field Group. A background sample was taken, in most cases, during the 2 hr prior to detonation.

Approximately 10 hr after detonation the first group of air samples was collected by the field crews and transported to the laboratory by courier team. The first sample analyses were possible at approximately H+18 hr.

Throughout D-day members of the Field Group obtained monitoring information; the teams operated under the direction of the squad leader responsible for an assigned area within the fall-out pattern. At H+24 hr the Field Group secured the sampling equipment, collected the various types of fall-out samples, and returned to the laboratory at Mercury.

Owing to changes in the wind directions which could not be relayed to the field because of inadequate radio communications, deviations in the actual fall-out patterns of about 45° from that predicted resulted in total misses on three detonations. When adequate communications were obtained by use of a relay station carried in a USAF C-47 flying at an altitude of 12,000 ft, a revision of station locations according to a later weather prediction (H−5 hr) was possible, and a more complete coverage was achieved.

2.2 FIELD SAMPLING STATIONS

2.2.1 Station Locations

Prior to the test series, sampling and reference locations were selected and posted. These served the following purposes: (1) permitted mapping of the fall-out patterns with reasonable accuracy, (2) permitted selection of areas where topographic influence was minimized so that results at each station could be more easily correlated, and (3) greatly facilitated the mobile operation of the Field Program.

Stations were selected according to the following criteria whenever possible:

1. At predetermined intervals along roads and trails which approximated arcs of 20, 40, and 80 miles around the test site.
2. At least 200 ft from the road in the direction toward the test site.
3. On level terrain, preferably with only grassy vegetation.
4. In areas where no trees or shrubs over 2 ft high grew within 100 ft.

At each station a general description of soil surface, slope, vegetation, and other observations was recorded. Each station was permanently marked with a vertical post with a reflector and a station code number. The first word or number of the code identified the arc or road, and the remainder of the code identified the station in sequence. Station locations are given in Table 2.1.

Figure 2.1, the operational map of Project 27.1, presents the relative locations of sampling stations.

2.2.2 Types of Sampling Stations

A distinction was made between the types of stations according to the equipment used as follows:

(a) Routine Air-sampling Station. This station consisted of either a Low-volume (Lo-Vol) Automatic Sampler (20-mile arc) or a High-volume (Hi-Vol) Automatic Sampler (40- and 80-mile arcs) plus a gummed-tray assembly, film badge, and soil sample.

(b) Master Air-sampling Station. This station consisted of all the equipment of a routine station plus extra equipment intended for correlative work, e.g., many gummed trays for uniformity of fall-out distribution studies and both Lo-Vol and Hi-Vol Automatic Samplers for comparison of efficiencies.

(c) Tray Station. This station consisted of only a gummed-tray assembly and a film badge. One tray station was located midway between the air-sampling stations.

Field station equipment is illustrated in Figs. 2.2 and 2.3 and is described in Sec. 2.3.

Table 2.1—SAMPLING STATION LOCATIONS

Station No.	Approximate station interval, mi	Location
201 to 211	2–3	Along arc, ~20 mi from GZ*
401 to 452	5	Along arc, ~40 mi from GZ
801 to 828	10	Along arc, ~80 mi from GZ
K-1 to K-8	5	In Kawich Valley, from ~7 to 40 mi from GZ, oriented north and south
Nye 1 to Nye 5	2	In Nye Canyon, oriented north and south, ~10 mi east of Yucca Flat
P-1 to P-10	2	In Papoose Lake area, north of Nye Canyon
EV-1 to EV-10	2	In Emigrant Valley from Groom Lake to Nye Canyon

*GZ refers to Ground Zero.

2.3 FIELD SAMPLING EQUIPMENT AND TECHNIQUES

The primary requirements of field sampling equipment and techniques for this type of program may be stated as follows:

1. Ability to withstand shock, vibration, and exposure to weather.
2. Stable automatic operation without constant attention.
3. Reproducibility of sample rates and volumes in the case of air samplers.
4. Ability to obtain the representative sample required.
5. Minimum error due to sample contamination or loss of sample.
6. Portability and ease of setting up under adverse weather conditions.

Inasmuch as previously available air-sampling equipment generally failed to satisfy these requirements, specially designed air samplers were obtained. These units were, in one case, prototype models and in another were modified Chemical Warfare air samplers used at the Dugway Proving Grounds.

All air sampling, gummed-paper fall-out collections, and film-badge exposures were made at 3 to 4 ft above the ground surface. Survey-meter readings were likewise taken 3 ft above the ground surface.

2.3.1 High-volume Automatic Air Sampler

Thirty automatic air samplers, which were prototype models of a design intended for field use, were purchased from the Ralph M. Parsons Company of Pasadena, Calif. These Hi-Vol samplers were primarily used at distances of from 40 to 80 miles from Ground Zero.

This sampler consists of two basic integral units. One unit contains a belt-driven positive displacement air pump powered by a ½-hp constant-speed motor and the necessary timing and control devices for automatic operations and intermittent sample changing. The second unit, a sample magazine, contains eight 4-in.-diameter air filters designed to be completely interchangeable. However, in practice it was found that better results were obtained by matching pump and magazine units. A time-delay mechanism permits a delay in the initiation of air sampling until the desired hour. Programming is controlled by a synchronous motor which is set for the desired 2-hr sample interval. An over-all accuracy in timing and sampling rate of 5 per cent was claimed by the manufacturer.

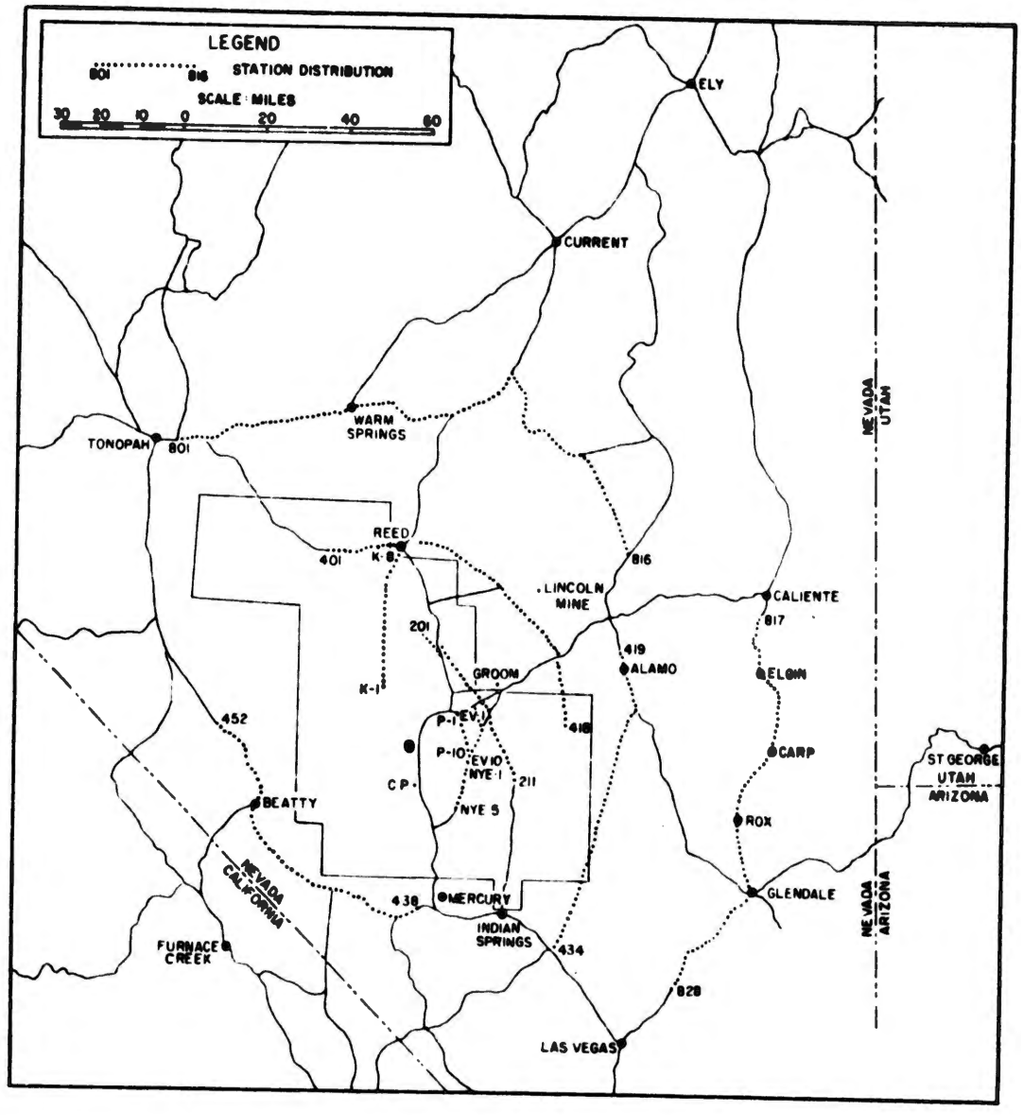

Fig. 2.1—Operational map showing relative locations of all sampling stations established by Project 27.1.

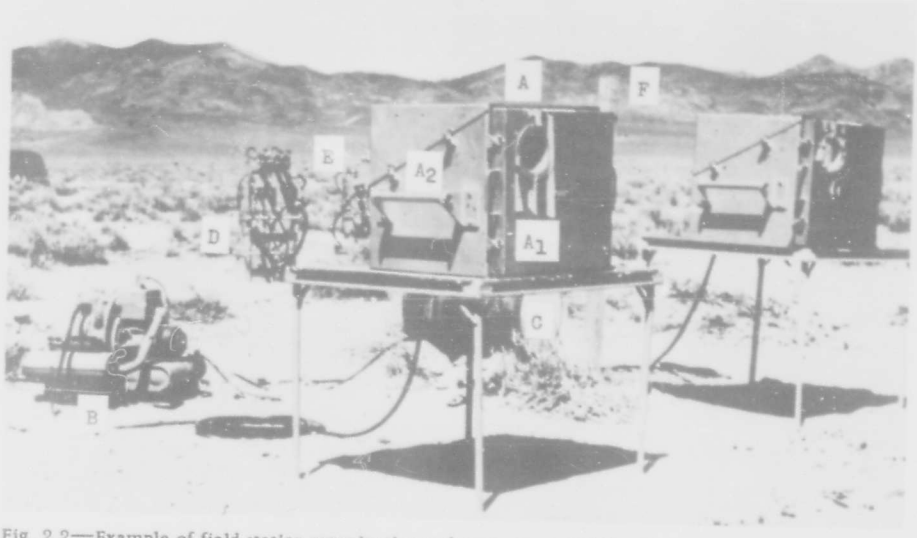

Fig. 2.2—Example of field station organization and equipment. (A) Hi-Vol air sampler. (A_1) sample magazine unit. (A_2) pump unit. (B) 1.5-kw Homelite generator. (C) auxiliary gasoline tank. (D) cascade impactor assembly attached to Lo-Vol sampler. (E) Lo-Vol sampler. (F) station marker.

Fig. 2.3—Detail of Lo-Vol air sampler and gummed-tray assembly. (A) Lo-Vol sampler. (A_1) filter magazine unit with attached sampling heads. (A_2) pump unit. (A_3) initial and auxiliary battery boxes. (A_4) second series of sampling heads. (B) gummed-tray assembly. (C) film badges.

The sampler requires a source of 110-volt 60-cycle a-c power. Homelite 1.5-kw portable power units, loaned to this project by LASL, were used primarily. Generators with 2.5-kw output were found to be preferable because of the high current required to start the pump motor and to change samples. An inadequate source of power was the cause of the majority of the equipment failures.

Mine Safety Appliance Company (MSA) Type BM-2133 filter pads were used in the Hi-Vol samplers. This type pad was selected because of its routine usage by other air-monitoring programs during Operation Upshot-Knothole and earlier test series. Type AA Millipore (membrane) filters, manufactured by the Lovell Chemical Co., were used to a limited extent at master stations for use in particle-size determinations. Calibration by means of a Back-Rack velometer yielded the following flow rates for these samplers and the two filter media:

Filter media	Flow rate, m^3/min	2-hr sample volume, m^3
MSA BM-2133	0.706	84.8
Type AA Millipore	0.466	56.0

2.3.2 Modified Electrolux Air Sampler

Six air samplers consisting of Electrolux tank-type vacuum cleaners modified to draw air through MSA BM-2133 filter pads were obtained from the Rad-Safe Unit for use in comparative studies only. The Electrolux sampler operates quite satisfactorily as an air sampler within the limits imposed by manual changing and the variations in sample rates with voltage and load due to the speed characteristics of a series-wound motor.

A sample rate of 1.16 m^3/min at 110 volts was determined from the average flow rates of the six Electrolux samplers measured with a Back-Rack velometer. This yielded a 2-hr sample of 140 m^3.

The Electrolux samplers were used at master stations to determine the effect of the orifice position upon sampling efficiency and to obtain data directly comparable to those of the Rad-Safe Unit.

2.3.3 Low-volume Automatic Air Sampler

Twenty-five Lo-Vol Automatic Air Samplers were obtained from the Dugway Proving Grounds. These units were initially radio controlled but were modified to operate in the same manner as the Hi-Vols.

This sampler consists of three basic units. The first unit consists of a battery box containing a 6-volt storage battery and programming devices. The second, the pump unit, contains control devices and a 6-volt motor-driven positive displacement vacuum pump. The third, a filter magazine unit, consists of a vacuum manifold which is connected in sequence to each of seven sampling ports by means of solenoid-operated valves. The sampling heads, each containing one filter paper, are locked in position in these ports by rubber compression fittings. An auxiliary battery connected in parallel with the first was necessary to obtain a 24-hr period of continuous operation.

Type AA Millipore filter paper 1 in. in diameter was used. A flow rate of 10.2 liters/min yielded a total 2-hr sample of 1.23 m^3.

2.3.4 Modified Casella Cascade Impactor

As one method to determine the size distribution of airborne material, cascade impactors were substituted for the regular sampling heads of the Lo-Vol samplers. The impactors were connected to two intake ports of the Lo-Vol by means of "tee" connections, giving a sample interval of 4 hr per impactor.

The impactor used was a "Casella" four-stage to which was added a fifth stage containing a 1-in.-diameter Whatman #41 paper. A flow rate of 14.6 liters/min was obtained. The calcu-

lated mass median diameter of each stage at this flow rate, based upon spherical particles having a density of 2.5, is as follows:

Stage	Mass median diameter, μ
5	0.49
4	0.81
3	1.56
2	3.82
1	8.97

2.3.5 Gummed-tray Fall-out Sampler

At each air-sampling station and midway between stations, two 8- by 9-in. Kum-Kleen gummed cellophane sheets were exposed to collect primary fall-out material. The cellophane sheets (covered with a protective kraft paper) were taped to squares of 10-gauge galvanized metal in the laboratory prior to each detonation. In the field these were attached to angle-iron fence posts by means of thumb screws with corner irons for supports. Finally the protective paper was removed. After an exposure of approximately 24 hr following a detonation, a single fold was made in each sheet to form a 4- by 9-in. sample within which the collected material was sealed. The thickness value of this cellophane is 5 mg/cm^2.

2.3.6 Soil Samples

Surface soil samples were collected from selected areas where fall-out was known to have occurred. A single sample consisting of the composited surface soil of three 1-ft^2 areas, as defined by a template, was collected with a hand trowel at each contaminated location. The depth of soil was not critical but generally approximated 1 in. To provide for the possibility that prior contamination might account for appreciable activity, a background sample was collected at each air-sampling station in the same manner prior to each detonation.

2.3.7 Film-badge Dosimetry

In addition to the sampling equipment described in Secs. 2.3.1 to 2.3.5, film-badge packets were placed at each sampling station. They were suspended 3 ft above the ground, by wire, from one of the fall-out trays. Each badge was exposed for approximately 24 hr following detonation.

In order to minimize the effect of transporting the films across a contaminated area and to reduce contamination of the film badges, the following procedure was used: Each team was issued a lead-shielded container for the transportation of the film packets. A "control" film was carried in the shielded container throughout each operation. Each film pack was enclosed in a "pliofilm" envelope which was removed after exposure and before placing the exposed film in the container for transportation to the laboratory in Mercury. The film packs were packaged and shipped to the Health Physics Section, AEP, UCLA, for development under standard conditions and evaluation.

Densitometer readings were made in the standard manner for gamma and beta-gamma exposures. Results are reported in roentgens and rems, respectively. The films used were Eastman type K and Du Pont 558 with a shielding due to the pliofilm container of 0.065 g/cm^2. The film packets were developed and evaluated.[1]

2.3.8 Background Recorders

Ten portable battery-operated background recorders were used to determine fall-out time at the various sampling stations. These units consisted of either a Victoreen Model 263 G-M survey meter or a Tracerlab Model SU-10 ionization chamber survey meter, followed by a d-c amplifier whose output was connected to an Esterline-Angus spring-wound recording milliam-

meter. These units were developed by the Electronics Section, AEP, UCLA, and are described in detail elsewhere.[2]

2.3.9 Field Monitoring

The survey meters used in field monitoring were the Tracerlab Model T1B (ion chamber), the Jordan Model AG 500 (ion chamber), and the Precision Model 106 (G-M). All survey meters were calibrated with a Co^{60} source having a radiation field of 11,628 mr/hr at a distance of 1 ft. A calibration table was prepared and sent with each instrument. With the survey meters enclosed in disposable plastic bags, all readings were obtained uniformly at a distance of 3 ft above the ground and at least 30 ft from the vehicle. Only gamma radiation was measured. At the time of monitoring, all readings were recorded as dial reading and corrected reading in terms of milliroentgens per hour, gamma.

Monitor readings were taken at each station in the standard manner at times of station activation and sample change. These readings, when extrapolated to a common time (H+12 hr), serve to correlate the various determinations made at each station. The instrument calibration and extrapolation of readings to a common time, by means of the mixed fission product decay formula, are apparently valid. This is indicated by the fact that individual readings, taken at the same location at different times by the same or different instruments, resulted in very good correlation. During the day of detonation and the following day, each team monitored its area of operations within the fall-out pattern, and a limited number of "roving" monitors, usually the squad leaders, completed the definition of the fall-out pattern along the passable roads or trails.

The instrument which proved to be the most satisfactory for this operation was the Jordan survey meter. This instrument utilizes a low-voltage pressurized ionization chamber with an open grid electrometer tube amplifier. The open grid circuit results in a logarithmic response to radiation. The response of this instrument is essentially energy independent to gamma radiation from 0.1 to 1.25 Mev. The instrument has a characteristic of long battery life with a very low calibration drift. The small over-all dimensions, light weight, and simplicity of operation were also desirable. The principal disadvantage of the instrument is the small scale length and the difficulty in interpolating between dial divisions on a logarithmic scale. However, this was largely overcome with practice and use of the instrument. Further information can be found in reference 3.

2.3.10 Identification of Field Samples

All field samples were identified by means of a code number which indicated in sequence the station number, the type of equipment, the sequence of the sample, and the shot. For example, a sample identified as 427-HV-2-U7 was from Station 427, a Hi-Vol air sample, the second serial sample, and from Shot 7.

Equipment was identified by the following abbreviations: HV, Hi-Vol Automatic Sampler; EL, modified Electrolux; LV, Lo-Vol Automatic Sampler; GP, gummed paper; SOIL, soil sample; FB, film badge; and CI, cascade impactor.

A data sheet bearing the proper code accompanied each sample or serial group of samples. Pertinent information, such as time of sampling, equipment operation, weather observations, terrain features, and mr/hr readings, was entered upon this data sheet.

2.4 RADIOACTIVITY ASSAYS

2.4.1 Equipment and Techniques

Radioactivity determinations were generally limited to standard counting procedures. The possible numbers of samples to be processed for each detonation (in excess of 1200) and past field experience indicated that laboratory equipment and techniques should fulfill the following requirements:

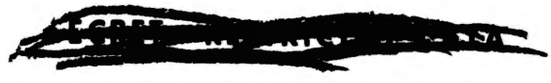

1. Ability to detect sample activities between 10 μμc and 1 μc.
2. Ability to radio-assay samples in the presence of high instrument background rate.
3. Minimum error due to cross-contamination.
4. Minimum time of assay.
5. Accuracy of assay within 5 per cent probability.

The primary counting instruments used, according to activity and physical size of the collected samples, were as follows:

1. For high activity and large area samples, an unshielded thin window (mylar hydrochloride film) 4- by 9-in. flat plate beta proportional counter followed by a linear amplifier (CMR-7, Model PA-6) and a binary scaler (CMR-7, Model SC-3B, scale of 1024). These units were purchased from LASL.

2. For low activity and small area samples, a Tracerlab Model TGC-2A end-window G-M tube (approximately 1.5 mg/cm^2) mounted in a 2-in. lead shield and followed by a Keleket Autoscaler Model K-280 (scale of 256).

Counting efficiencies were determined by the use of standards which were prepared by plating out aliquots of radium D + E standardized solution on filter paper. The standards were enclosed in aluminum foil to absorb the soft components and to prevent contamination. Individual standards approximated the physical size and shape of each of the various collected samples. The radium D + E standards compared favorably to the Sr^{90} standards used by the Off-site Rad-Safe Unit. Differences in energy characteristics between fission products and the radium standards result in an error of undetermined magnitude. Such an error would be present regardless of the standardizing isotope chosen because of the rapidly changing energy spectra of the fission products during the early decay period.

Depending on the distance of the sample from the window, the proportional counters had counting efficiencies of from 5 to 25 per cent and the G-M instruments of from 0.5 to 10 per cent.

Coincidence corrections were determined from data obtained by counting two samples individually and together.

Radioactivity values are presented in terms of microcuries wherever possible, the validity being dependent upon energy spectra, as previously described. Since the activity of mixed fission products varies with time to the −1.2 power (approximately), all values are corrected accordingly either to a common time or to the midtime of sampling for purposes of comparison. The common time was arbitrarily chosen as H+12 hr.

The following equation, which describes the decay rate of mixed fission products, was used in calculations involving decay of collected field samples:

$$A = A_0 T^{-1.2} \tag{2.1}$$

where A = activity or dose rate at any time t
A_0 = activity or dose rate at an initial time t_1
T = ratio of time t to time t_1

Accumulated dosage over the time interval t_1 to t_2 was calculated using the equation

$$\text{Dose} = \int_{T_1}^{T_2} A_0 T^{-1.2}\, dT \tag{2.2}$$

which on solution yields

$$\text{Dose} = 5A_0 \left[\frac{1}{t_1^{0.2}} - \frac{1}{t_2^{0.2}} \right] \tag{2.3}$$

In practice extrapolation factors for decay and dosage determinations were obtained from prepared tables and nomographs based upon Eqs. 2.1 to 2.3.

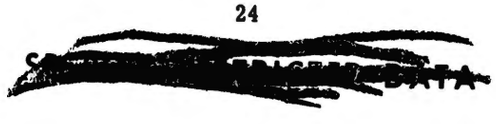

2.4.2 Determination of Airborne Radioactivity Concentrations

The radioactivity of Hi-Vol samples was determined on proportional counters and that of Lo-Vol samples on G-M counters. The activity concentrations were calculated in the following manner:

$$\mu c/m^3 \text{ (midtime)} = \frac{\text{counts/min}}{\text{geometry} \times (2.2 \times 10^6) \times \text{volume}} \times T^{-1.2} \tag{2.4}$$

where $T = \dfrac{\text{midtime of sample interval}}{\text{time of assay}}$ (H + hr)

The activities of the cascade impactor slides were determined on G-M counters. The necessary calculations for particle-size determinations, based upon cascade impactor samples, are described elsewhere.[4]

2.4.3 Determination of Fall-out Activity per Unit Area

The folded 4- by 9-in. gummed papers were counted directly on the proportional counters, and unit area activities at H+12 hr were determined from the average count rate of the two samples as follows:

$$\mu c/ft^2 \text{ (H + 12 hr)} = \frac{\text{av. counts/min}}{\text{geometry} \times (2.2 \times 10^6) \times 0.5 \text{ ft}^2} \times T^{-1.2} \tag{2.5}$$

where $T = \dfrac{12}{\text{time of assay}}$ (H + hr)

Soil samples required the following preparation and counting techniques:

1. Samples representing 3 ft^2 of surface soil were dry-sieved through a 2-mm screen for 10 min, and the coarse fraction was discarded. (Pulverization prior to sieving was generally not required; in exceptional cases a mortar and rubber-tipped pestle were used to break up agglomerates.) The total weight of the <2 mm soil fraction was determined, using a 4-kg-capacity torsion balance.

2. Triplicate 200-g samples of <2 mm soil fraction were uniformly distributed over the surface of 4 by 9 by 1 in. deep cardboard containers and were counted on the proportional counters.

3. Self-absorption of beta radiation by the soil required that activities be extrapolated to zero mass. (On D+2 days the half-thickness of soil was less than 4 mm.) The necessary factor was determined by selecting one soil sample from each detonation and assaying mass increments from 5.00 to 250.00 g per 36 $in.^2$, the area of the cardboard container. The resulting activities per gram were plotted as a function of sample weight, and the activity at zero mass was determined by extrapolation. A self-absorption factor (activity at zero mass : activity per 200 g) was then calculated. This factor was determined periodically to account for changes in the energy spectrum with time.

4. A small number of samples, having high activities which resulted in very large coincidence corrections or exceeded the capacity of the scaler, were counted through an aluminum absorber to reduce the count rate. In such cases a weight series (as above) was counted with and without the absorber and the per cent transmission through the aluminum at zero sample mass determined. The factor was introduced into Eq. 2.6 when required.

Unit area activities based upon soil samples were determined as follows:

$$\mu c/g = \frac{\text{av. counts/min/200 g} \times \text{correction factor to zero thickness}}{\text{geometry} \times (2.2 \times 10^6) \times 200 \text{ g}} \tag{2.6}$$

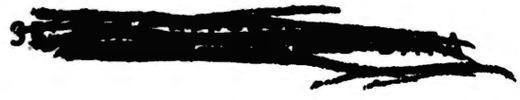

$$\mu c/ft^2\ (H + 12\ hr) = \frac{\mu c/g \times g/3\ ft^2\ sample}{3} \times T^{-1.2} \qquad (2.7)$$

where $T = \frac{12}{\text{time of assay}}\ (H + hr)$

2.4.4 Determination of Particle Size of Fall-out Material by Means of Soil Samples

The <2 mm soil fraction described in Sec. 2.4.3 was subjected to the following treatment for the determination of particle-size distribution: Single 200-g samples per sampling location were fractionated by 30-min dry-sieving in nests of sieves having openings of 833, 350, 175, 125, 88, and 44 μ. Fraction weights were determined by torsion balance. The <44 μ fraction was further fractionated by a method of air-elutriation of 10- or 15-g samples into 5- to 44-μ and 0- to 5-μ fractions, and their weights were determined by analytical balance.

Triplicate 1.000-g samples for each fraction (with the exception of the 5- to 44-μ and 0- to 5-μ fractions) were placed in plastic cups $1\frac{5}{8}$ in. in diameter and $\frac{1}{4}$ in. deep and assayed on the G-M counters. Activities of all fractions of each sample were generally determined within 30 to 60 min of each other. Corrections for decay were therefore necessary in only the few cases where counts of different fractions were not performed on the same day. Activities were not corrected for sample self-absorption on the assumption that difference in the self-absorption characteristics of soil samples of different particle size but of equal weight would be negligible.

In the case of the 5- to 44-μ and 0- to 5-μ fractions, single samples of equal weight were assayed, as determined by the weight yield of the 0- to 5-μ material. The relative activities of the 5- to 44-μ and 0- to 5-μ fractions were then applied to the percentage of the total activity which is represented as the total <44 μ fraction previously determined.

Where sampling areas had been contaminated by previous detonations, the background activities of comparable fractions were deducted prior to the determination of distribution percentages.

The distribution of activity with respect to particle size was determined as follows:

$$\text{Activity per fraction} = \frac{\text{av. counts/min/g}}{\text{geometry}} \times \text{weight of fraction, g} \qquad (2.8)$$

$$\text{Total activity} = \text{sum of fraction activities} \qquad (2.9)$$

$$\text{Per cent total activity per fraction} = \frac{\text{activity per fraction}}{\text{total activity}} \times 100 \qquad (2.10)$$

REFERENCES

1. R. Baker and L. B. Silverman, An Improved Film-badge Method in the Accurate Determination of Personnel Exposures, Report UCLA-53, March 1950.
2. W. R. Kennedy, A Continuously Recording Radiation Background Monitor for Field Use, AEP-UCLA Report UCLA-258, June 1953.
3. F. H. Day, Quarterly Progress Report on Radiological Instrument Calibration, National Bureau of Standards, Report NBS-2594, March 1953.
4. Los Alamos Scientific Laboratory, "The Effects of Atomic Weapons," U. S. Government Printing Office, Washington, 1950.

CHAPTER 3

RESULTS

Project 27.1 participated in the following test detonations:

Shot	Type	Date	Fireball yield, kt
2	300-ft tower	3/24/53	24.2 ± 10%
3	300-ft tower	3/31/53	0.18 ± 25%
4	~6000-ft airdrop	4/6/53	10.8 ± 10%
5	300-ft tower	4/18/53	27.4 ± 10%
7	300-ft tower	4/25/53	51.5 ± 10%

For each of the tower shots, stations were activated at distances ranging from 10 to 80 miles from Ground Zero in a direction dependent upon predicted weather conditions. The geometrical distribution of these stations was according to the basic plan set forth in Sec. 2.1.3. In the case of the airdrop the operational plan was altered to cover the area between 80 and 200 miles while adhering to the basic geometry as closely as possible.

In terms of completeness of fall-out sampling, the Shot 7 operation was the most successful. Changes in wind conditions caused the fall-out patterns of Shots 2 and 5 to differ considerably from those predicted approximately 8 hr before shot time. As a result the stations established for Shot 2 received neither airborne nor fall-out activity, and only a small percentage of those established for Shot 5 received either airborne or fall-out activity. However, following each of these tests, soil sampling and field monitoring were used to describe the primary fall-out areas.

The detonations of Shots 3 and 4 yielded very little fall-out material, as was expected, considering the small size and the height of burst of the respective devices.

3.1 SHOT 2 (24.2 KT ± 10 PER CENT)

3.1.1 Dose Rate and Integrated Dosage Measurements

Figure 3.1 presents in graphical form the distribution of fall-out material originating from Shot 2. The distribution is indicated by isointensity lines (at H + 12 hr) as determined by field monitoring and is further described by plotting the mr/hr and calculated integrated dosage values detected along two roads crossing the fall-out path.

Since the fall-out pattern was displaced from the pattern of established sampling stations, neither film-badge nor background recorder measurements were available. The integrated dosages were therefore calculated from the estimated fall-out times as indicated by trajectory analysis (see Table 4.7 for wind velocities).

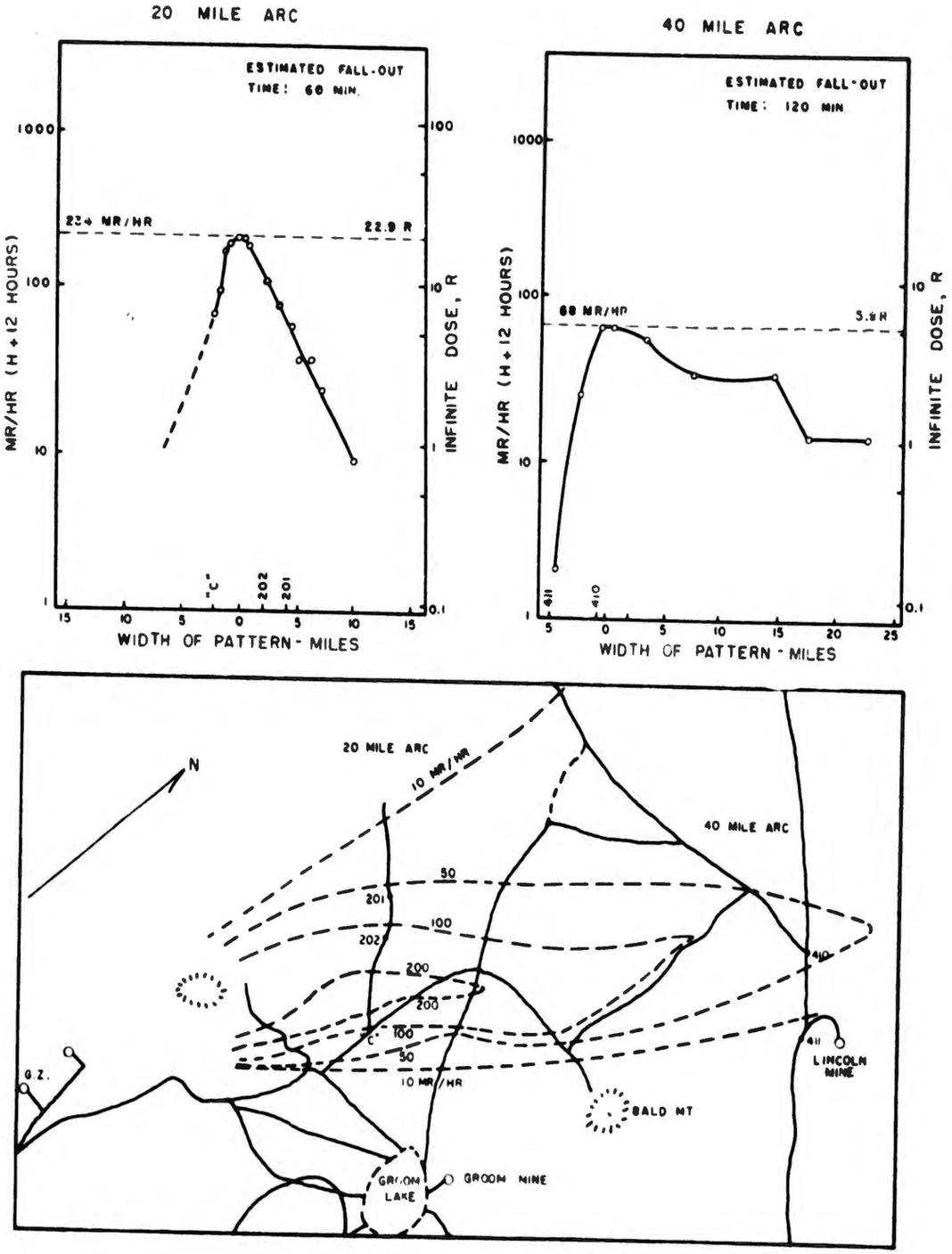

Fig. 3.1—Pattern of fall-out distribution from Shot 2; dose-rate contours at H + 12 hr and detailed lateral distribution along arc.

3.1.2 Primary Fall-out Activity

(a) Soil Samples. Samples from off-site areas contaminated by Shot 2 were collected 6 days following detonation. No determinations of activity per unit area were made, the samples being used for particle-size analysis and to establish laboratory techniques necessary for unit area analysis.

The results of particle-size analysis of soil samples are presented in Table 3.1. For comparison mr/hr values are included.

(b) Gummed Papers. Collections were successful only at those stations located within the bowl. One station was located in the primary fall-out area downwind from the detonation, and the remainder were in fringe areas. The station in the primary fall-out (8 miles, 355° east of north from Ground Zero) collected 272 $\mu c/ft^2$, whereas those in fringe areas collected activities which varied from 10^{-3} to 10^{-1} $\mu c/ft^2$ at H+12 hr. Since the location of these stations with respect to the midline of fall-out was not determined, the values cannot be interpreted.

3.1.3 Airborne Radioactivity

Two air-sampling stations within the bowl collected measurable amounts of airborne radioactivity. Airborne activities detected at one station (5 miles, 178° east of north from Ground Zero) averaged 2.7×10^{-2} $\mu c/m^3$ for the period H to H+4 hr. The activity at the other station (4 miles, 75° east of north from Ground Zero) was 1.6×10^{-3} $\mu c/m^3$ during the 2 hr following detonation. All other samples had negligible activity.

3.2 SHOT 3 (0.18 KT ± 25 PER CENT)

3.2.1 Dose Rate and Integrated Dosage Measurements

Shot 3 was detonated under conditions of relatively low wind velocities; therefore it yielded a very small cloud of debris rising to approximately 15,000 ft and did not provide detectable levels of fall-out activity at most stations.

The cloud traveled toward the southeast with a wide shear. Known passable roads were monitored, but, though "hot spots" (approximately 10 mr/hr) were located, a general pattern of fall-out was unobtainable owing to the inaccessibility of the contaminated area.

3.2.2 Primary Fall-out Activity

(a) Soil Samples. No soil samples were collected owing to the low mr/hr values.

(b) Gummed Papers. Seven sampling stations from approximately 15 to 80 miles from Ground Zero collected measurable amounts of primary fall-out material. All concentrations were less than 0.5 $\mu c/ft^2$. The values are presented in Table 3.2.

3.2.3 Airborne Radioactivity

Four sampling stations collected measurable amounts of airborne activity. The airborne concentrations persisted for only 2 to 4 hr at each location. The concentrations, which varied from 10^{-4} to 10^{-3} $\mu c/m^3$, are presented in Table 3.3.

3.3 SHOT 4 (10.8 KT ± 10 PER CENT)

Owing to the absence of scavenging debris and surface material, the quantity of fall-out from a high airburst does not approach that produced by a tower shot. The extremely small particles expected to be produced may be regarded as being primarily airborne rather than fall-out material. Project 27.1 functioned during this test primarily to determine the distance from Ground Zero at which these small particles might produce significant ground-level activity.

Table 3.1—SOIL CONTAMINATION AND SIZE DISTRIBUTION OF PRIMARY FALL-OUT, SHOT 2*

Distance from target, mi	Bearing, degrees E of N	Mr/hr†	Per cent total activity associated with various soil size fractions, μ						
			2000 to 833	833 to 350	350 to 175	175 to 125	125 to 88	88 to 44	44 to 0
3.5			3.7	9.7	12.2	10.4	19.0	22.7	22.3
12	26	176	3.2	81.6	5.7	0.5	0.5	0.6	7.9
19.5	31	147	0.4	14.6	80.2	0.5	0.7	1.2	2.4
25.5	28	137	0.3	1.8	84.5	0.4	0.6	2.6	9.8
34.5	28	72	1.8	1.8	57.9	0.8	24.3	2.4	11.0
42.0	27	48	0.2	23.5	66.0	1.2	1.5	5.6	2.0
43.0	34	48	0.5	0.7	65.9	20.5	0.6	3.3	8.5

*Soil samples were collected Mar. 30, 1953.
†Corrected to H + 12 hr.

Table 3.2—GUMMED-PAPER COLLECTION OF PRIMARY FALL-OUT, SHOT 3*

Stations ~15 mi from Ground Zero		Stations ~80 mi from Ground Zero	
Station	μc/ft²	Station	μc/ft²
Nye 4†	0.48	828.5	0.052
Nye 5	0.34	829	0.38
Nye 5.5	0.031	830	0.43
		831	0.18

*Values are corrected to H + 12 hr.
†See Fig. 3.2 for detailed station locations.

Table 3.3—AIRBORNE ACTIVITY CONCENTRATIONS, SHOT 3

Station	Miles from Ground Zero	Midtime of sample interval	$\mu c/m^3 \times 10^{-4}$
Yucca Flat	~7.5*	H + 3	3.8
		H + 5	1.7
434	~51	H + 3	7.6
829	~79	H + 11†	28.0
831	~69	H + 5	4.3

*Bearing from Ground Zero: 170° E of N.
†Midtime correct to nearest hour.

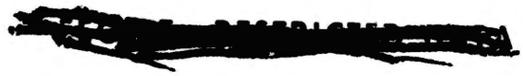

3.3.1 Dose Rate and Integrated Dosage Measurements

The monitoring teams, using field-survey instruments, did not detect any levels of gamma radiation above background within the (approximate) 200-mile distance from Ground Zero which was studied.

3.3.2 Primary Fall-out Activity

One gummed-paper sample having an activity of 1.4×10^{-3} $\mu c/ft^2$ was collected approximately 175 miles from Ground Zero (61 miles northeast of Kingman on U. S. Highway 66). Stations on either side of this location (3-mile intervals) did not collect measurable primary fall-out.

3.3.3 Airborne Radioactivity

The radioactivity values of air samples collected following Shot 4 are presented in Table 3.4.

Table 3.4—AIRBORNE ACTIVITY CONCENTRATIONS, SHOT 4

Location, and distance from Kingman, Ariz., mi	Miles from Ground Zero	Midtime of sample interval*	$\mu c/m^3 \times 10^{-4}$
15 S	~190	H+18†	0.42
46 NE	~175	H+3	27.0
		H+7	3.4
		H+17	2.1
		H+19	0.66
		H+21	1.0
52 NE	~175	H+7	2.4
		H+9	2.4
58 NE	~175	H+3	7.2
		H+7	6.1
		H+9	1.5
		H+11	1.1

*Midtime correct to nearest hour.

†Total sample interval of H+12 to H+24 hr; programming device failed.

3.4 SHOT 5 (27.4 KT ± 10 PER CENT)

3.4.1 Dose Rate and Integrated Dosage Measurements

Although the fall-out pattern again failed to coincide with the sampling station pattern, a detailed study was made by means of field-monitoring and soil-analysis techniques.

The distribution of fall-out from Shot 5 is presented in the form of an isointensity plot in Fig. 3.2. As was the case with Shot 2, neither film-badge nor background-recorder measurements were obtained. Therefore the integrated dosages were calculated from the estimated time of arrival of fall-out activity (see Table 4.7 for wind velocities).

3.4.2 Primary Fall-out Activity

(a) Soil Samples. Samples from areas contaminated by Shot 5 were collected at approximately H+24 hr from locations known to be within the primary fall-out area. The results of

Table 3.5—SOIL CONTAMINATION AND SIZE DISTRIBUTION OF PRIMARY FALL-OUT, SHOT 5*

Reference location	Distance from target, mi	Bearing, degrees E of N	Mr/hr†	Surface soil activity, †‡ μc/ft²	Per cent total activity associated with various soil size (μ) fractions							
					2000 to 833	833 to 350	350 to 175	175 to 125	125 to 88	88 to 44	44 to 5§	5 to 0
Yucca	~3		110		1.3	2.6	70.9	10.5	8.8	2.5	3.1	0.3
EV-10	16.5	122	31.8	1,420	7.0	36.9	47.5	1.6	0.7	1.9	3.8	0.6
1 mi S of EV-10	16.6	125	1018		3.7	22.5	67.9	2.3	1.9	0.3	1.5	
1.4 mi S of EV-10	16.6	126	900	18,300	0.2	86.9	1.5	1.7	1.7	2.3	3.4	2.4
2.5 mi S of EV-10	17.5	129	771	21,950	0.5	91.6	2.8	1.1	0.7	1.4	1.2	0.7
5.0 mi S of EV-10	18.5	134	32.9	994	1.5	4.0	13.7	70.8	3.9	4.0	0.9	1.1
14 mi S of Sta. 210	31	121	578	9,410	0.07	10.1	79.2	1.0	1.4	3.6	3.3	1.3
429	50.2	111	1.0	64.1	2.1	4.3	5.1	6.2	3.2	30.1	46.2	2.8
429.5	51	113	172	3,580	0.1	0.3	46.2	43.8	1.7	2.6	5.0	0.3
430	52.5	116	10.9		4.4	1.6	2.1	5.3	62.8	14.9	8.5	0.4
430.5	53.5	118	9.0	218	0.8	6.3	3.3	2.8	46.5	13.8	26.9	
17 mi SW of Glendale	86	120	153	575	1.2	0.8	2.9	31.2	21.9	31.9	8.5	1.6

*Soil samples were collected Apr. 19, 1953.

†Corrected to H + 12 hr.

‡Soil activities in terms of μc/ft² correspond approximately to μc/kg of surface soil (1 ft², ½ cm deep with apparent density of 2.0).

§Represents 0- to 44-μ percentages where 0- to 5-μ values are omitted because of insufficient quantities of 0- to 5-μ material for separation.

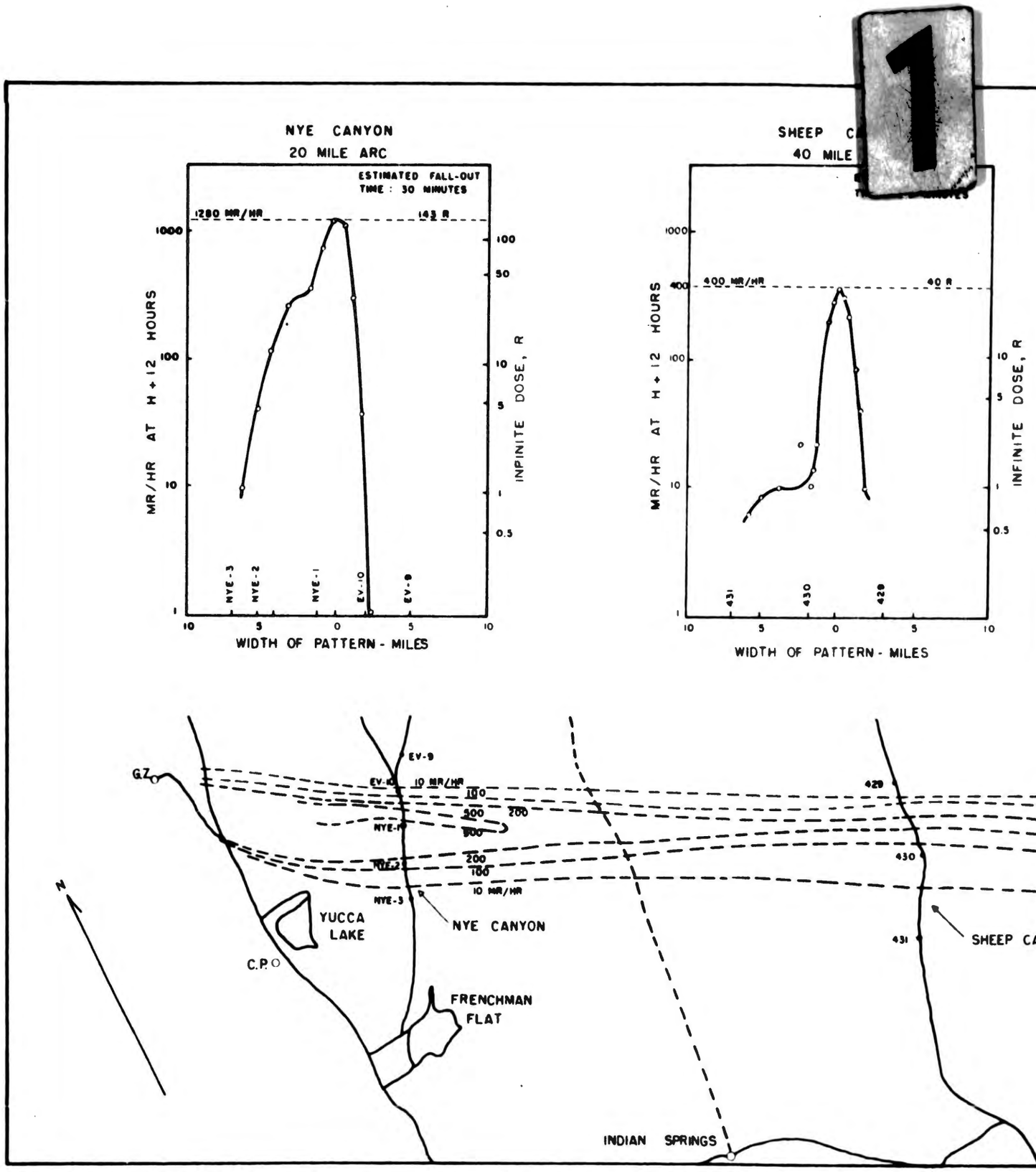

Fig. 3.2—Pattern of fall-out distribution from Shot 5; dose-rate contours at H + 12 hr and deta

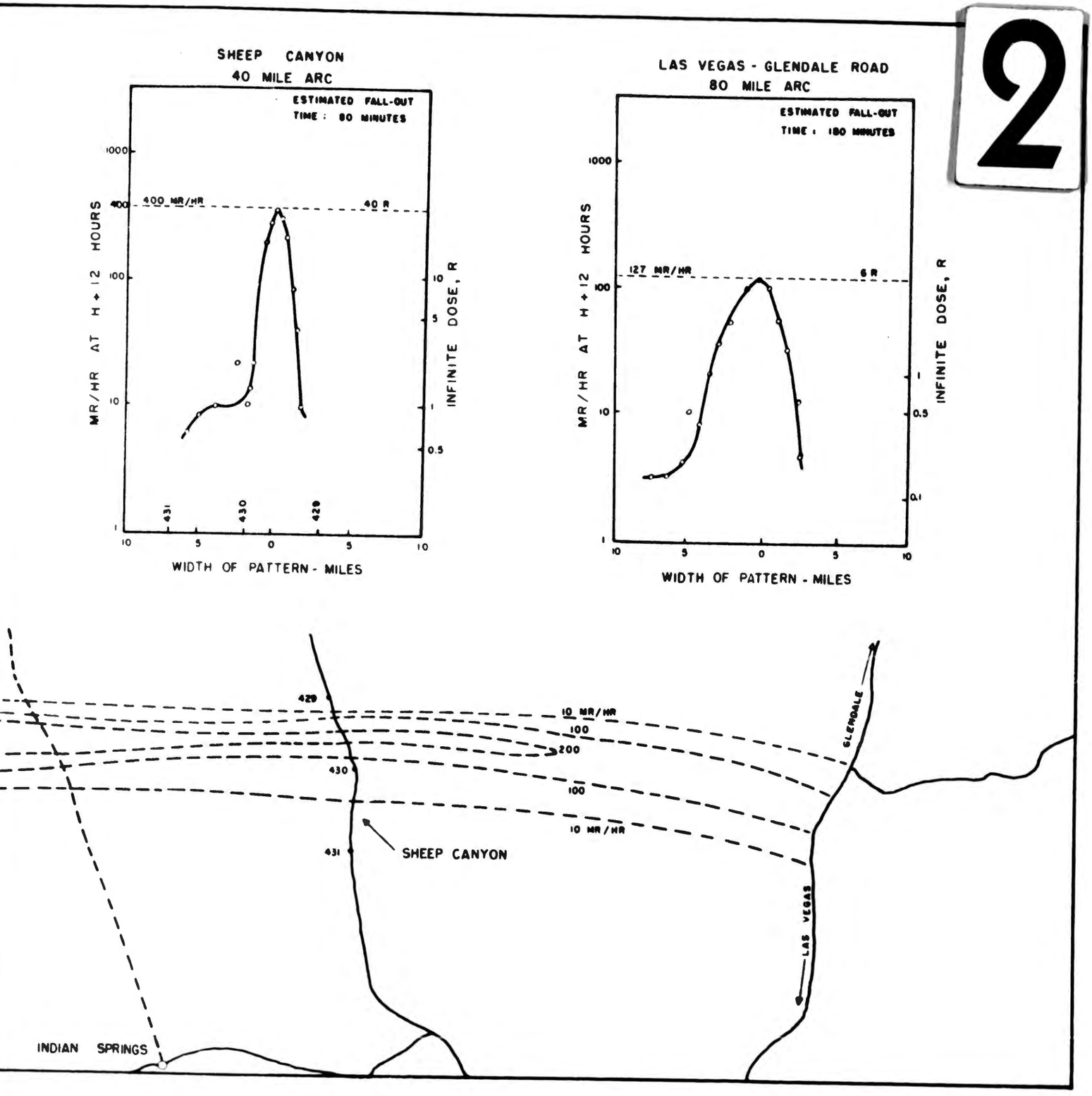

-out distribution from Shot 5; dose-rate contours at H + 12 hr and detailed lateral distribution along arc.

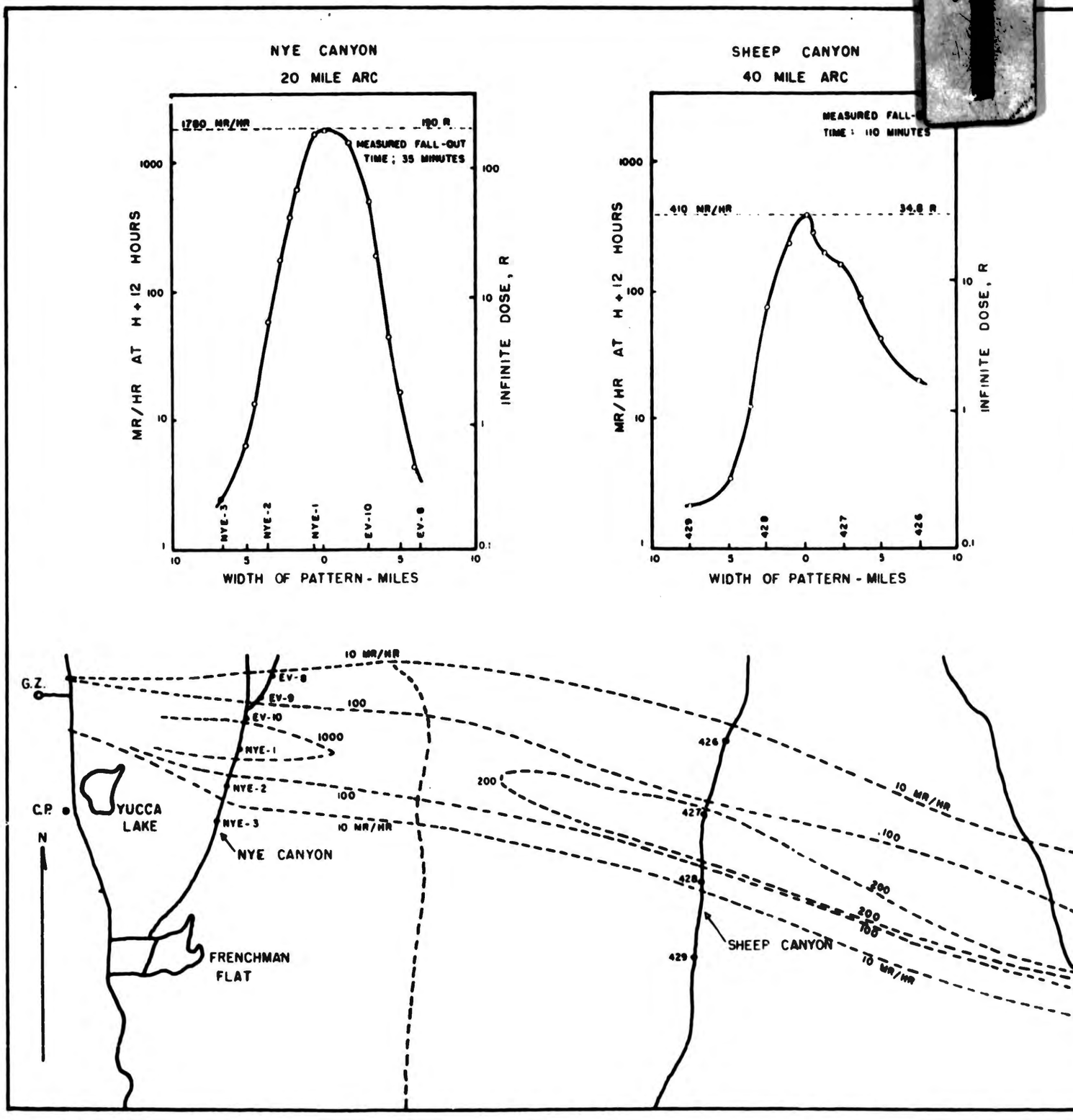

Fig. 3.3—Pattern of fall-out distribution from Shot 7; dose-rate contours at H + 12 hr and detailed la

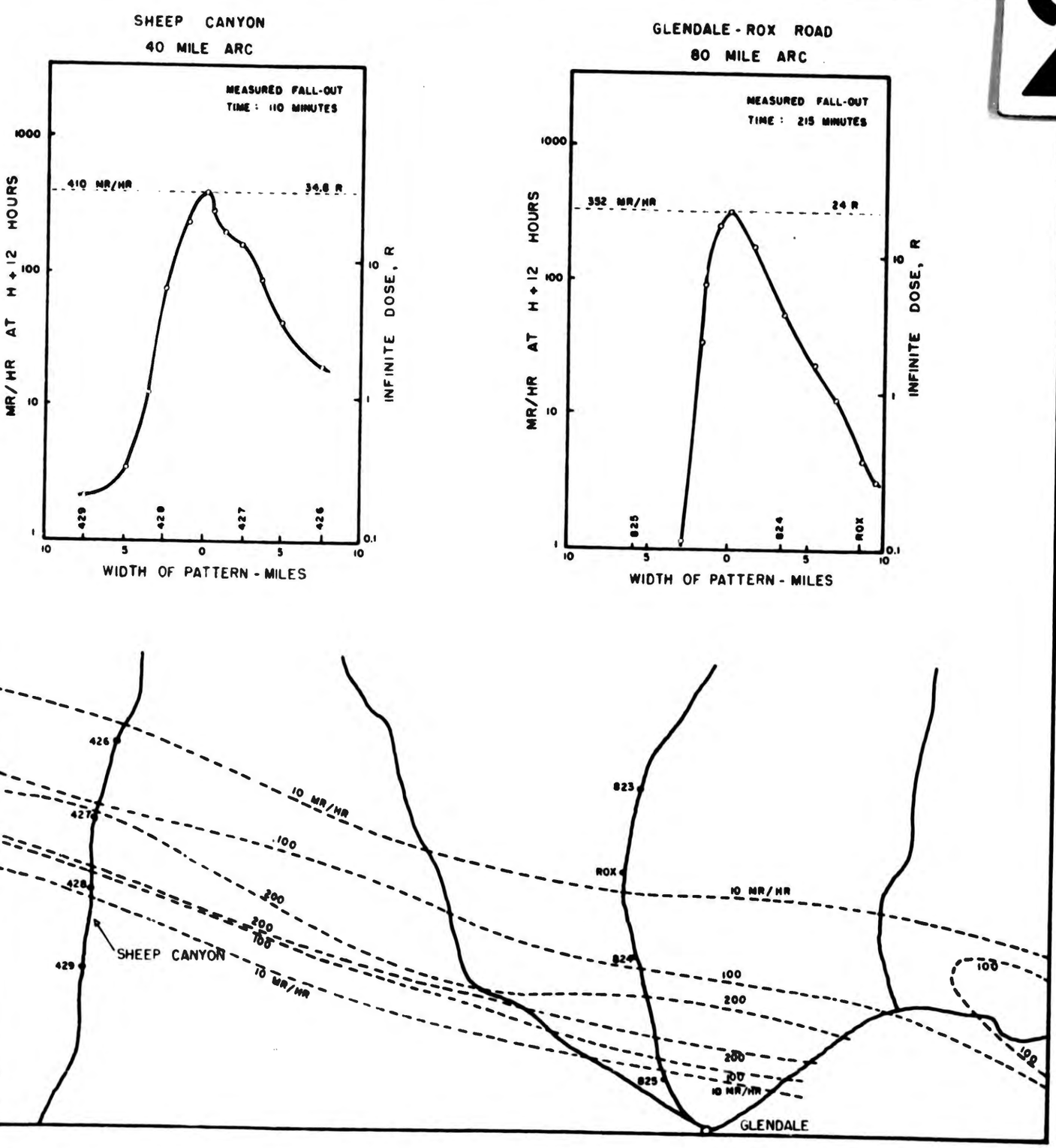

ibution from Shot 7; dose-rate contours at H + 12 hr and detailed lateral distribution along arc.

activity per unit area and particle-size analyses of the collected samples are presented in Table 3.5. For purposes of comparison, mr/hr values are included.

(b) Gummed Papers. The placement of fall-out trays resulted in fringe area sampling only. Fall-out activities in these areas were too low for correlative data to be obtained by field monitoring. The complete results of laboratory analysis of gummed papers are presented in Table 3.6.

3.4.3 Airborne Radioactivity

Four stations collected measurable amounts of airborne radioactivity which are summarized in Table 3.7.

3.5 SHOT 7 (51.5 KT ± 10 PER CENT)

A total of 31 sampling stations were activated and located according to a special 2300 D−1 day forecast. This late fall-out prediction, in conjunction with a satisfactory revised communication system, permitted a more accurate placement of equipment and all of the stations activated received relatively high levels of both primary fall-out and airborne activity. The station locations with reference to the measured midline of fall-out are illustrated in Fig. 3.4 (page 36).

3.5.1 Dose Rate and Integrated Dosage Measurements

(a) Field Monitoring. Figure 3.3 presents the isointensity lines within the fall-out area as determined by field monitoring. The presented values of integrated dosage are based on monitoring data and time of arrival of fall-out as measured by background recorders.

The background recorders in the main line of fall-out recorded an initial burst of activity at fall-out time which then decayed with time. Though the drift characteristics of the instrument prohibited precise decay determinations, the decay was similar to that of mixed fission products. This would indicate that the majority of the fall-out material at these locations was deposited during a short time interval (approximately 5 min at 16 miles and 20 min at 100 miles) and that subsequent arrival of additional material was not appreciable. This being the case, the integrated dosages based upon monitoring data and calculated from measured fall-out time should be valid.

(b) Film-badge Dosimetry. Film badges exposed at each of the air-sampling and tray stations gave results which are compatible with the calculated dosages from instrument readings. The results of film-badge dosimetry are summarized in Table 3.8.

(c) Beta-Gamma Ratio. To expand the information regarding beta to gamma ratios, several exposed gummed papers and Electrolux air samples were surveyed with a Juno ionization chamber. The measurements were made at D+40 hr at maximum geometry for the instrument. Measurements were made through approximately 10 mg/cm^2 of cellophane. The results are presented in Table 3.9.

3.5.2 Primary Fall-out Activity

(a) Soil Samples. Samples were collected at approximately H+24 hr from areas known to have received significant primary fall-out. Many of these samples were taken at locations where there were other types of samples, which permits comparison of the activities collected by each method.

The results of activity per unit area and particle-size determinations are presented in Table 3.10. Corresponding mr/hr values and gummed-paper activities are included for purposes of comparison where soil samples were collected at routine sampling stations.

(b) Gummed Papers. Primary fall-out activity at all sampling stations resulted from Shot 7. Gummed-paper activities ranged from 0.3 to 25,700 μc/ft^2, depending upon the distance from Ground Zero and the location relative to the midline of fall-out.

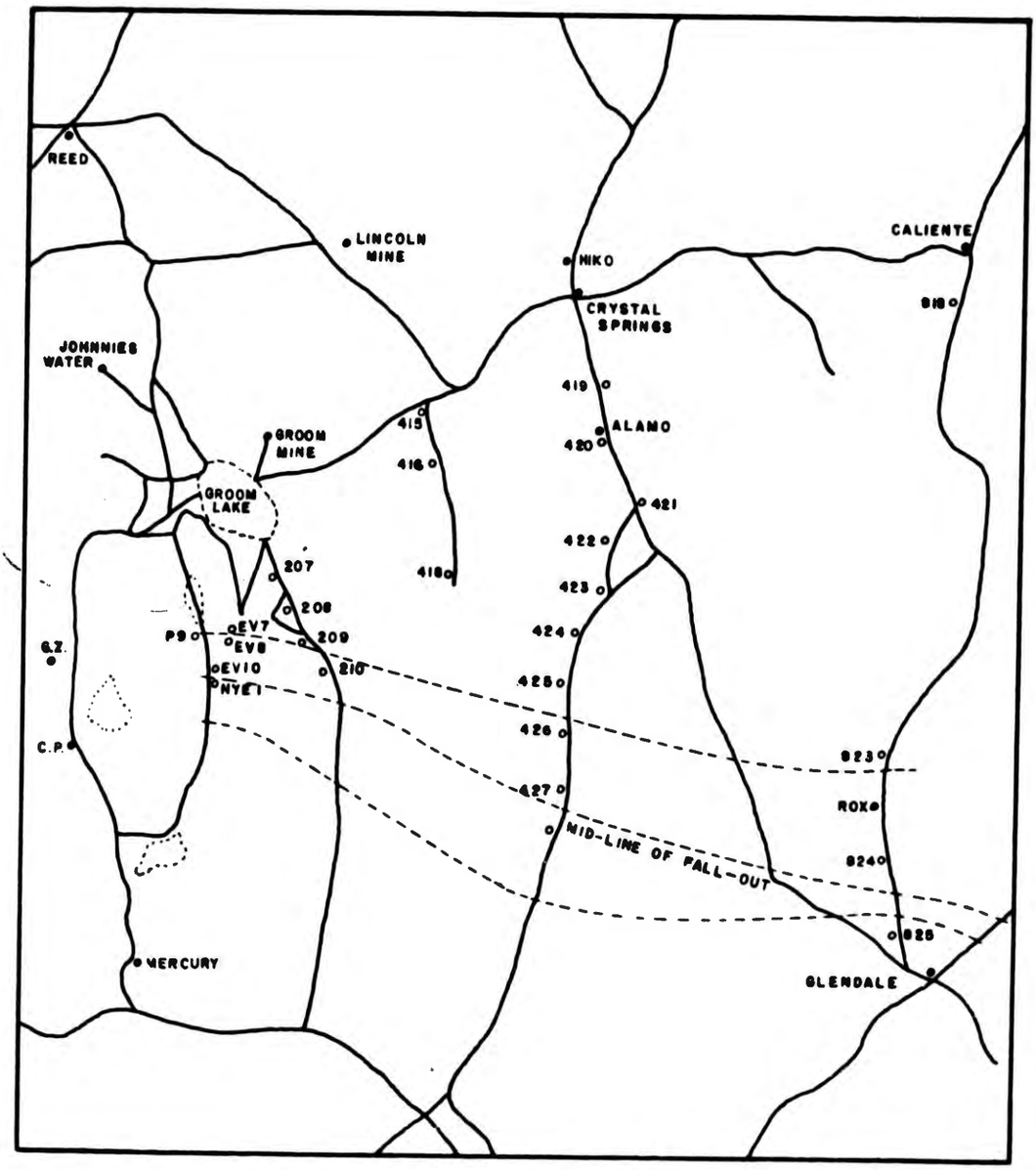

Fig. 3.4—Locations of activated air-sampling stations and general pattern of fall-out from Shot 7.

Table 3.6—GUMMED-PAPER COLLECTION OF PRIMARY FALL-OUT, SHOT 5*

Station	$\mu c/ft^2$	Location of stations
209.5	0 076	~25 mi from GZ†; from 13.5 to 12 mi N of midline of fall-out
210	0.011	
421.5	0.10	~45 mi from GZ; from 41 to 10 mi N of midline of fall-out
422	0.11	
422.5	0.088	
423	0.074	
424	0.089	
425.5	0.085	
426	0.060	
426.5	0.12	
427	0.11	
427.5	0.054	
819	0.14	~85 mi from GZ; from 68 to 3 mi N of midline of fall-out
819.5	0.091	
820	0.17	
823	0.056	
823.5	0.14	
5 mi SW of Glendale	0.090	
10 mi SW of Glendale	1.00	
15 mi SW of Glendale	79.3	

*Values are corrected to H + 12 hr.
†GZ is used here for Ground Zero.

Table 3.7—AIRBORNE ACTIVITY CONCENTRATIONS, SHOT 5

Station	Miles from Ground Zero	Midtime of sample interval*	$\mu c/m^3 \times 10^{-4}$
424	~49	H + 15	0.74
425	~50	H + 12	3.8
825	~88	H + 9	8.5
		H + 12	6.5
827	~86	H + 7.5	110†

*Midtime correct to nearest hour; 2-hr sample intervals.
†Maximum concentration detected; average midtime concentration, H + 6 to H + 24 hr: 0.0026 $\mu c/m^3$.

Table 3.8—SUMMARY OF FILM-BADGE DOSIMETRY, SHOT 7

Reference location	Calculated 24-hr gamma dose, r*	Measured film exposure, corrected to common exposure time of H + 24 hr†		
		Gamma, r	Beta, rem	Total, rem
Nye 1	87	95	237	332
EV-10‡	30	39	166	205
427‡	5.8	9.5	28.5	38
426.5	1.5	1.05	3.70	4.75
426	0.75	0.95	1.9	2.85
824	1.4	2.2	3.96	6.16

*Calculated from monitoring data.

†"The reported readings ... are greater than a theoretical interpretation based on the gross density ratio of unshielded to shielded area of the film. These interpretations do not include dosage received from β radiation received below an effective energy of 0.265 Mev, this assumption being based on the amount of absorber surrounding the film (0.065 g/cm^2)..." (From memorandum to K. H. Larson from Louis B. Silverman, Chief, Health Physics Section, AEP, UCLA, June 17, 1953.)

‡Station at which background recorder was located.

Table 3.9—RATIO OF BETA DOSE RATE TO GAMMA DOSE RATE, SHOT 7

Sample location	Dial reading, shield open	Dial reading, shield closed	Beta : gamma
	Gummed Papers		
Nye 1	1100	15	73 : 1
EV-10	2800	40	70 : 1
210.5	165	1*	165 : 1
426	400	2*	200 : 1
426.5	900	4	225 : 1
427a	2200	25	88 : 1
427b	1400	17	82 : 1
427c	1400	22	64 : 1
427d	1300	23	57 : 1
427e	2200	30	73 : 1
427f	1250	15	83 : 1
427g	2300	21	109 : 1
824	800	4	200 : 1
824.5	1500	15	100 : 1
	Electrolux		
427a	1450	3	483 : 1
427b	1500	1*	1500 : 1
427c	2200	6	367 : 1

*Those gamma readings which are less than 3 are questionable.

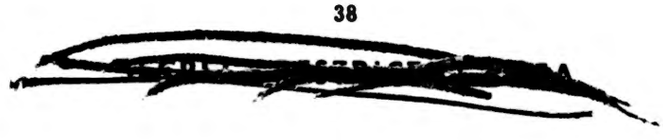

Table 3.10—SOIL CONTAMINATION AND SIZE DISTRIBUTION OF PRIMARY FALL-OUT, SHOT 7*

Reference location	Distance from target, mi	Bearing, degrees E of N	Mr/hr†	Surface activity†		Per cent total activity associated with various soil size (μ) fractions							
				Gummed-paper, $\mu c/ft^2$	Soil,‡ $\mu c/ft^2$	2000 to 833	833 to 350	350 to 175	175 to 125	125 to 88	88 to 44	44 to 5§	5 to 0
Yucca	~3					38.4	15.8	42.6	2.4	0.8	0.03	0.01	
EV-7	17.4	82	2.5	41.5	24.9	0.3	0.8	5.8	19.5	15.5	14.5	43.6	
EV-8	16.8	87	4.2	54.5	37.1	1.3	2.5	3.5	3.0	5.7	34.8	49.2	
EV-10	14.7	103	515	5,220	6,740	0.0	90.3	0.0	0.6	1.0	5.0	2.9	0.2
Nye 1	14.7	108	1630	25,700	18,580	0.0	0.0	85.2	5.2	1.9	4.9	2.5	0.3
426	46.8	93	20.3	296	94.4	0.2	5.7	43.6	17.6	3.2	19.2	10.5	Nil
427	46.5	99	169	2,950	1,597	0.1	0.3	52.5	9.6	2.1	5.2	30.0	0.2
427.5	45.8	102	293		3,084	0.6	0.4	9.2	58.6	8.3	7.6	14.8	0.5
428	46.7	104	77		330	0.3	0.5	0.3	26.2	50.5	3.4	16.5	2.3
428.5¶	47.4	106	3.6		3.3	2.3	2.2	6.2	1.3	0.6	5.7	70.6	11.1
429¶	47.7	109	2.2		4.8	0.0	0.4	2.5	0.0	1.9	60.8	33.9	0.5
429.5¶	48.5	111	23.0		254	0.2	0.3	27.3	51.9	1.4	2.3	16.5	0.1
ROX	80.4	98	4.6	78.9	17.9	0.7	4.3	3.9	2.1	5.6	37.9	43.6	1.9
824	81.9	100	52.8	87.5	261	0.1	0.6	5.5	64.7	1.1	5.2	17.1	5.7
9.7 mi E of Glendale	95.2	105	288		740	0.01	0.2	2.9	6.5	61.2	11.5	17.7	

*Soil samples were collected Apr. 26, 1953.

†Corrected to H+12 hr.

‡Soil activities in terms of $\mu c/ft^2$ correspond approximately to $\mu c/kg$ of surface soil (1 ft^2, ½ cm deep, with apparent density of 2.0).

§Represents 0- to 44-μ percentages where 0- to 5-μ values are omitted because of insufficient quantities of 0- to 5-μ material for separation.

¶Stations possibly contaminated by Shot 5.

In addition to the standard horizontal gummed trays, a pair of gummed trays was mounted in a vertical plane at each sampling location on the 20- and 40-mile arcs. The vertical pair of gummed papers formed a "vee" pointing toward Ground Zero. The results of the gummed-paper collection by the standard horizontal, as well as vertical, papers are summarized in Table 3.11. Stations included are those stations at which air samplers were located (see Fig. 3.4). Field-monitoring data are presented for correlative purposes.

Table 3.11—GUMMED-PAPER COLLECTION OF PRIMARY FALL-OUT, SHOT 7*

Location of stations	Station	Field survey, mr/hr	Gummed-paper activity, $\mu c/ft^2$	
			Horizontal assembly	Vertical assembly
~16 mi from GZ† at 2- to 3-mi intervals; from 8 to 1 mi N of midline of fall-out	EV-7	2.52	41.5	9.07
	P-9.5	3.45	13.1	2.52
	EV-8	4.22	54.5	11.5
	EV-10	515	5,220	34.5
	Nye 1‡	1630	25,700	4015
~22 mi from GZ at 2- to 3-mi intervals; from 17 to 9 mi N of midline of fall-out	207	0.92	8.75	1.74
	208	Nil	2.08	15.6
	209	Nil	1.87	8.83
	210‡	3.50	87.2	No sample
~45 mi from GZ at 5-mi intervals; from 31 to 2.5 mi N of midline of fall-out	415	Nil	1.54	0.75
	416	Nil	2.21	1.85
	419	Nil	3.85	No sample
	420	Nil	5.30	No sample
	421	Nil	18.6	20.7
	422	Nil	13.0	Nil
	423	1.33	15.5	3.15
	424	Nil	16.4	5.02
	425	4.1	22.8	4.13
	426	20.3	296	8.17
	427‡	169	2,950	214
~80 mi from GZ; from 59 mi N to 6 mi S of midline of fall-out	Caliente	Nil	0.386	No sample
	818	Nil	20.2	No sample
	823	2.2	52.3	No sample
	ROX	4.56	78.9	No sample
	824‡	52.8	875	No sample
	825	Nil	0.256	No sample

*Values corrected to H+12 hr.
†GZ is used here for Ground Zero.
‡Station closest to midline of fall-out.

Although the activities collected by the vertical trays are, with very few exceptions, lower than those collected by the horizontal ones, a rather high efficiency of collection by impingement is indicated. Such data also suggest that samples collected by gummed papers may not be strictly representative of residual ground-surface activity, owing to subsequent collection of wind-blown dust or even airborne material.

3.5.3 Airborne Radioactivity

(a) Maximum and Average Concentrations. (See Appendix A for detailed tabulation.) The concentrations of airborne radioactivities collected during the 24 hr following detonation are given in Table 3.12. Values presented are the maximum concentrations detected and the average concentration through H+24 hr.

Table 3.12—AIRBORNE ACTIVITY CONCENTRATIONS, SHOT 7*

Location of stations	Station	Surface activity at H+12 hr (gummed paper), $\mu c/ft^2$	Maximum air concentration† (midtime), $\mu c/m^3$	Interval of maximum	Average concentration through H+24 hr,‡ $\mu c/m^3$	Periods station inoperative
~16 mi from GZ§ at	EV-7	41.5	0.25	H+2 to H+4	0.048	H+10 to H+14
2- to 3-mi intervals;	P-9.5	13.1	0.044	H+2 to H+4	0.0054	
from 8 to 1 mi N of	EV-8	54.5	0.16	H to H+2	0.030	
midline of fall-out	EV-10	5,220	2.08	H to H+2	0.20	
	Nye 1¶	25,700	9.9	H to H+2	1.1	
~22 mi from GZ at	207	8.75	0.021	H+2 to H+4	0.0050	H to H+12
2- to 3-mi intervals;	208	2.08	0.0051	H+20 to H+22	0.0017	
from 17 to 9 mi N of	209	1.87	0.16	H to H+2	0.027	
midline of fall-out	210¶	87.2	0.57	H to H+2	0.084	
~45 mi from GZ at	415	1.54	0.00099	H+12 to H+14	0.00050	H to H+12; H+16 to H+24
5-mi intervals;	416	2.21	0.61**	H to H+2	0.18	H+8 to H+12; H+14 to H+24
from 31 to 2.5 mi N	418	No sample	0.0076	H+2 to H+4	0.0045	H+4 to H+12; H+16 to H+24
of midline of fall-out	419	3.85	0.032	H+12 to H+14	0.011	H+4 to H+12; H+14 to H+24
	420	5.30	0.034	H+10 to H+12	0.0045	
	421	18.6	0.0037	H+12 to H+14	0.0012	H+8 to H+12; H+22 to H+24
	422	13.0	0.15	H+8 to H+10	0.027	
	423	15.5	0.020	H+18 to H+20	0.0063	
	424	16.4	0.011	H+12 to H+14	0.0058	H to H+12; H+16 to H+24
	425	22.8	0.14	H+6 to H+8	0.020	H+10 to H+12; H+22 to H+24
	426	296	0.85	H+4 to H+6	0.14	
	427¶	2,950	4.18	H+2 to H+4	0.95	
~80 mi from GZ;	Caliente	0.386	0.088	H+12 to H+14	0.020	
from 59 mi N to 6	818	20.2	0.33	H+6 to H+8	0.052	H+10 to H+12
mi S of midline	823	52.3	0.11	H+8 to H+10	0.023	
of fall-out	ROX	78.9	0.14	H+6 to H+8	0.062	H+10 to H+12; H+14 to H+24
	824¶	875	0.74	H+6 to H+8	0.14	
	825	0.256	0.0063**	H to H+2	0.0014	H+10 to H+12; H+16 to H+24

*For calculation, 100 per cent sampling efficiency is assumed.

†Based on Lo-Vol air samples at all stations 16 and 22 mi from Ground Zero and at Stations 423 and 427; remainder based on Hi-Vol air samples.

‡Average of activities at midtimes of sampling; intervals where no samples were obtained are not included.

§GZ is used here for Ground Zero.

¶Station nearest midline of fall-out.

**Probable cross-contamination of samples in magazine.

Where more than one type of sampler was operating at a location, the values presented are those obtained by the sampler having the fewest periods of inoperation due to equipment failure. Where failures occurred, the time that the station was inoperative is noted, and the average value represents only those intervals during which a sample was obtained. For comparison purposes the primary fall-out activities, as determined by gummed-paper sampling, are included in the tabulation.

As has been noted in previous field investigations,[1] no definite relation between airborne and primary fall-out activities is indicated. This may be attributed to the fact that airborne radioactivity is a transient phenomenon, influenced by such factors as diffusion, thermal effects, and vegetative cover, whereas the primary fall-out becomes relatively fixed to the soil and vegetation surfaces.

The data presented indicate that the greater the distance along an arc from the path of major fall-out, the later the time interval during which the maximum concentration occurs. This may be attributed to lateral dispersion due to local meteorological conditions.

Shot 7 resulted in widespread distribution of airborne, as well as fall-out, material in concentrations which were several orders of magnitude greater than those detected for Shot 5 when similar wind conditions prevailed.

(b) Particle-size Determinations. Detailed tabulation of cascade impactor data is not included since comparatively few of the impactor sets collected sufficient radioactivity during the 4-hr sampling period for an accurate analysis. Sets of cascade impactor slides were disregarded if the count rate of any two stages was less than twice the background. Since the time required to process the samples for each detonation was several days, with priority being given to analysis of airborne concentrations and primary fall-out collections, many of the impactor samples had decayed to this level before assay. When time permitted, many of these impactor slides were recounted, and some 14 size-distribution studies were made. However, since large extrapolation factors were necessary, the validity and accuracy of the data are questionable.

The data may be summarized as follows: The median diameter of the radioactive airborne material (based on the disintegration rate of the radioactive material collected per stage, rather than numerical count or weight of the particles per stage) varied between 0.5 and 8 μ with, in some cases, as much as 70 per cent of the radioactivity being associated with particles of less than 1 μ in diameter.

Several impactor slides were examined by electron microscope. An electronmicrograph of the collected particles is included in the discussion of particle characteristics (see Sec. 3.6.1 and Fig. 3.6).

An experimental sedimentation technique for the determination of airborne particle-size distributions was also investigated. This technique is based upon the rate of sedimentation of the material in suspension as determined by a scintillation counter surveying a narrow slit in a sedimentation cell. Suspensions of airborne material were obtained by the solution of Hi-Vol membrane filters in acetone. Significant results were not obtained, however, because of instrument instability. This technique warrants further study and is presently being evaluated at AEP, UCLA.

(c) Evaluation of Air-sampling Techniques. The many failures of air-sampling equipment indicated in Table 3.12 were primarily due to power failure. The generator used was a 1.5-kw Homelite portable power unit. In some cases a 2.5-kw unit was available and used to obtain better results.

Comparison of results obtained by means of Lo-Vol and Hi-Vol samplers at the same locations indicates that the two methods yield compatible results. However, individual variations suggest that a considerable error may be inherent in any single determination due to failure to obtain a truly representative sample of the aerosol.

A similar comparison of results obtained by modified Electrolux samplers oriented in different directions (the orifice up, down, and horizontal) at the same location indicates that, while activities are of the same order of magnitude, the horizontal sampler consistently collects the sample having the highest activity.

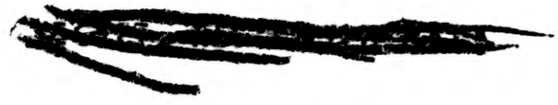

Such variations, associated with different types of air samplers and sampler orientation, suggest that only by isokinetic sampling with proper instrumentation would truly representative samples be obtained.

The Hi-Vol Automatic Samplers were delivered following Shot 2 of Operation Upshot-Knothole, and detailed engineering and calibration studies were not possible prior to their use. Subsequent to the test series, examination of the air-flow pattern with luminescent zinc sulfide powder indicated that some of the air can bypass the filter pad, resulting in errors due to sampling-rate inaccuracies and possible cross-contamination.

Investigations of the filter efficiency of the MSA BM-2133 filter pad are currently in progress at AEP, UCLA. Preliminary data indicate that retention efficiency varies with "face" velocity and dust concentration. Laboratory sampling of a test cloud of 0.47-μ particles of dust at a concentration of 0.27 mg/ft^3 indicates a retention efficiency of over 99 per cent at a flow rate of 0.52 m^3/min.

The magnitude of the error to which the air-sampling data are subject is undetermined and probably varies with each sampling unit. Since the results are reported in terms of 100 per cent efficiency of sampling, the values may be expected to be lower than actual concentrations.

3.6 THE NATURE OF THE FALL-OUT PARTICLE

3.6.1 General Observations

Photomicrographs of selected fall-out particles are presented in Fig. 3.5. Fall-out particles from tower shots are generally black, glossy, often magnetic, beads which appear to have solidified in the air. However, individual particles have been isolated which vary from the so-called "norm" (based on study of relatively few particles) in that they have clusters of smaller particles adhering to the surface, have pitted surfaces, are sponge-like, or appear to be crystalline with a milky-white coloring. These variations are thought to be due to the conditions under which solidification occurs in the "dust cloud."

Figure 3.6 presents an electronmicrograph of sub-micron particles collected by cascade impactors. Again, the particles appear to have originated from molten material which has solidified in air.

Solubility studies of fall-out particles, collected within 100 miles from Ground Zero, indicate that generally less than 1 per cent of the activity is soluble in H_2O and approximately 2 per cent in 0.1N HCl. Individual beads have been found in which the solubility is several times greater than the norm. This appears to be related to the characteristics of the surface of the particle.

Radiochemical studies have been reported[1] for particles obtained from Operation Tumbler-Snapper. There is reason to believe that the particles from Operation Upshot-Knothole are similar because the decay and energy characteristics are approximately the same.

3.6.2 Activity per Particle as a Function of Particle Size

Results from Operation Tumbler-Snapper[2] indicated that fall-out particles having diameters from 300 to 900 μ have activities which are a direct function of the surface area of the particle. Additional investigations were made during Operation Upshot-Knothole to determine if this relation is maintained as the particle size is decreased.

The relation of activity per particle to particle size was investigated by two methods: (1) individual particles were isolated, measured, and radio assayed, and (2) samples of selected soil size fractions were mounted on gummed paper, radio assayed, and autoradiographed. The total activity detected was then divided by the number of particles, as indicated by the autoradiograph, to yield the average activity per particle.

Figure 3.7 presents the series of autoradiographs from which data were obtained and illustrates the relative activities per size fraction. An autoradiograph reflecting relative activities of the separated particles shown in the photomicrographs in Fig. 3.5 is also included.

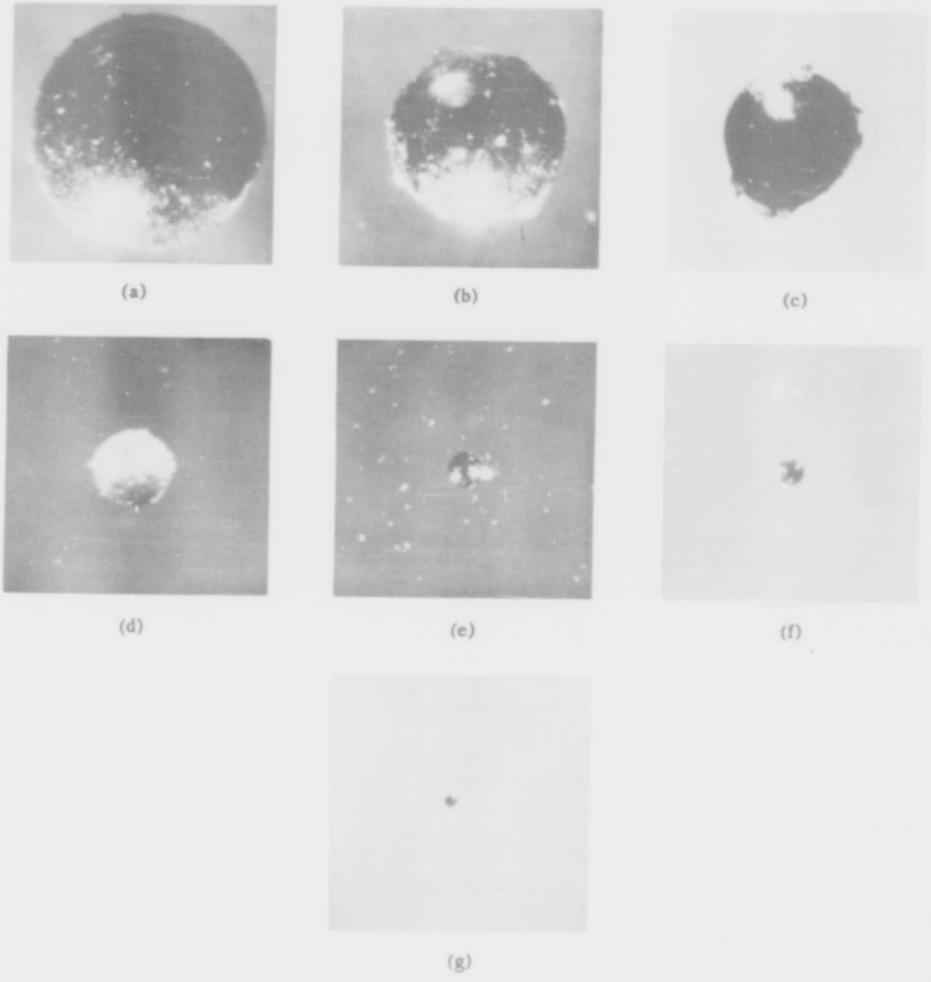

Fig. 3.5—Photomicrographs of selected fall-out particles from Shot 7. (Radioactivity values corrected to H + 12 hr.) (a) 723-μ diameter, 65.9 μc. (b) 555-μ diameter, 25.6 μc. (c) 387-μ diameter, 47.3 μc. (d) 234-μ diameter, 8.7 μc. (e) 115-μ diameter, 0.95 μc. (f) 81-μ diameter, 0.59 μc. (g) 20-μ diameter, 0.01 μc.

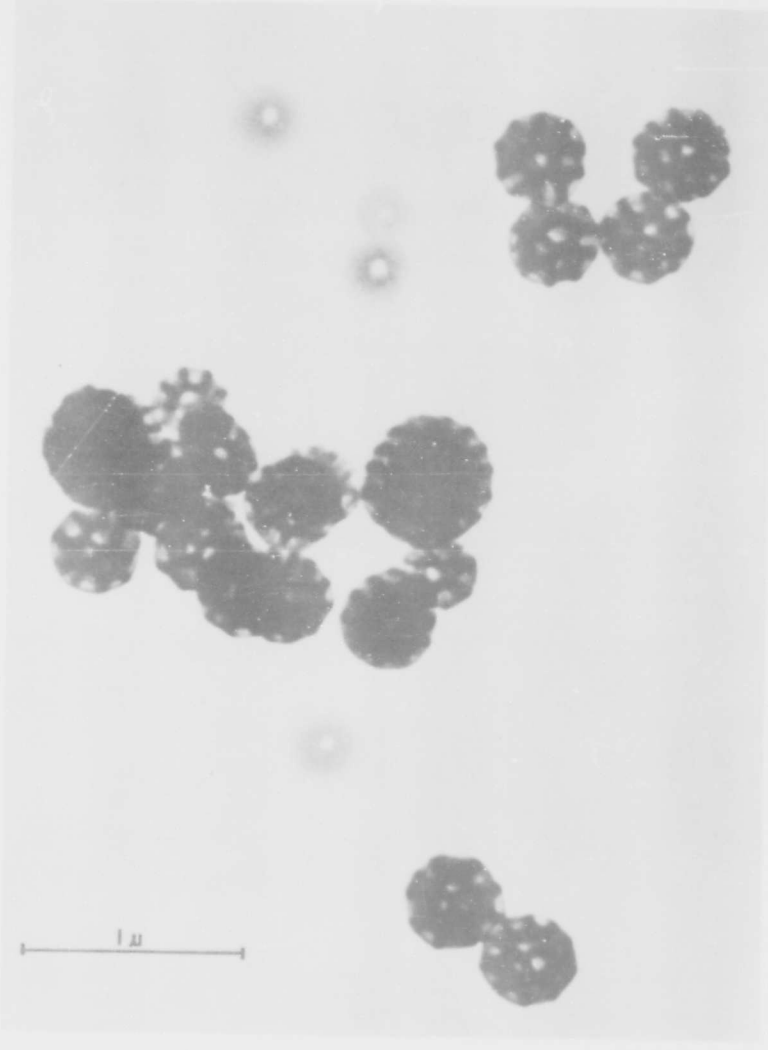

Fig. 3.6—Electronmicrograph of airborne particles collected by cascade impactor.

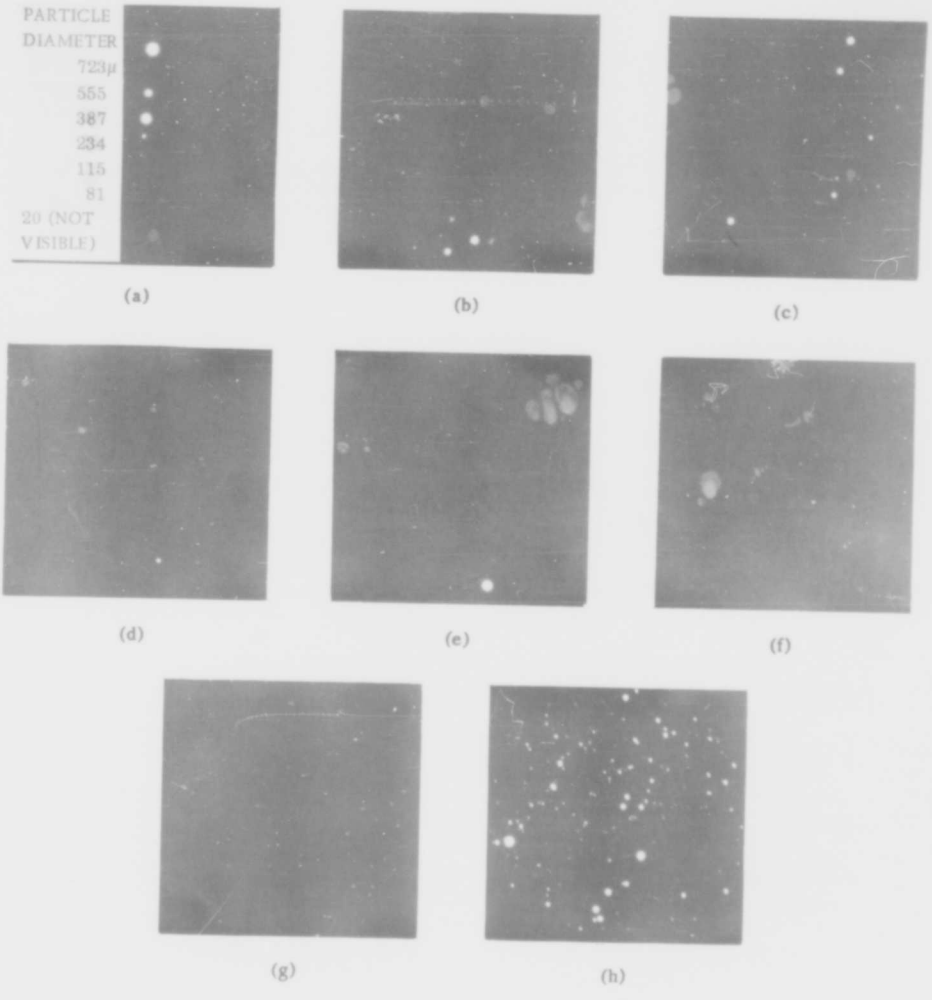

Fig. 3.7—Autoradiographs indicating relative radioactivity per particle as a function of particle size. (Exposure at D + 75 days; radioactivities corrected to H + 12 hr.) Individual particles described in Fig. 3.5 are shown in a; b through h show selected soil samples. (a) Relative activity per particle; 5-min exposure. (b) 833 – 350-μ diameter, 76.2 μc; 5-min exposure. (c) 350 – 175-μ diameter, 67.0 μc; 5-min exposure. (d) 175 – 125-μ diameter, 6.6 μc; 5-min exposure. (e) 125 – 88-μ diameter, 0.17 μc; 36-hr exposure. (f) 88 – 44-μ diameter, 0.16 μc; 36-hr exposure. (g) 44 – 5-μ diameter, 0.17 μc; 36-hr exposure. (h) 44 – 0-μ diameter, 1.56 μc; 36-hr exposure.

Data for the relation of activity per particle to particle size appear in Table 3.13.

Figure 3.8 presents the data of Table 3.13 in graphical form with counts per minute per particle plotted as a function of diameter or range of diameters. The figure indicates that as particle size is decreased, the activity per particle approaches a direct function of the volume of the particle. The divergence of points is probably due to variations in specific activity of particles of the same size.

Table 3.13—RELATION OF ACTIVITY PER PARTICLE TO PARTICLE SIZE

Single-particle diameter, μ	Description	Counts/min on D + 73 days	μc/particle at H + 12 hr
723	Spherical, brown-black, glassy, with a few smaller beads attached	121,000	65.9
555	Spherical, brown-black, glassy	47,000	25.6
387	Spherical, black, glassy	87,000	47.3
234	Spherical, black, glassy	16,000	8.7
115	Spherical, black, glassy	1,750	0.95
81	Spherical, black, glassy	1,080	0.59
20	Spherical, black, glassy	21	0.01

Soil-fraction* diameter range, μ	Total counts/min on D + 73 days	No. of particles	Counts/min per particle	μc/particle at H + 12 hr
350–833	113,000	11	10,273	6.93
175–350	123,000	10	12,300	6.70
125–175	12,100	2	6,050	3.3
88–125	301	1	301	0.17
44–88	262	8	32.7	0.02
5–44	384	87	4.4	0.002
0–44	3,050	312	9.8	0.005

*Fractions do not represent single soil sample.

3.6.3 Distribution of Activity Within a Particle

A fall-out particle was measured microscopically by a sliding micrometer and radio assayed through a 1331 mg/cm^2 aluminum absorber. This particle was then treated with hydrofluoric acid for 90 sec, rinsed in distilled water, reassayed for radioactivity, and measured for size reduction, if any. This procedure was repeated three times. The results are given in Table 3.14.

It is apparent that a large percentage of the activity is on or near the surface of the particle. However, this should be largely dependent upon the type of particle, e.g., glassy, sponge-like, or blister-like.

3.7 RADIATION DECAY RATES AND ENERGY SPECTRA OF FALL-OUT MATERIAL

The investigation of the decay rates and energy spectra of the collected fall-out material was designed to determine:

1. The magnitude of variations in decay and energy characteristics of the bomb products from the published values of mixed fission products.
2. The basic decay and energy relations necessary to perform dosage calculations.
3. The degree of confidence which should be placed in data obtained by various field and laboratory techniques and methods of making such data more compatible.

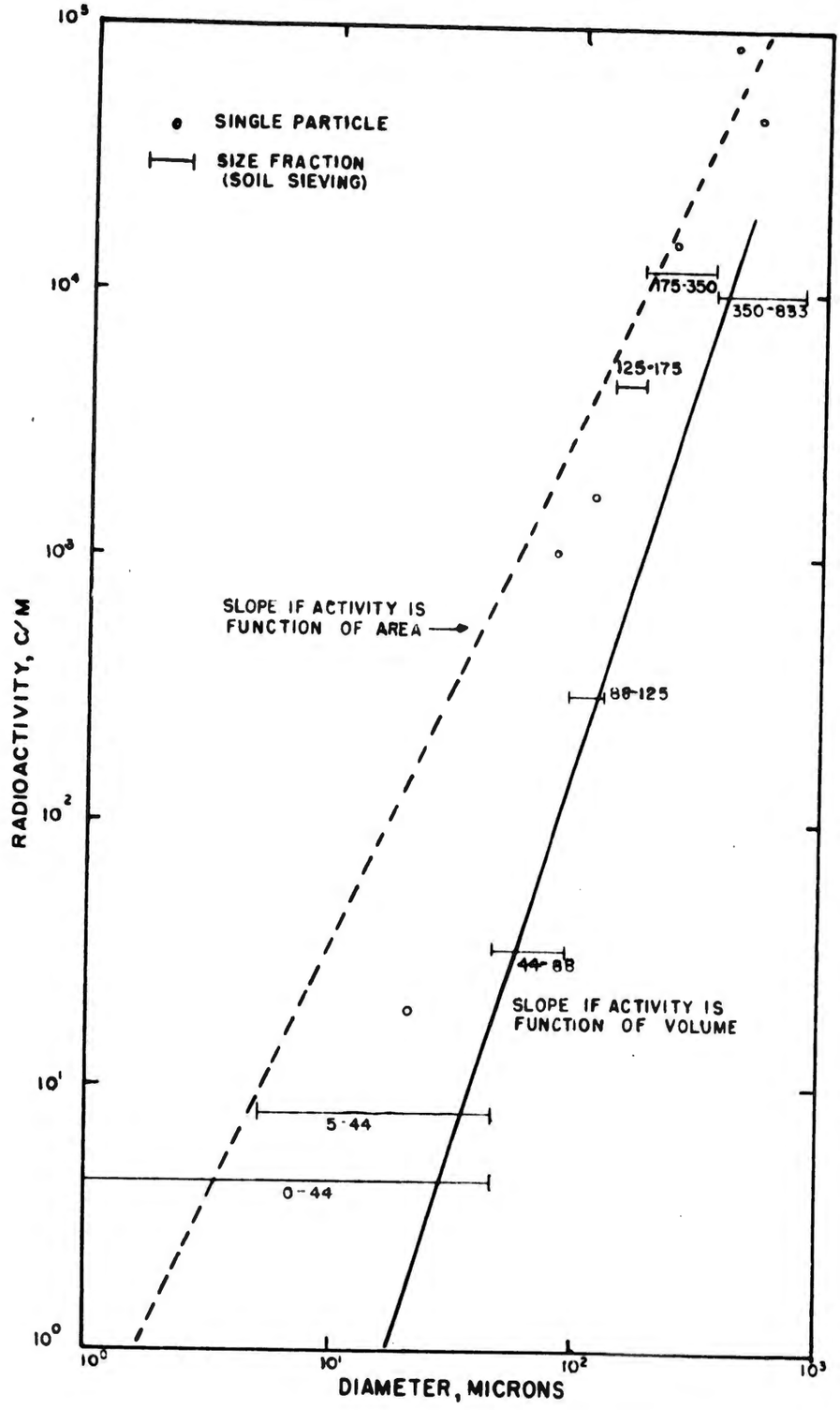

Fig. 3.8—Relation of radioactivity per particle to particle size.

The determinations of decay and energy were limited to the use of routine counting equipment and aluminum and lead absorbers. Consequently quantitative data, including isotope identification, were not obtainable. However, for the purpose of evaluating field-sampling and laboratory techniques, these data were considered acceptable.

Table 3.14—REDUCTION OF SIZE AND RADIOACTIVITY OF ONE PARTICLE FROM SHOT 7 UPON SUCCESSIVE TREATMENTS WITH HYDROFLUORIC ACID

Stage	Diameter of particle, μ	Activity remaining, %	Original volume, %
Before treatment	1101.6	100	100
After first treatment	1086.9	55	96
After second treatment	967.8	24	67
After third treatment	490.0	6.5	8.75

Table 3.15—APPARENT DECAY RATES OF VARIOUS SAMPLES FROM SHOTS 5 AND 7*

Type of sample	Radiation detector	Shot 5		Shot 7	
		No. of samples	Av. decay constant†	No. of samples	Av. decay constant†
Gummed-paper	G-M	3	−1.23	10	−1.20
Soil	G-M	5	−1.38	7	−1.27
Lo-Vol	G-M	0		2	−1.34
Hi-Vol	Proportional	2	−1.71	5	−1.43

*Rate of decay measured between H + 100 and H + 1000 hr.

†Decay constant is k in the equation $A = A_0T^k$. The values are averages derived by normalizing individual decay curves to a common activity at H + 100 hr, averaging the resulting H + 1000-hr activities, and then substituting in the above equation.

3.7.1 Variations in Gross Decay Rates of Field Samples

Table 3.15 summarizes the apparent decay rates of various types of samples from Shots 5 and 7 over a time interval of 100 to 1000 hr following detonation.

As is indicated, a considerable variation in decay rate can be expected among samples radio assayed by different types of detectors, samples from different detonations, and different types of samples from the same detonation. Samples from each group varied within the limits of counting error.

It should be noted that no conclusions as to isotopic differences can be based upon such evidence. Variations in instrument characteristics and in the distribution of activity in or on the samples are sufficient to account for the above variation in decay rates.

3.7.2 Absorption Studies: Variation in Energy Characteristics with Respect to Time

The energy spectra of each of the various types of samples from Operation Upshot-Knothole were studied periodically from the time of collection. The effect of changes in sample self-absorption with time, as indicated by decay curves, is even more pronounced when aluminum-absorption curves are compared. This effect precludes the direct comparison of energy determinations of the several types of samples.

Figure 3.9 compares the aluminum-absorption curves of a gummed-paper sample from Shot 7 at various times following detonation. Decay of activity is indicated by the displacement of the curves. The change in shape of the curves, indicating variation of energy with time, is apparent.

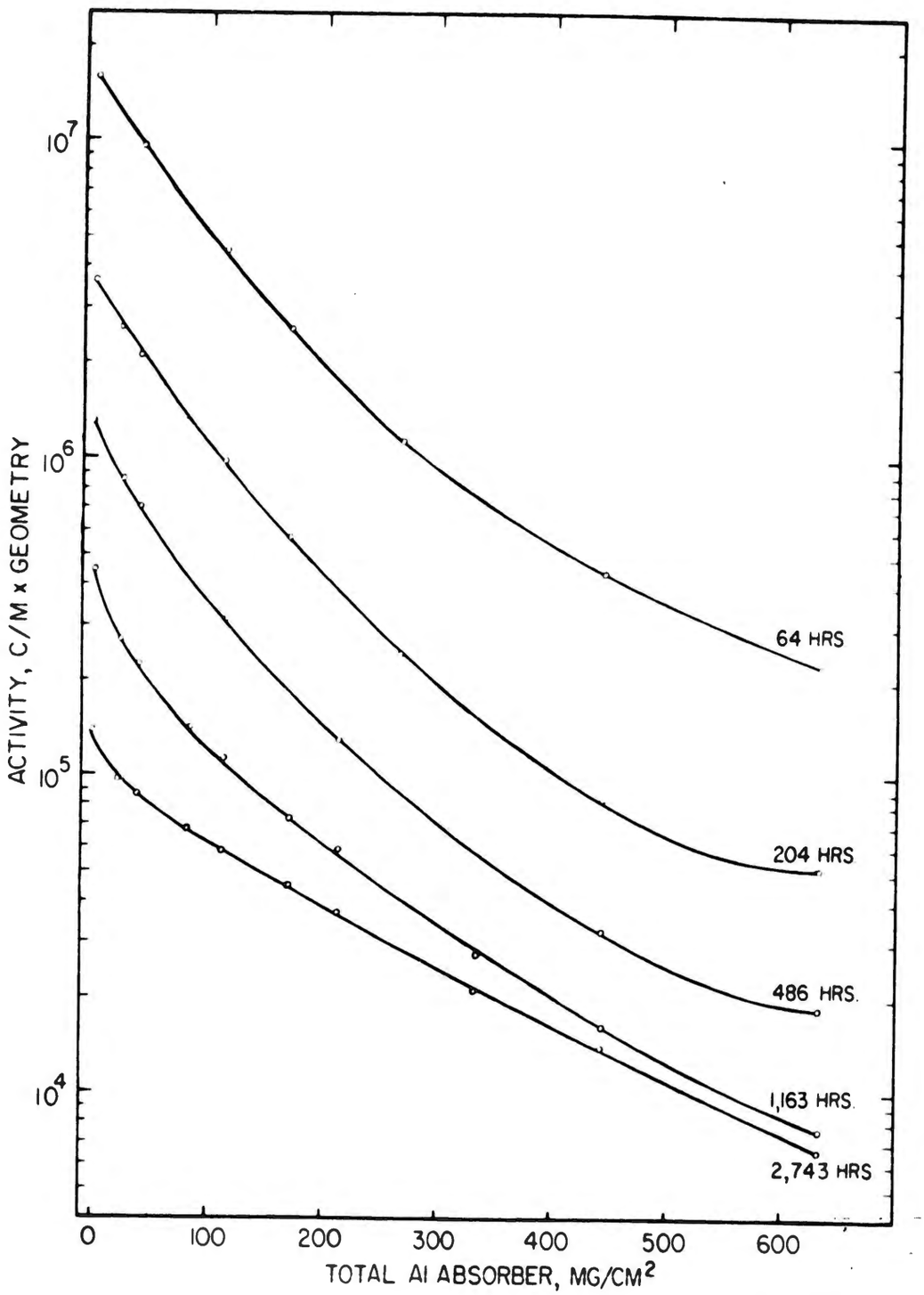

Fig. 3.9—Comparison of aluminum-absorption curves determined from gummed-paper collected samples at times shown following Shot 7.

In order to better illustrate the variation of energy with time, the following approach was employed:

1. The best curve was drawn through the plotted points of each absorption series.
2. At absorber thicknesses of 20, 50, 100, 200, 300, 400, 500, and 600 mg/cm^2, the relative change in count rate per milligram added absorber over an increment of 40 mg/cm^2 was determined. The plot of change in count rate per mg/cm^2 of added absorber vs total absorber indicates the rate of change in absorption as absorber thickness is increased. (Curves so derived are only intended to demonstrate variation in energy with time and not definite energy measurements.)

Table 3.16—EFFECTIVE ENERGY OF BETA EMITTERS*

Decay period, H + hr	Energy components	Half thickness, mg/cm^2	Maximum energy, Mev	Contribution, %	Effective energy of composite sample, Mev
5	A	187	2.8	51.2	0.594
	B	38	1.15	26.4	
	C	4	0.21	24.3	
				Total 101.9	
64	A	106	2.0	33.5	0.462
	B	43	1.16	61.8	
	C	Could not resolve third component			
				Total 95.3	
204	A	96	1.9	28.4	0.440
	B	49	1.29	60.5	
	C	Could not resolve third component			
				Total 88.9	
486	A	96	1.9	30.4	0.406
	B	43	1.16	48.0	
	C	8	0.35	24.0	
				Total 102.4	
1163	A	109	2.05	39.6	0.414
	B	30	0.90	36.8	
	C	8	0.35	26.5	
				Total 102.9	
2743	A	146	2.40	60.8	0.547
	B	14	0.52	34.9	
	C	Could not resolve third component			
				Total 95.7	

*Gummed-paper samples collected from Shot 7.

A family of curves derived in this manner from the absorption curves presented in Fig. 3.9 appears in Fig. 3.10.

3.7.3 Effective Energy of Beta Radiation

The effective energy of a beta emitter is necessary for dosage calculations and experiments. Table 3.16 presents the results of resolution of the aluminum-absorption curves into straight-line components by which the effective energy was determined. The effective energy was approximated as being one-third the maximum energy.[3]

Standard graphical techniques and published relations between half thickness and energy were used.[4] Resolution by this method has two readily apparent sources of error. First, the

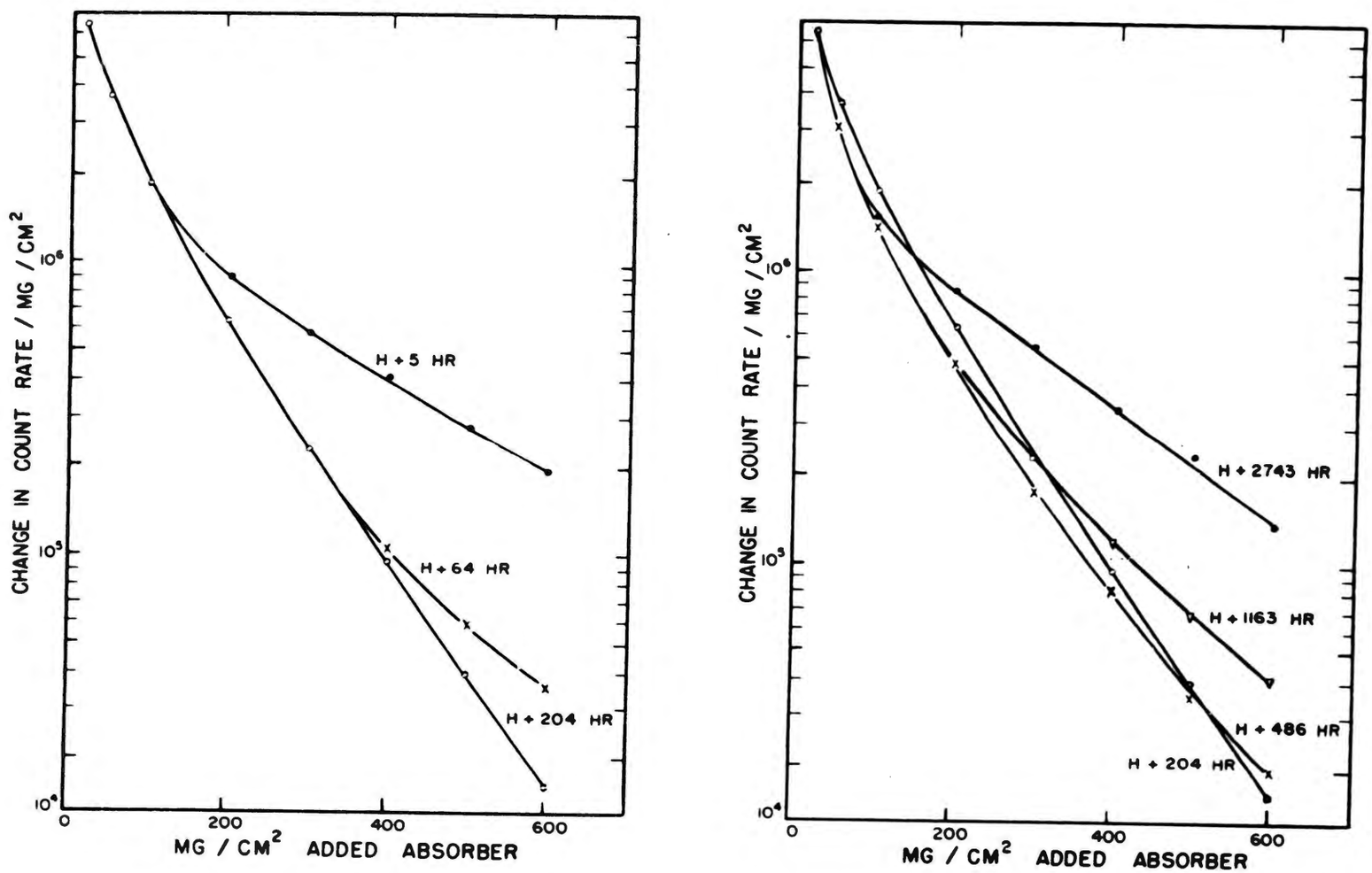

Fig. 3.10—Illustration of beta-energy variation with time, determined from gummed-paper collected samples, Shot 7.

method depends upon successive subtraction with the result that errors are compounded. Second, in the extrapolation to zero absorber, where the minimum irreducible absorber (due to the sample, window, and air thickness) is approximately 7 mg/cm^2, it is possible to lose a considerable portion of the beta spectra of the low energy emitters.

REFERENCES

1. J. H. Olafson et al., Preliminary Study of Off-site Airborne Radioactive Materials, Nevada Proving Grounds. I. Fall-out Originating from Snapper 6, 7, and 8 at Distances of 10 to 50 Miles from Ground Zero, AEP-UCLA Report UCLA-243, February 1953.
2. J. H. Olafson et al., Preliminary Study of Off-site Airborne Radioactive Materials, Nevada Proving Grounds. I. Fall-out Originating from Snapper 6, 7, and 8 at Distances of 10 to 50 Miles from Ground Zero, AEP-UCLA Report UCLA-243, February 1953, p. 52.
3. W. E. Siri, "Isotopic Tracers and Nuclear Radiations," p. 417, McGraw-Hill Book Company, Inc., New York, 1949.
4. C. D. Coryell and N. Sugarman, "Radiochemical Studies: The Fission Products," National Nuclear Energy Series, Division IV, Volume 9, Book 1, p. 18, McGraw-Hill Book Company, Inc., New York, 1951.

CHAPTER 4

DISCUSSION AND ANALYSIS OF RESULTS

4.1 INTEGRATED DOSAGE IN PRIMARY FALL-OUT AREAS

The biological significance of the integrated dosage values determined in primary fall-out areas must be evaluated in light of the following terms:

1. The total dose and the time interval over which the dose is received.
2. The type of radiation.
3. The effective energy of the radiation and its variation with time.

Shots 2, 5, and 7, each of which was a tower shot larger than a nominal bomb, resulted in widespread distribution of moderate to high-level primary fall-out activity and correspondingly high dose rates. Shots 3 and 4 because of their small size and height of detonation, respectively, resulted in relatively low, although not insignificant, concentrations of fall-out activity and negligible dose rates (see Secs. 3.1 to 3.5).

4.1.1 Gamma Radiation

The calculated total body exposure within the areas contaminated by Shots 2, 5, and 7 are presented by means of an isodose plot in Fig. 4.1. The isodose lines describe the areas within which infinite integrated gamma doses greater than 1, 5, 25, and 125 r were received. The gamma dose rate at each location, as determined by field monitoring, was integrated over the time interval of measured or estimated fall-out time to infinity. The accepted decay characteristic of mixed fission products was assumed.

Shot 2, which was detonated under conditions of considerable wind shear, resulted in a wide fall-out pattern within which the maximum infinite isodose line of 25 r extended approximately 20 miles from Ground Zero. Shots 5 and 7, detonated under conditions of little shear, resulted in narrow fall-out patterns within which the maximum infinite isodose lines of 125 r extended approximately 22 miles from Ground Zero, and the 25 r isodose lines extended 55 and 65 miles, respectively, from Ground Zero.

Since the integrated dosage is a function of fall-out time, the region between Ground Zero and the operational area of Project 27.1 would be expected to have received correspondingly greater doses. However, no field measurements were made because of the inaccessibility of this region, and no attempt was made to extrapolate isodose lines toward Ground Zero, owing to the large errors which would result from slight errors in fall-out time estimation. The occurrence of a "skip" distance within this region is also a possibility.

Within the areas described by the integrated infinite isodose lines, the fraction of the infinite dose which would be received during a shorter time interval is likewise dependent upon the fall-out time. Table 4.1 gives the time intervals during which given percentages of the integrated infinite dose would be received, as influenced by the time of fall-out. (See Figs. 3.1, 3.2, and 3.3 for Shots 2, 5, and 7 fall-out times along arcs crossing the respective fall-out paths.)

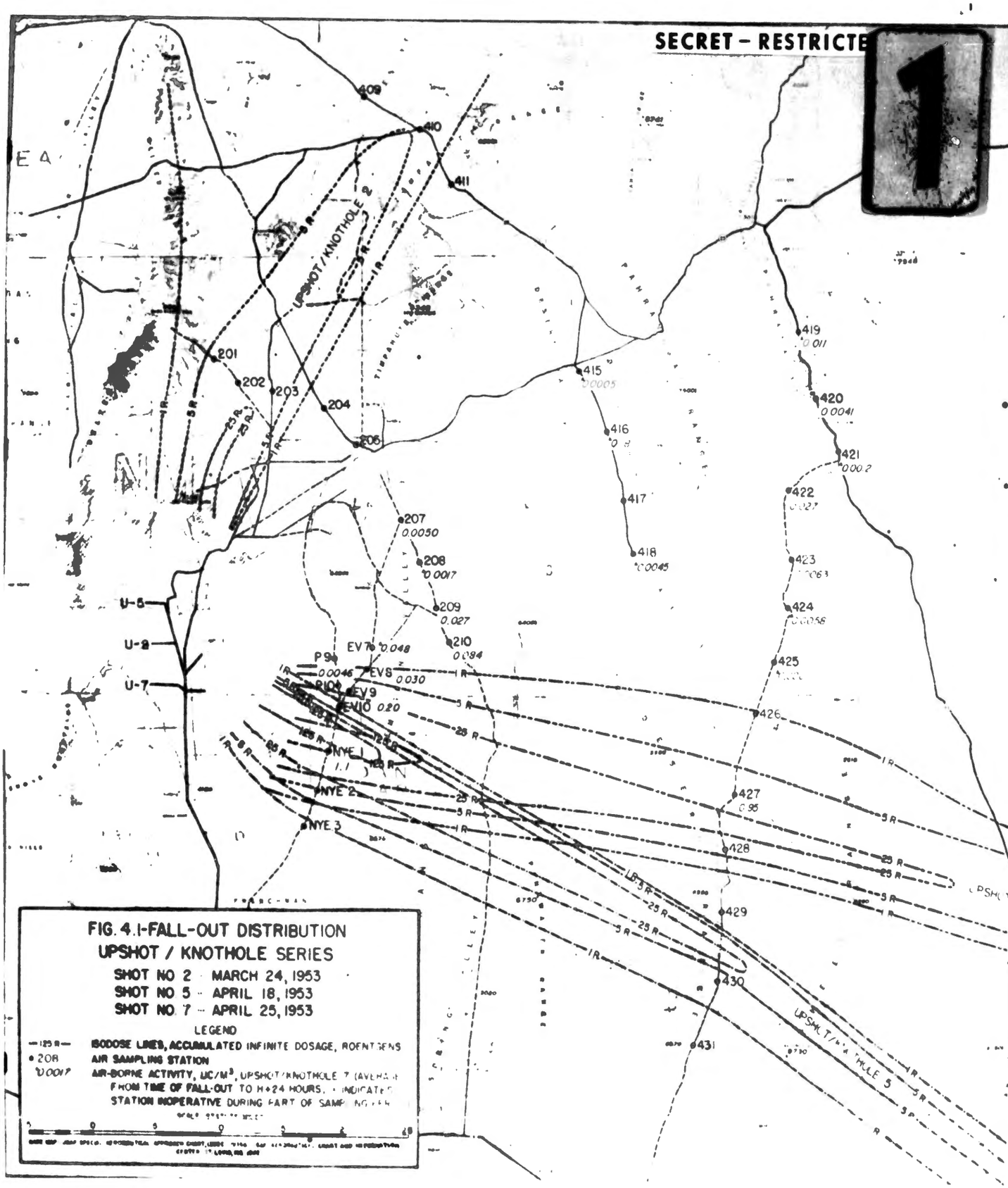

Fig. 4.1—Fall-out distribution for Shots 2, 5, and 7. Isodose lines show accumulated infinite dosage in roentg
▲, airborne activity, μc/m³, Shot 7 (average from time of fall-out to H + 24 hr); ●, station inoperat

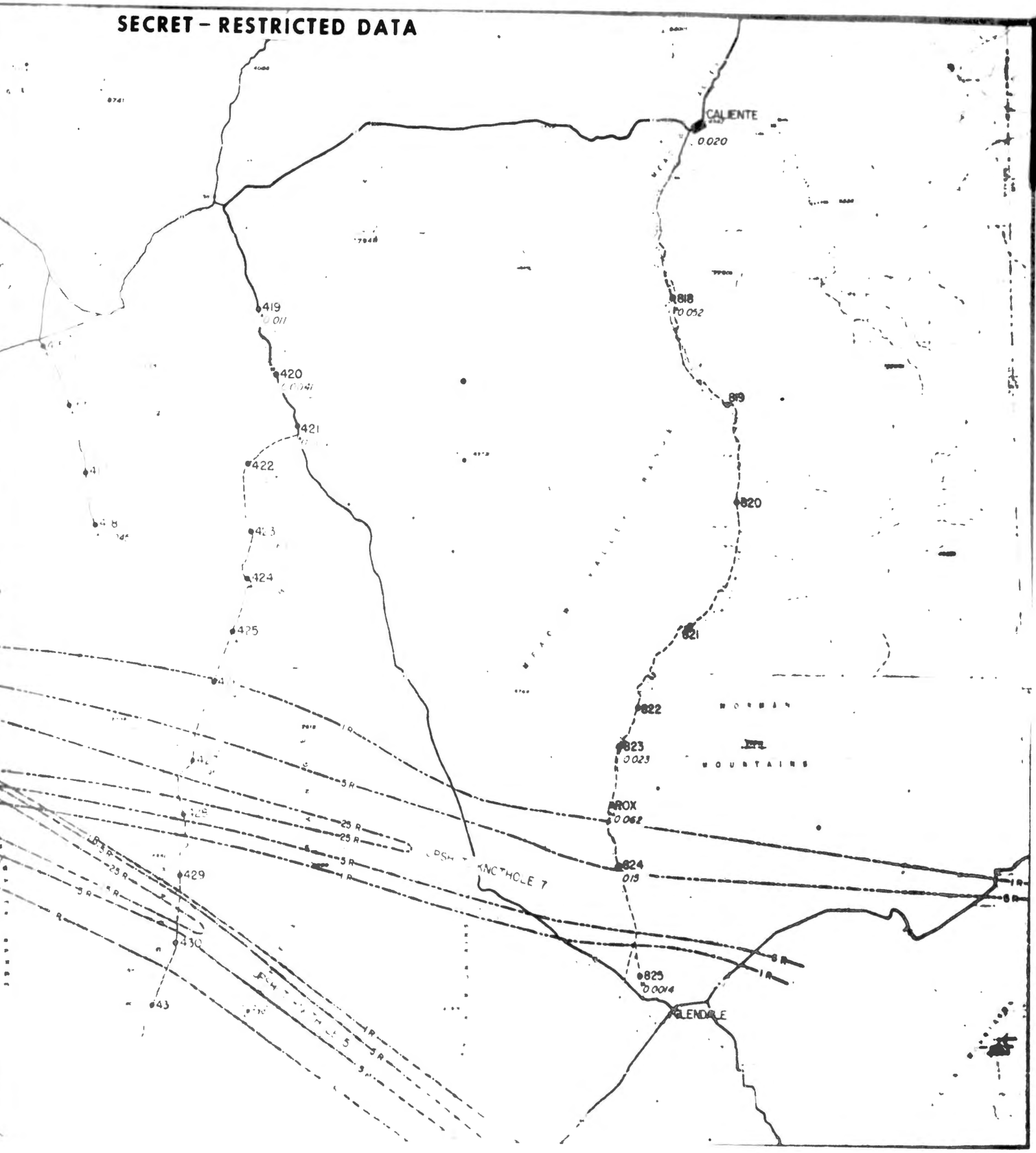

2

ts 2, 5, and 7. Isodose lines show accumulated infinite dosage in roentgens. Station 208 is an air-sampling station.
, Shot 7 (average from time of fall-out to H + 24 hr); ●, station inoperative during part of sampling period.

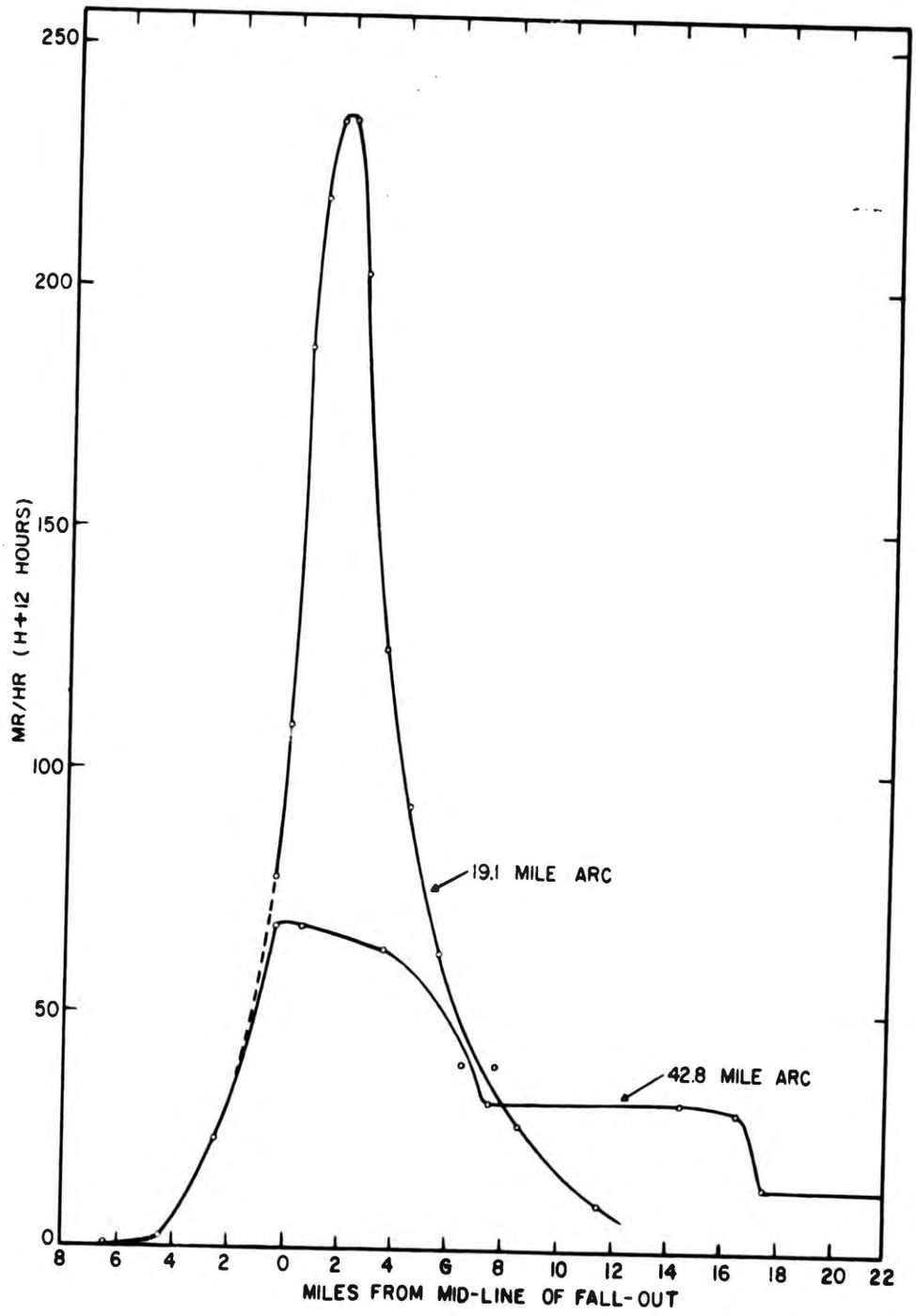

Fig. 4.2—Lateral distribution of residual fall-out, Shot 2, along two arcs.

4.1.2 Beta Radiation

The rem dose due to the beta components of the fall-out material was approximately three times that due to the gamma components. This ratio was determined by film badges suspended 3 ft above the surface and would be expected to increase manyfold as the distance from the source is decreased. Measurement of the beta-gamma and the gamma dose rates from collected air samples and gummed papers, at approximately 50 per cent geometry, indicates that the ratio may range from 50:1 to 500:1. (See Sec. 3.5.1.)

The effective beta energy of the bomb-product material was experimentally determined to vary from 0.4 to 0.6 Mev during the time interval studied, which was 5 to 2743 hr after detonation (Sec. 3.7.3). By use of the observed values of effective energy and the assumption of geometry conditions, the beta dose may be calculated.

Table 4.1—INFLUENCE OF FALL-OUT TIME ON INTEGRATED DOSE

Fall-out time, H+hr after detonation	Approximate time required to receive indicated percentage of infinite dose, hr			
	10%	20%	50%	75%
0.5	0.35	1.0	15.5	500
1	0.7	2.0	31	1000
2	1.4	4.0	62	2000
4	2.8	8.0	124	4000

4.2 DISTRIBUTION OF CONTAMINATION IN PRIMARY FALL-OUT AREAS

The residual radioactive material becomes significant as a part of the environmental system in proportion to its availability to the biological cycle. The availability in turn is a function of (1) the concentrations of fall-out material per unit area, (2) the size and other physical and chemical characteristics of the fall-out particle, and (3) the chemical properties of the elements contained in the particle. Measurement of these factors is basic to the estimation of availability, either by direct ingestion by animals or by selective uptake by plants.

4.2.1 Distance Relations

The relation between residual fall-out material and distance from Ground Zero is illustrated in Figs. 4.2 to 4.4, which present the mr/hr readings (corrected to H+12 hr) for Shots 2, 5, and 7 plotted with respect to location along those roads which crossed the fall-out paths and approximated arcs about Ground Zero.

Integration of the area beneath each curve by means of a polar planimeter results in a measure of the total fall-out activity deposited along each arc, the resulting unit being mr/hr × miles. Since the dose rate will be proportional to the contamination per unit area, mr/hr × miles is equivalent to

$$\frac{\text{Activity} \times \text{distance}}{\text{Distance}^2}$$

or activity per unit distance.

From the curves and the integrated areas it is evident that, as the distance from Ground Zero is increased, the activity deposited per unit distance consistently decreases.

Table 4.2, which was derived from data presented in Figs. 4.2 to 4.4, presents the ratios of average mr/hr : maximum mr/hr occurring along the several arcs about Ground Zero for Shots 2, 5, and 7. A consistent relation is indicated; with but two exceptions the ratio of average mr/hr : maximum mr/hr closely approximates 1 : 3.

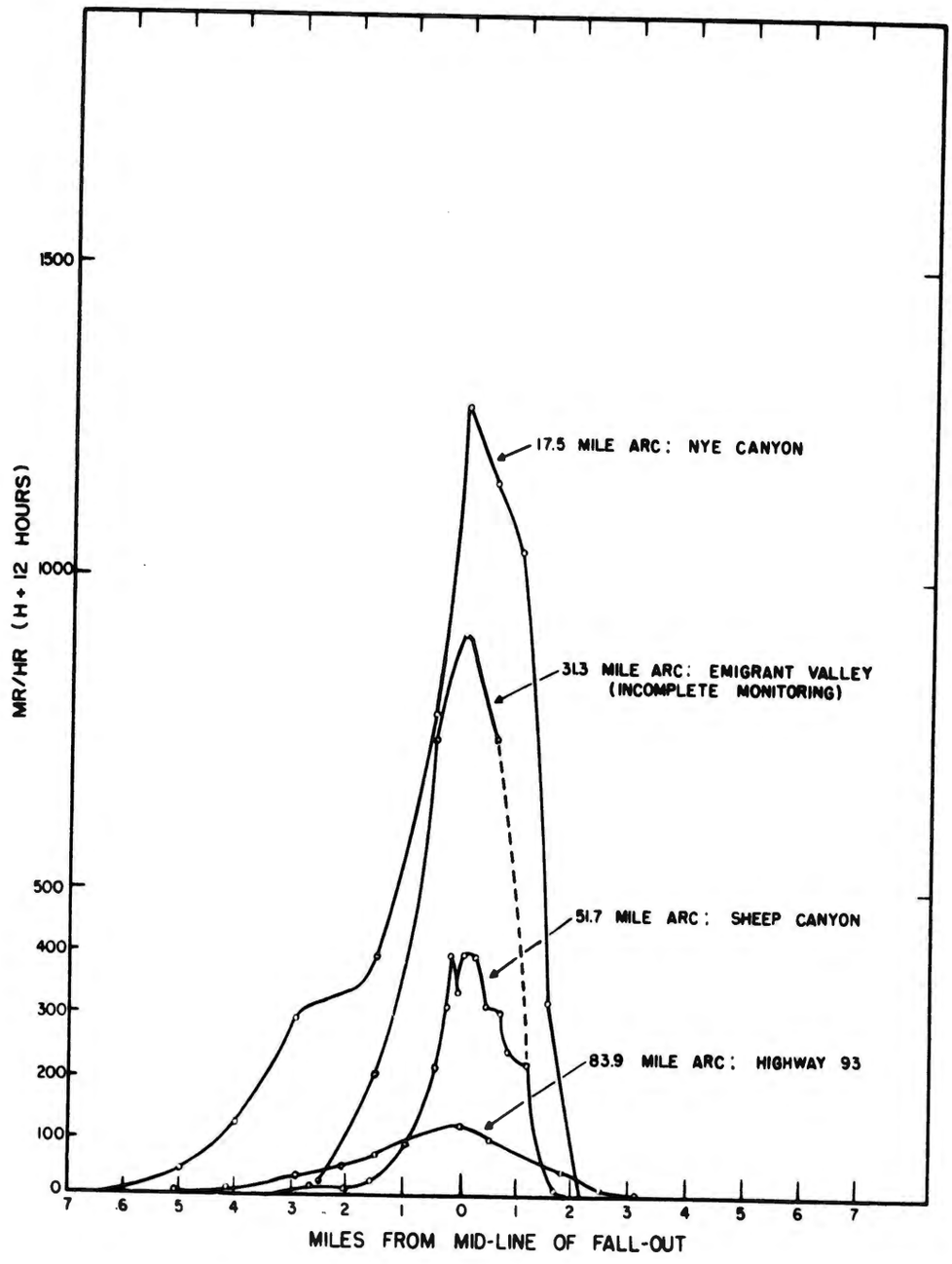

Fig. 4.3—Lateral distribution of residual fall-out, Shot 5, along four arcs.

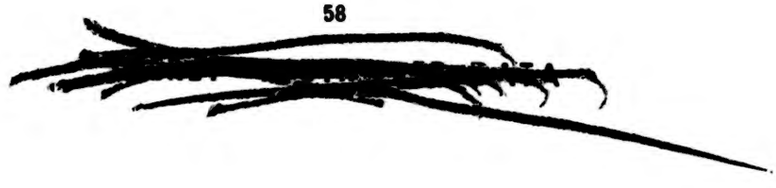

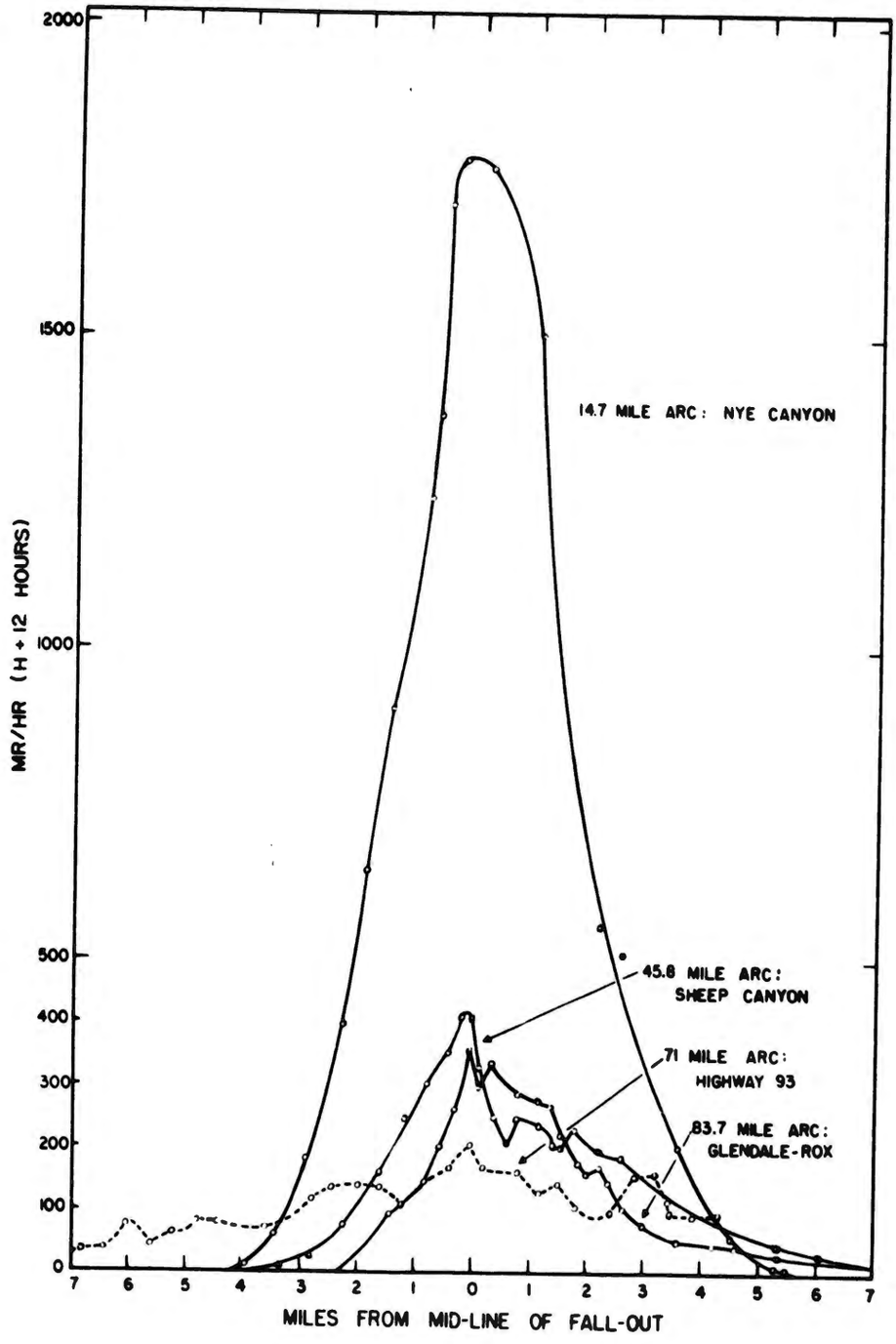

Fig. 4.4—Lateral distribution of residual fall-out, Shot 7, along four arcs.

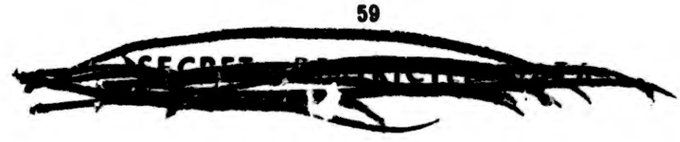

The ratio of 1:3 suggests that fall-out material is dispersed laterally according to a standard distribution curve which is skewed according to the effects of prevailing winds and local terrain.

Table 4.2—RATIO OF AVERAGE TO MAXIMUM MR/HR VALUES ALONG ARCS CROSSING THE FALL-OUT PATTERNS OF SHOTS 2, 5, AND 7

Distance to arc, mi*	Width of fall-out, road mi	Total activity,† mr/hr × mi	Calculated average mr/hr along arc	Maximum mr/hr detected	Ratio average : maximum mr/hr
		Shot 2			
19.1	15‡	1200	80.0	234	1:2.93
42.8§	32‡	930	29.1	68	1:2.34
		Shot 5			
17.5	8.8	3410	440	1280	1:2.91
31.3	5‡	1350	272	910	1:3.35
51.7	5.5	680	124	407	1:3.29
83.9	8.8	400	45.5	128	1:2.81
		Shot 7			
14.7	10.7	6390	597	1780	1:2.96
45.8	12.0	1510	125	410	1:3.28
71§	15.3	1220	79.7	205	1:2.57
83.7	10.9	1080	99	352	1:3.55

*Distance from Ground Zero to point along arc receiving maximum fall-out.
†Derived from Figs. 4.2 to 4.4.
‡Complete width of arc not determined.
§Roads monitored do not approximate arcs as closely as desired.

Table 4.3—LOCAL VARIATION IN FALL-OUT DISTRIBUTION, SHOT 7

Station	Residual mr/hr*	No. of samples	Mean activity,* $\mu c/ft^2$	Standard deviation	Coefficient of variation, %
423	1.33	12	19.52	4.45	22.8
EV-7	2.52	12	34.49	4.97	14.4
427	169	12	3373	237	7.03

*Corrected to H + 12 hr.

In order to determine the magnitude of the local variation in distribution of fall-out activity to be expected at any given location, six pairs of fall-out trays were mounted within an area of 12 ft^2 at three sampling locations. The individual papers were collected and radio-assayed, and the data were summarized as a group per location. Table 4.3 presents the statistical variations of the samples collected.

Although the trays were mounted in areas receiving relatively high levels of contamination, a trend toward greater variation with decrease in concentration is indicated. Such a trend is to be expected in so far as the activity level reflects, in part, the number of contributing particles.

4.2.2 Activity per Unit Area Relations

It was originally intended to base measurements of activity per unit area primarily upon gummed-paper collections. However, placement of gummed papers generally yielded fringe area sampling (as indicated in Chap. 3), necessitating the use of soil samples as the primary source of activity per unit area measurements as well as particle-size distributions.

In general, gummed papers yielded slightly higher activity values than corresponding soil samples. This may be attributable to the ability of gummed paper to collect residual material being translocated by local winds after fall-out time, the error being compounded by corresponding losses in soil activity and/or to differences in radio-assay efficiencies evolving from self-absorption corrections for soil samples.

Within the areas receiving the most concentrated primary fall-out measured, maximum concentrations up to and greater than 20,000 $\mu c/ft^2$ (H+12 hr) were detected. In the fringe areas, and in the cases of Shots 3 and 4, activities from 10^{-6} to 10 $\mu c/ft^2$ were recorded.

The relation between mr/hr and activity per unit area, as determined by the comparison of field and laboratory measurements, is presented in Fig. 4.5. It will be noted that the ratio of mr/hr : $\mu c/ft^2$, as determined by gummed-paper sampling (Shot 7), is lower than that by soil sampling, which reflects the activity differences described earlier.

A variation in the ratios associated with Shots 5 and 7 also occurs. This variation may be the result of detonation characteristics or of errors inherent in the extrapolation of soil activities and monitoring data by use of the standard decay formula. As the reason for this deviation is undetermined, the results of the analyses for Shots 5 and 7 have been consolidated. Based upon all values presented, the ratio of mr/hr : $\mu c/ft^2$ approximates 1 : 10.

4.2.3 Particle-size Relations

The examination of particle-size analyses of fall-out from Shots 2, 5, and 7 (Tables 3.1, 3.5, and 3.10) indicates two relations between particle size and distance. The particle size associated with the major portion of the fall-out activity decreases as (1) the distance from Ground Zero along the main line of fall-out increases and (2) the distance from the main line of fall-out along any arc increases.

The first relation is illustrated by Fig. 4.6, which presents activity (cumulative per cent) as a function of mean particle size for three Shot 5 samples collected at different distances from Ground Zero along the midline of fall-out. The median diameter of the radioactive material decreases consistently with distance. The presence of relatively high percentages of total activity in the smaller size fractions at short distances from Ground Zero may be attributed either to the initiation of fall at low elevations or to the entrainment of particles. The possibility of small particles adhering to larger ones or forming large agglomerates, which are broken up by sieving, may also be contributive.

The second relation of decrease in particle size with increasing distance from the midline of fall-out along an arc is more subtle, and the data are not conducive to graphic presentation.

A pronounced size fractionation in fall-out material sampled at adjacent stations near the midline of fall-out is also indicated. This effect is illustrated in Table 4.4, which summarizes a portion of the original Shots 5 and 7 particle-size analysis data obtained from soil samples. Size fractions, containing the majority of activity at adjacent stations, are tabulated in order of decreasing size range. It is evident from Table 4.4 that there is no consistency of fractionation with reference to the midline of fall-out. This phenomenon is probably explainable only by detailed meteorological investigations.

The lack of a uniform particle-size distribution laterally through the fall-out path suggests that considerable error may be inherent in basing the relation between particle-size distribution and distance from Ground Zero upon individual samples from each arc. Consequently, a method of analysis based upon the size distributions along entire arcs was investigated.

The method of analysis, similar to that presented in Sec. 4.2.1 for the determination of total activity per arc, had the following development:

1. Calculation of microcuries associated with each size fraction of the sieved soil samples. (Based upon the relation of 1 mr/hr = 10 $\mu c/ft^2$ rather than the results of corresponding labo-

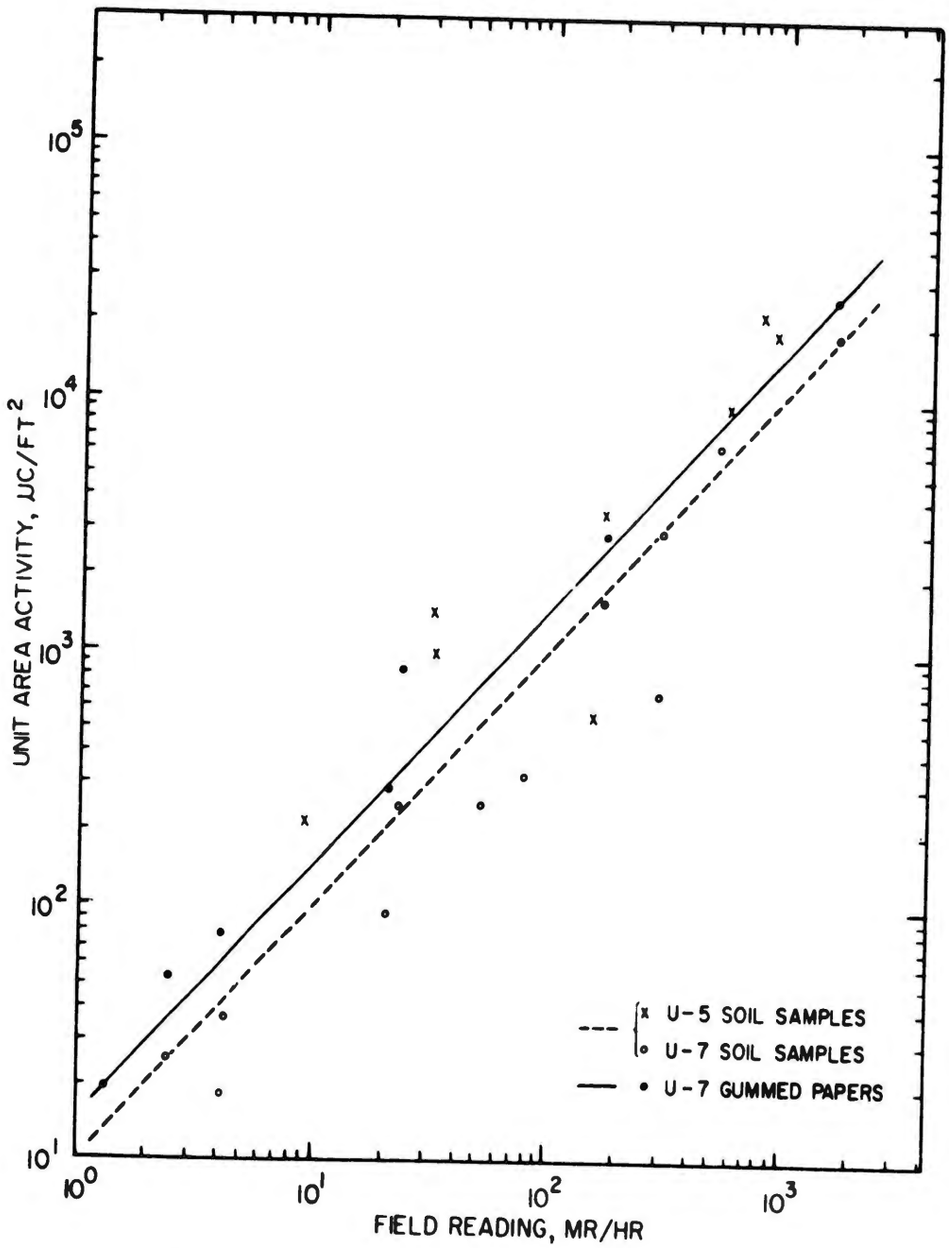

Fig. 4.5—Relation between unit area activity, μc/ft², and field measurements, mr/hr.

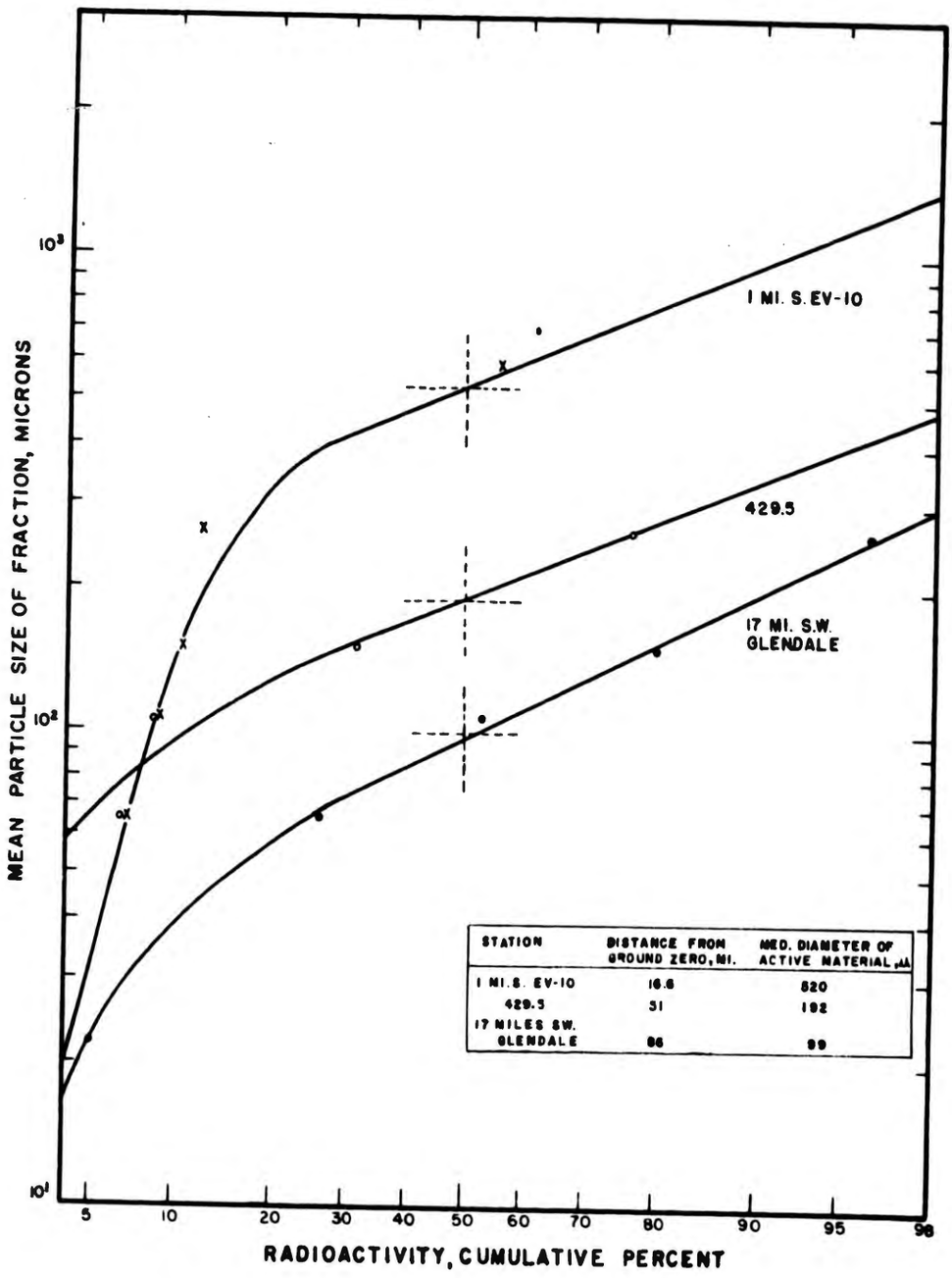

Fig. 4.6—Relation between particle-size distribution and distance from Ground Zero of fall-out, Shot 5. (Based upon individual soil samples collected at stations nearest midline of fall-out at three distances from Ground Zero.)

ratory determinations of activity per unit area. The resulting value should be subject to less sample variation.)

2. Drawing of a smoothed distribution curve through the plotted points of microcuries per fraction vs distance along each arc.

3. Integration of area beneath each size-fraction curve to yield a measure of total activity in each size fraction along the fall-out arcs with the resulting unit being $\mu c/ft^2 \times$ miles.

Soil samples collected from Nye and Sheep Canyons following Shot 5 present a fairly good cross section of the fall-out pattern. The distributions of the microcuries per size fraction of these samples are presented in Figs. 4.7 and 4.8. The indicated area under each curve was determined by means of a polar planimeter.

Table 4.4—SUMMARY OF FRACTIONATION OF PRIMARY FALL-OUT SAMPLES AT STATIONS ADJACENT TO MIDLINE OF FALL-OUT

Approximate distance from Ground Zero, mi	Reference location	Distance between adjacent stations, mi	Size fraction, μ	Total activity, %
		Shot 5		
17	1.4 mi S EV-10*	0.4	833 – 350	86.9
	1.0 mi S EV-10		350 – 175	67.9
52	429.5†	2.5	350 – 125	90.0
	430*		125 – 88	62.8
		Shot 7		
15	EV-10	2.0	833 – 350	90.3
	Nye 1*		350 – 175	85.2
46	427	2.5	350 – 175	52.5
	427.5*		175 – 125	58.6
81	824*	5.0	175 – 125	64.7
	ROX		88 – 5	81.5

*Station nearest midline of fall-out.

†Stations 429.5 and 430 were on either side of midline of fall-out.

Table 4.5 gives the resulting particle-size distributions of the total radioactive material deposited along the two arcs in terms of total activity per size fraction and per cent activity per size fraction.

Figure 4.9 presents log-probability plots of activity, as cumulative per cent, vs mean particle size for the two arcs. The two curves closely approximate straight lines, which indicate skewed probability distributions. The effect of distance upon the total particle distributions is evident; the median diameter of the radioactive material at a distance of approximately 17 miles from Ground Zero is 450 μ, while at a distance of approximately 51 miles it is 225 μ.

The ratio of the gross activities of both arcs, as determined by the above method (26,120/5230 = 4.99), is approximately the same as the ratio of the integrated mr/hr distributions for the same arcs as plotted in Fig. 4.3 (3410/680 = 5.01). This comparison checks the accuracy of the method.

Since the reliability of the method depends upon the number of soil samples collected along each arc, the results presented indicate the development of a valuable method for the determination of total particle-size distributions and the function of particle size in the mechanics of fall-out.

The activity per particle has been found to approximate a function of particle volume for particles less than 150 μ and of surface area for particles larger than 150 μ (Sec. 3.6.2). Using

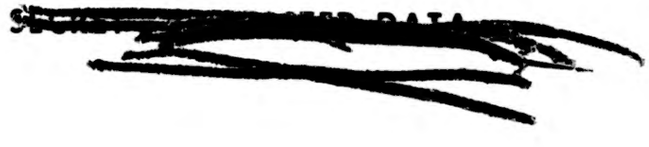

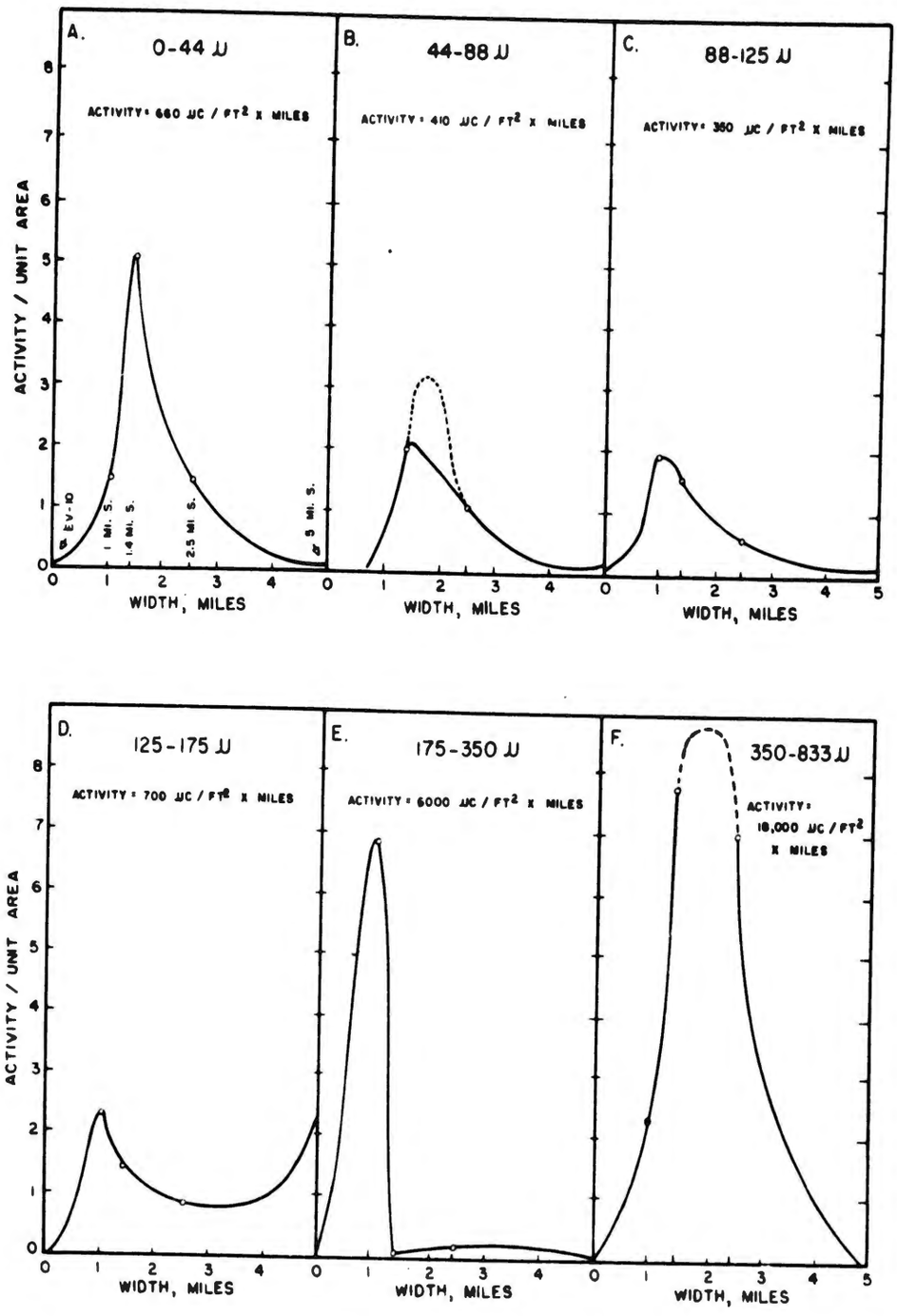

Fig. 4.7—Distribution of fall-out from Shot 5 with respect to particle size along 17-mile arc. Scale: for a through d, 1 cm^2 = 100 $\mu c/ft^2$ x miles; for e and f, 1 cm^2 = 1000 $\mu c/ft^2$ x miles. (Soil samples are from Stations EV-10 and 1, 1.4, 2.5, and 5 miles south of EV-10.)

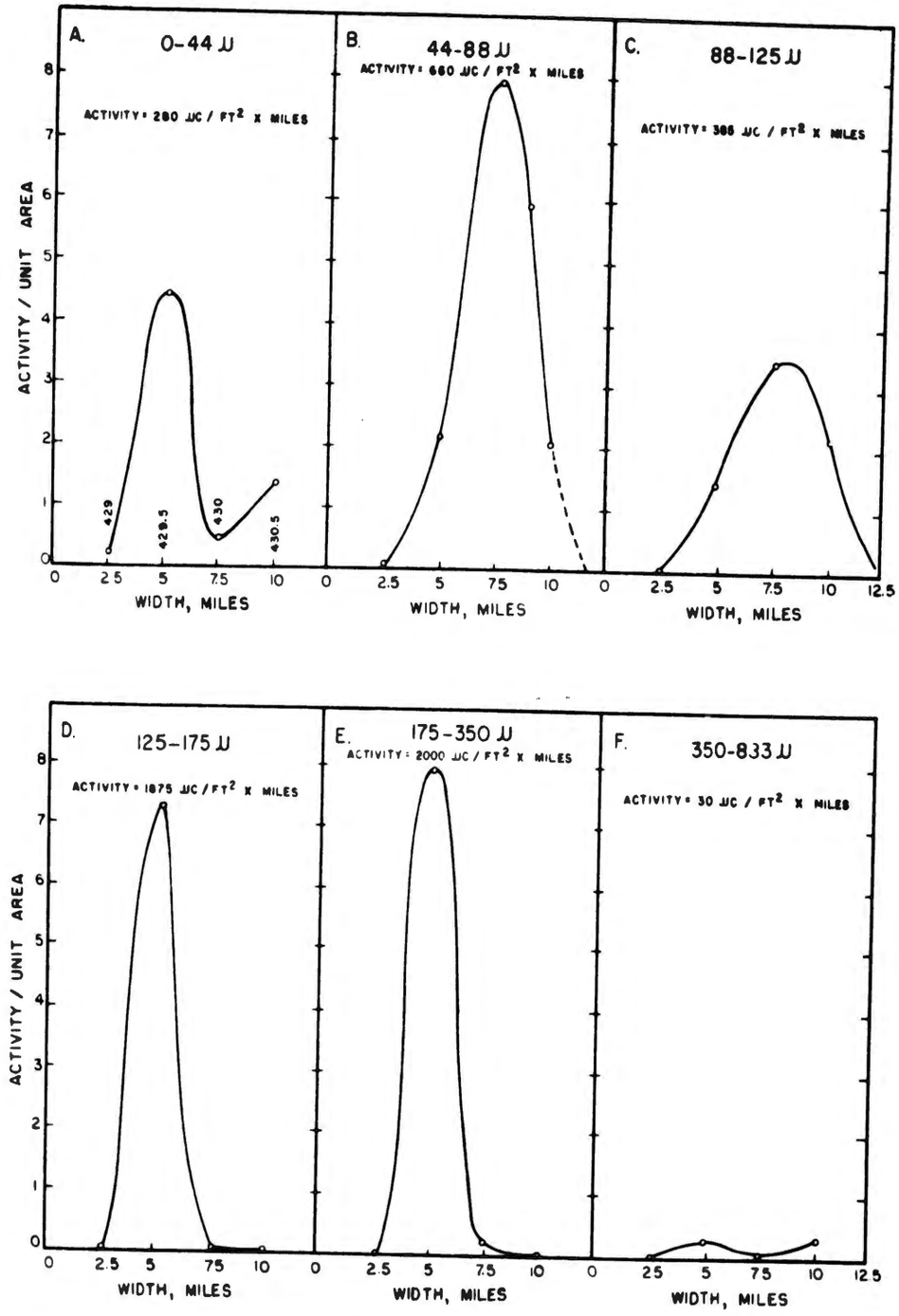

Fig. 4.8—Distribution of fall-out from Shot 5 with respect to particle size along 51-mile arc. Scale: for a through c and f, 1 cm^2 = 50 $\mu c/ft^2$ x miles; d and e, 1 cm^2 = 250 $\mu c/ft^2$ x miles. (Soil samples are from Stations 429, 429.5, 430, and 430.5.)

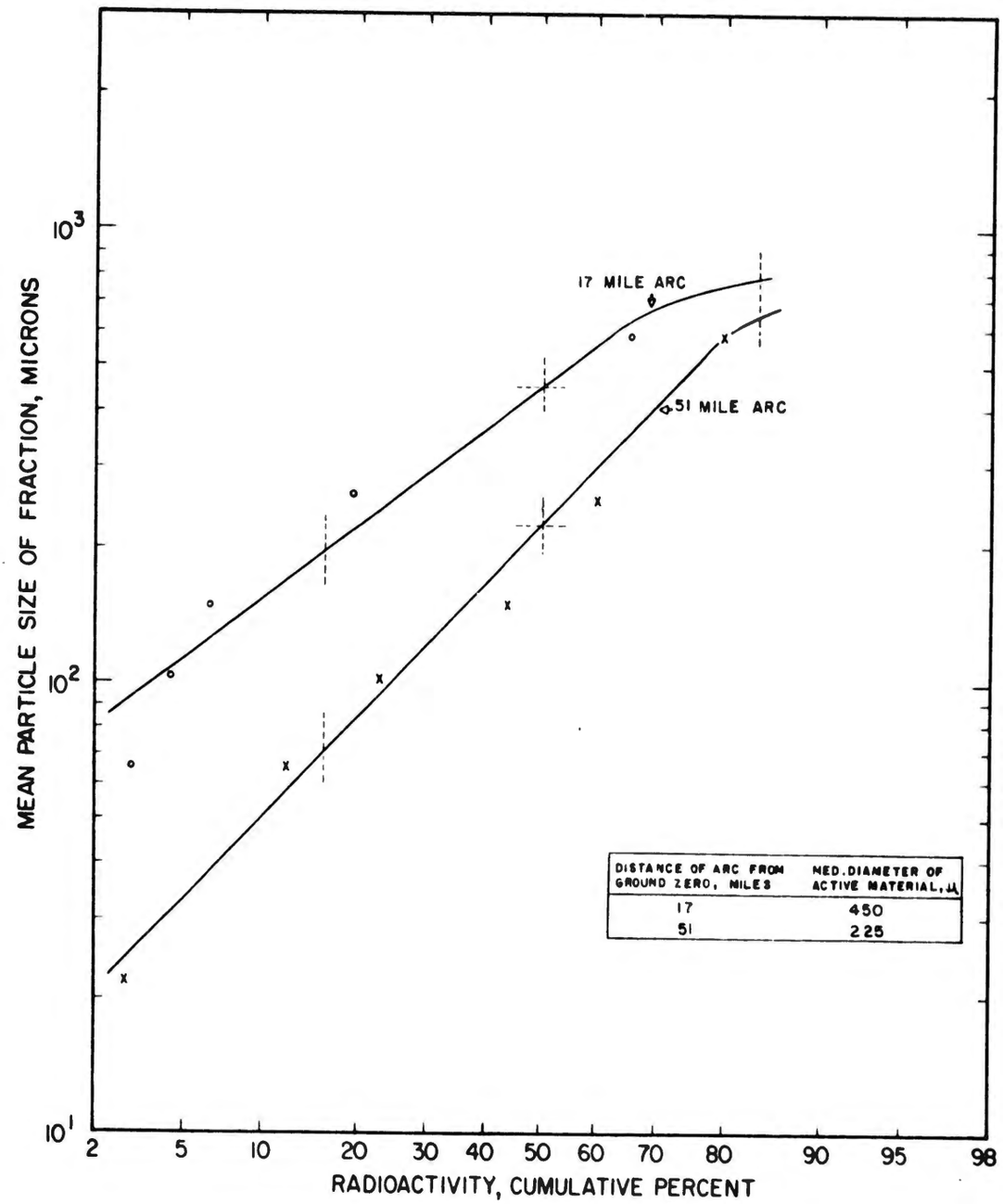

Fig. 4.9—Relation between particle-size distribution and distance from Ground Zero, Shot 5, based on total material distributed along two arcs.

Table 4.5—PARTICLE-SIZE DISTRIBUTION OF TOTAL MATERIAL DEPOSITED ALONG TWO ARCS CROSSING SHOT 5 FALL-OUT PATH

Particle-size range, μ	Nye Canyon stations (~17 mi from Ground Zero) Total activity, μc/ft² × mi	Total, %	Sheep Canyon stations (~51 mi from Ground Zero) Total activity, μc/ft² × mi	Total, %
833 – 350	18,000	68.9	30	0.6
350 – 175	6,000	23.0	2000	38.2
175 – 125	700	2.7	1875	35.8
125 – 88	350	1.3	385	7.4
88 – 44	410	1.6	660	12.6
44 – 0	660	2.5	280	5.4
Total	26,120	100.0	5230	100.0

Table 4.6—RELATIVE NUMBER OF FALL-OUT PARTICLES PER SIZE FRACTION NECESSARY TO YIELD A GIVEN UNIT ACTIVITY*

Size range, μ	Assumed numerical median diameter, μ	Activity/particle as function of diameter†	Relative number of particles to yield unit activity
833 – 350	600	$\left(\frac{150}{600}\right)^2$	6.25
350 – 175	263	$\left(\frac{150}{263}\right)^2$	32.5
175 – 125	150	$\left(\frac{150}{150}\right)^2$	100
125 – 88	106	$\left(\frac{150}{106}\right)^3$	282
88 – 44	66	$\left(\frac{150}{66}\right)^3$	1,165
44 – 5	25	$\left(\frac{150}{25}\right)^3$	21,600
5 – 0	2.5	$\left(\frac{150}{2.5}\right)^3$	21,600,000

*One hundred 125- to 175-μ fraction particles yield unit activity.

†Exponent indicates relation between activity per particle and particle size; area function: exponent = 2; volume function: exponent = 3.

these relations, the relative numbers of particles of each size fraction necessary to yield a given activity may be calculated as shown in Table 4.6.

The data presented in Table 4.6, in conjunction with the particle-size distribution studies, suggest that two phenomena due to particle size may be expected:

1. The numerical size distribution of the total fall-out material is probably of the hyperbolic type, i.e., the number of particles increases with decreasing size until the particles reach the dimensions of molecules or atoms. This is indicated by the large numbers of small particles required to yield a given activity and the significant percentage contribution of the small fractions.

2. Since the activity is directly proportional to the surface area of particles greater than approximately 150 μ, the total area associated with the number of particles required to yield unit activity would be independent of particle diameter. However, since the activity of particles less than 150 μ in diameter is more nearly proportional to the volume, the total area per unit

activity would be inversely proportional to the diameter. Therefore the rate of solubility of the radioactive components, which should be a function of the surface area, would be independent of diameter for large particles and would increase as the diameter decreases for smaller particles. These speculations suggest that airborne material and fall-out which settle out at great distances would be more soluble than the material considered in this report.

4.3 AIRBORNE RADIOACTIVITY CONCENTRATIONS

The evaluation of the biological significance of airborne radioactivity concentration depends upon three primary considerations. These are (1) the magnitude and persistence of concentrations of radioactive material per unit volume of air; (2) the relative proportion of long-lived fission products; and (3) the size and other physical and chemical characteristics of the airborne particles.

This discussion is confined to the results of Shot 7, owing to the limited success of the air-sampling program on previous detonations. The small number and general low activity of samples collected during the earlier detonations indicate, however, that concentrations were generally lower and less widespread than for Shot 7.

Shot 7 produced a widespread distribution of high levels of airborne radioactive material, as has been indicated in Fig. 4.1, where the averages of the midtime concentrations over the 24-hr period following detonation are shown for each station. The maximum concentration detected for a 2-hr sample period was approximately 10 $\mu c/m^3$. This sample was collected at Station Nye 1, which was 14.5 miles from Ground Zero and near the midline of fall-out. The station receiving the minimum 24-hr average concentration, Station 415, had a maximum concentration of 0.0009 $\mu c/m^3$ over a 2-hr period.

The maximum airborne concentrations decreased with distance from Ground Zero and with distance from the midline of fall-out, as indicated by the airborne concentration data presented in Table 3.12. The maximum concentrations appeared at each station during a later time interval as the lateral distance from the midline increased.

The variations in airborne concentrations with time are further described in Figs. 4.10 to 4.12, in which are shown the concentrations at midtime of sampling, presented as assayed and also corrected to H+12 hr, at two selected stations along each arc. The correction of activity concentrations to a common time permits recognition of movements of radioactive material which might otherwise be obscured by decay.

Both midline and lateral stations were subject to additions of radioactive material subsequent to the original contamination. This occurrence is particularly noticeable in Stations EV-8 and 423, where large increases occurred at a sample midtime of H+19 hr. Presumably local surface-wind movements are responsible for such migrations of radioactive materials.

While the airborne concentrations generally decrease with time, subsequent concentrations of lower magnitude may be of equal or greater biological significance than higher levels collected earlier because of the greater proportion of long-lived fission products.

The lack of precise data with respect to particle-size distributions of airborne material prevents detailed consideration of potential lung deposition and retention. However, from the persistence of airborne concentrations of radioactive material, a low settling rate is indicated, and a high proportion of sub-micron size particles may be assumed.

If the relation between activity per particle and particle size established for fall-out material in Sec. 3.6.2 may be extended to sub-micron size ranges, the radioactivity per particle becomes almost insignificant. However, if the particle is formed by a different method, e.g., by chemical combination of the vaporized fission products without dilution by inert material, much higher activities per particle would be expected. No measurements of activity per particle of airborne material were obtained.

4.4 MECHANICS OF THE DISTRIBUTION OF PRIMARY FALL-OUT

In order to anticipate the nature and extent of the radioactive environments arising from

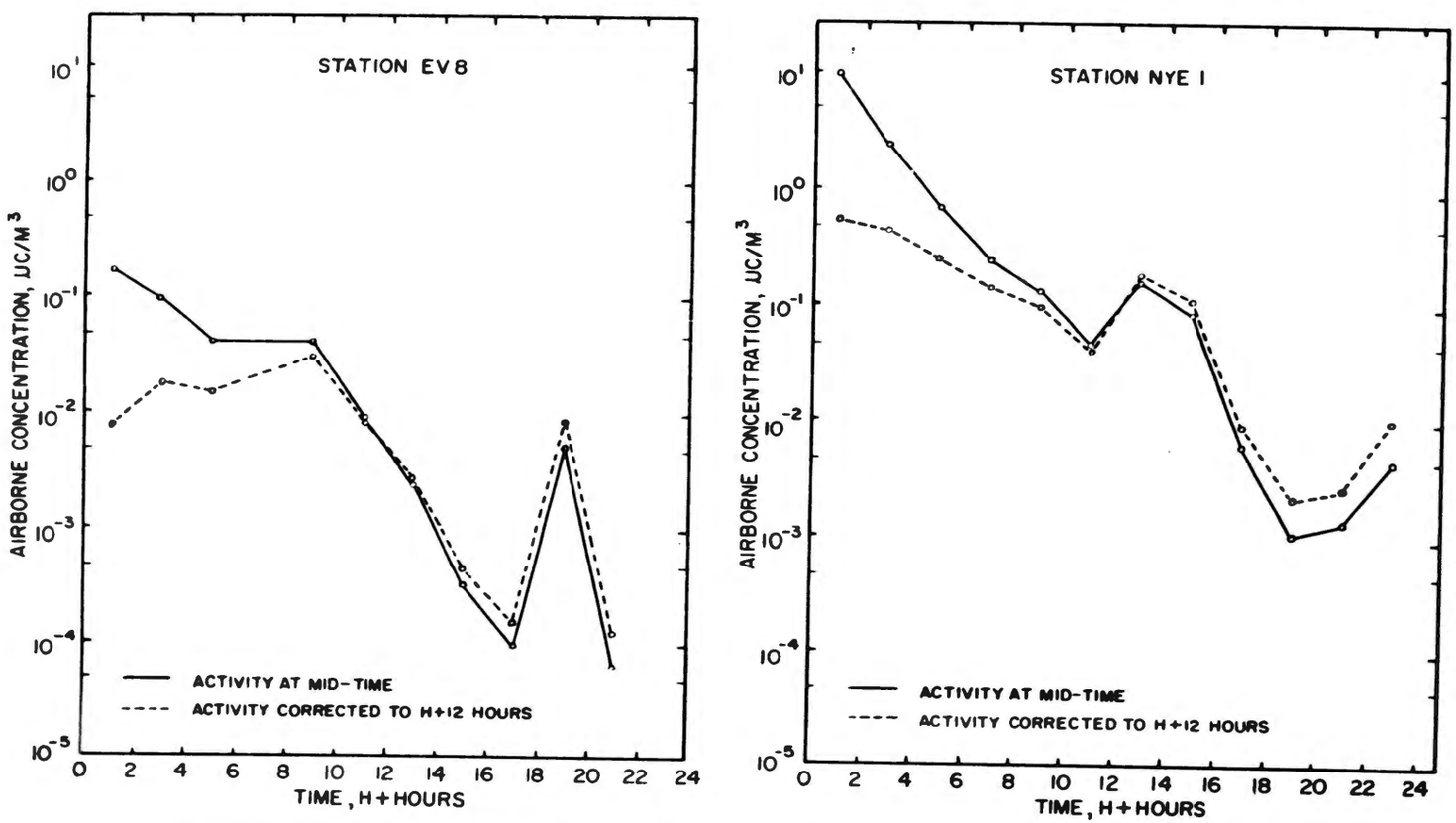

Fig. 4.10—Variation of Shot 7 airborne radioactivity concentrations with time at two sampling stations along 15-mile arc.

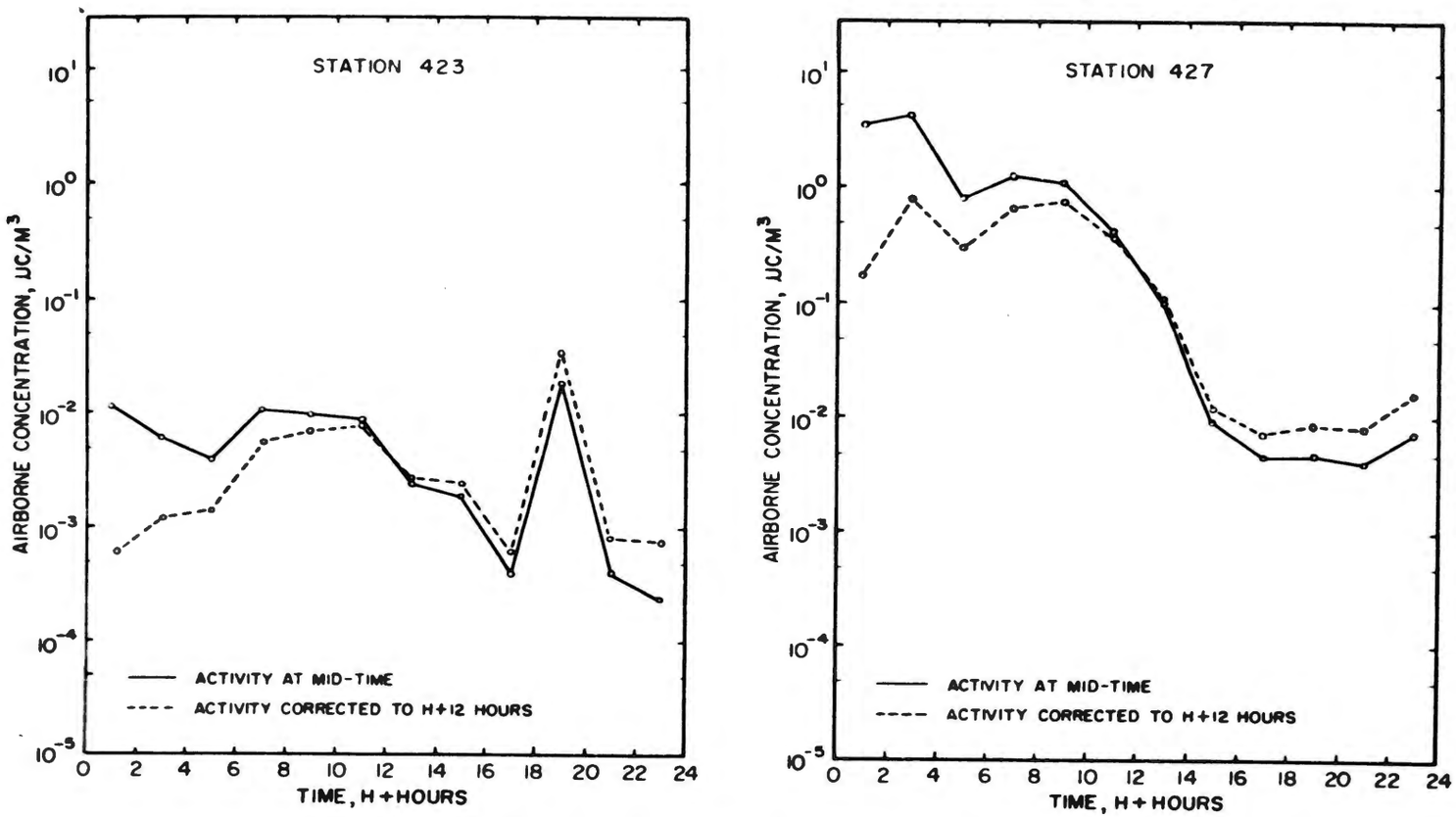

Fig. 4.11—Variation of Shot 7 airborne radioactivity concentrations with time at two sampling stations along 45-mile arc.

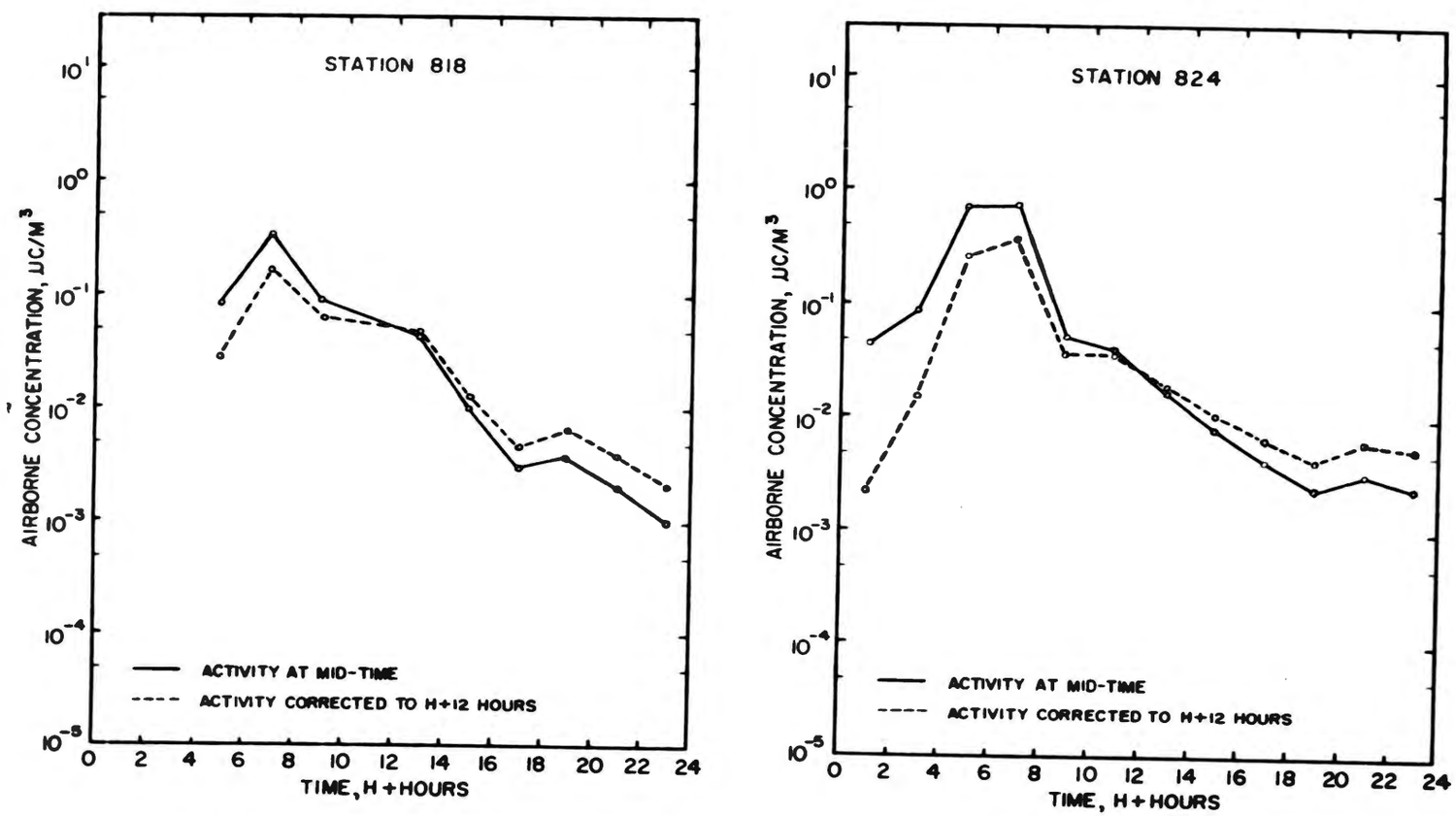

Fig. 4.12—Variation of Shot 7 airborne radioactivity concentrations with time at two sampling stations along 80-mile arc.

fall-out, such specific sampling data as those presented in the preceding sections must be made applicable to generalized conditions. This may be accomplished by the extraction of empirical relations by means of which the factors which characterize the fall-out phenomenon may be defined and correlated.

4.4.1 Trajectory Analysis of the Fall-out Particle

Table 4.7 presents the trajectories of particles falling from various elevations following Shots 2, 5, and 7. The trajectories are based on the assumptions that particles in free fall will

Table 4.7—RESULTANT HORIZONTAL VELOCITIES OF FALL-OUT PARTICLES INFLUENCED BY OBSERVED WINDS FROM SHOTS 2, 5, AND 7*

Initial elevation, ft, MSL	Observed winds		Resultant velocity	
	Direction, deg	Speed, knots	Direction, deg	Speed, mph
		Shot 2		
10,000	150	12	150	13.8
15,000	200	20	181	17.3
20,000	210	20	192	18.9
25,000	210	25	198	21.0
30,000	220	31	205	23.8
35,000	230†	33†	211	25.6
40,000	240	37†	216	27.6
		Shot 5		
10,000	270	17	270	19.6
15,000	320	30	302	24.8
20,000	290	35	297	29.8
25,000	290	43	295	34.6
30,000	310	46	299	37.9
35,000	300	54	299	42.1
		Shot 7		
10,000	260	9	260	10.4
15,000	290	9	275	10.4
20,000	280	26	277	16.7
25,000	280	22	277.5	18.7
30,000	280	41	278.5	24.4
35,000	280	36	279	27.2
40,000	270	48	277	31.2
45,000	270	30	276	31.7

*See Appendix C for examples of trajectory computation.
†No observations available; values estimated.

have a constant falling velocity and that the observed wind velocity at any elevation persists down to the next elevation at which there is a recorded observation. The values listed are the horizontal components of the resultant velocities of particles initiating their fall at various elevations above Ground Zero, as influenced by the winds observed immediately preceding or following the detonations. (See Appendix C for an example of vector analysis by which trajectory is calculated.)

The areas described by the particle trajectories are presented in Fig. 4.13 and very closely approximate the fall-out areas presented in Figs. 3.1 to 3.4.

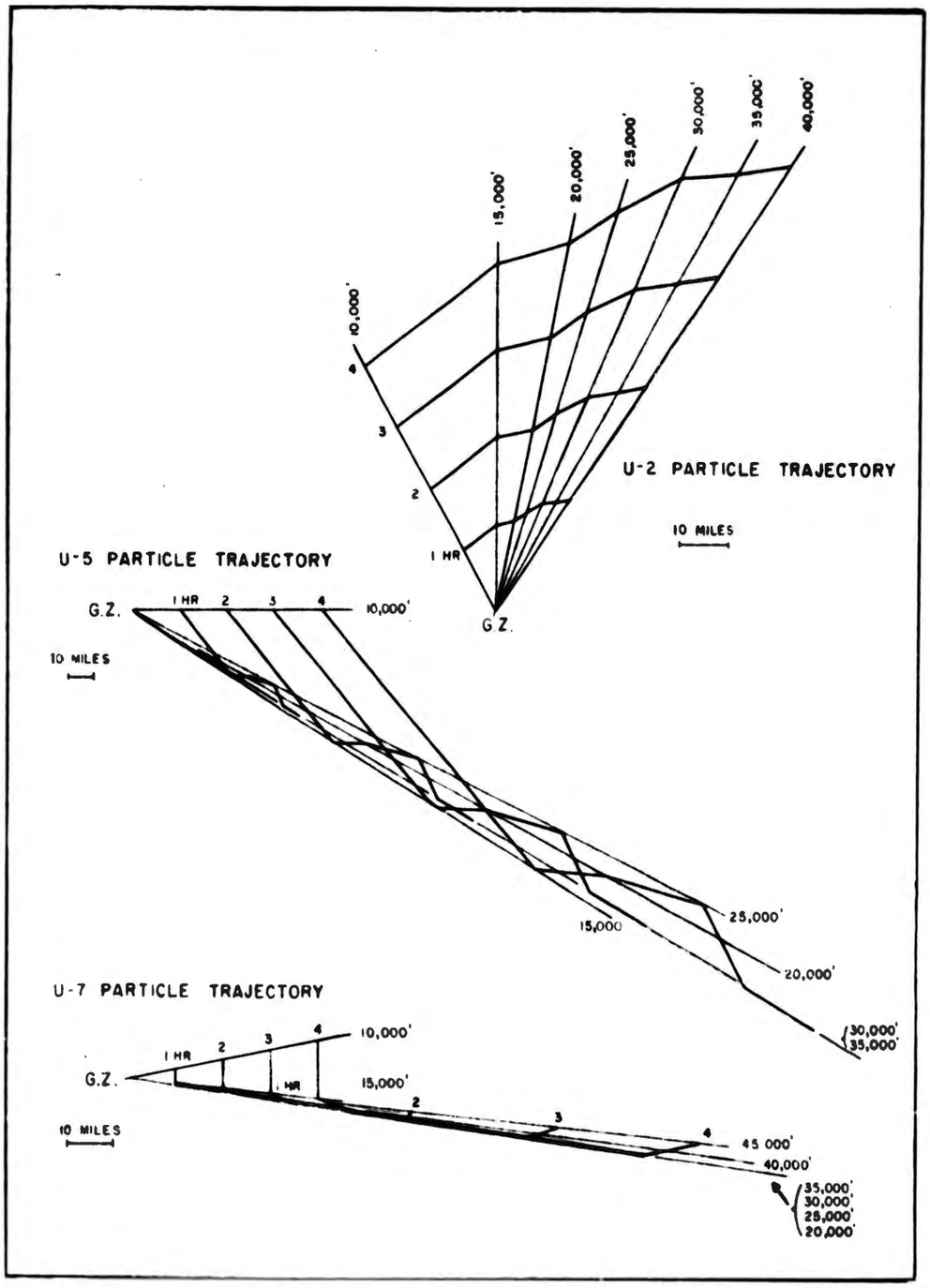

Fig. 4.13—Fall-out particle trajectories for Shots 2, 5, and 7.

4.4.2 Comparison of Calculated Fall-out Time to Field Observations

By means of the resultant horizontal velocities presented in Table 4.7, the fall-out times at each arc of particles originating at the various elevations may be predicted. Table 4.8 gives a comparison of the measured fall-out time at each arc to that predicted by trajectory analysis for Shot 7. Since no background recorders were in position near the midline of fall-out for Shots 2 or 5, comparable data are unavailable.

Table 4.8—COMPARISON OF MEASURED TO PREDICTED FALL-OUT TIME, SHOT 7*

Station†	Distance from Ground Zero, mi	Measured fall-out time, min	Predicted fall-out time from elevations indicated,‡ min			
			40,000 ft	35,000 ft	30,000 ft	25,000 ft
EV-10	14.7	35	28.3	32.4	36.2	47.2
427	46.5	110	89.4	102.7	114.4	149
824	81.9	215	157.2	180.3	201	262

*Fall-out time predicted by trajectory analysis.
†Stations nearest midline of fall-out at which background recorders were located.
‡Based on resultant particle velocities, Table 4.7.

The predicted fall-out times from the 30,000- and 35,000-ft elevations are in close agreement with measured values. Considering that fall-out time predictions are based on time of detonation rather than time of initiation of particle fall and that the effects of changes in air density are neglected, the predicted time of fall from any elevation will be shorter than the actual. Consequently, the agreement between the measured and the predicted fall-out time from 35,000 ft should be the most significant.

The elevation at which the Shot 7 fission cloud broke away from the dust column was approximately 38,000 ft. This elevation is in good agreement with the 35,000-ft elevation suggested by Table 4.8. As shown in Sec. 3.5.1, the background recorders indicated that the majority of fall-out material arrived during a short time interval. Therefore, for the purpose of further calculation, it can be assumed that the fall-out activity is initially most concentrated at a point which can be approximated as the maximum height of the dust column.

4.4.3 Comparison of Calculated Particle Size to Field Observations

Stokes' Law, which describes settling rates of spherical particles, may be approximated for fall in air as[1]

$$t = \frac{h}{0.35 d^2 \rho} \tag{4.1}$$

where t = time of fall
h = elevation
d = diameter, μ
ρ = density of particle (assumed to be 2.5)

This approximation neglects the changes in the velocity of fall resulting from increasing resistance of the air as the air density becomes greater at lower elevations. Owing to the method of size analysis by soil fractionation, the approximation is within the limits of error.

Table 4.9 compares the calculated maximum particle size to be found at various distances from Ground Zero, as determined by Eq. 4.1, to a summary of the observed particle-size distributions. The length of fall indicated is from the estimated maximum height of the dust column to 5000 ft, which approximates the average elevation of the off-site operational area.

The correlation between measured and calculated particle size further indicates the validity of assuming, for purposes of calculation, the initial distribution of activity above Ground Zero to be most concentrated at the top of the dust column.

The observed size fractionation at adjacent stations along individual arcs (Table 4.4) may be due to the error inherent in assuming the initial activity to be concentrated at a point. If, instead, the active material is initially distributed within a volume which may be approximated by a vertical cylinder over Ground Zero, a shearing effect by the winds and size fractionation resulting from the varying times of fall would be expected. Such assumption, while probably more exact, is unnecessary for the purposes of this calculation. In either case, the fall-out times and particle sizes indicate that the primary fall-out activity is more concentrated near the top of the column.

Table 4.9—COMPARISON OF MEASURED TO PREDICTED PARTICLE SIZE, SHOTS 2, 5, AND 7*

Reference location†	Distance from Ground Zero, mi	Fall-out time,‡ H+hr	Summary of measured particle-size distribution		Trajectory analysis§ maximum size, μ
			Fraction, μ	Activity, %	
		Shot 2, 25,000-ft fall			
	12	0.505	350 – 833	86.1	260
202.5	19.2	0.806	175 – 350	80.2	208
410.5	41.7	1.75	175 – 350	66	140
		Shot 5, 25,000-ft fall			
1 mi S of EV-10	16.6	0.438	175 – 350	67.9	280
14 mi S of Sta 210	31	0.818	175 – 350	79.2	205
429.5	51	1.35	125 – 350	90.0	160
17 mi SW of Glendale	86	2.27	44 – 175	85.0	123
		Shot 7, 33,000-ft fall			
Nye 1	14.7	0.584	175 – 350	85.2	270
427.5	45.8	1.83	125 – 175	58.6	155
824	81.0	3.59	125 – 175	64.7	110
9.7 mi E of Glendale	95.2	4.22	88 – 175	61.2	100

*Particle size of primary fall-out predicted by trajectory analysis and Stokes' law at distances >12 miles from Ground Zero.

†Stations nearest to the midline of fall-out at which soil samples were taken.

‡Fall-out time calculated for Shots 2 and 5 and measured for Shot 7.

§Values determined from plot of Eq. 4.1.

4.4.4 Concentration of Fall-out Material As a Function of Distance

The distribution of fall-out with respect to distance (or fall-out time) is probably a complex phenomenon determined by a number of variables such as kt yield, the height of the dust column, the particle-size distribution, wind velocity, and shear. Present information does not permit detailed evaluation of all of these factors.

An empirical relation between concentration of fall-out material and distance may be obtained as follows. If the total activities along each arc as presented in Sec. 4.2.1 are plotted against fall-out time, as determined by background recorders (Shot 7) or by trajectory analysis (Shots 2 and 5), the relation presented in Fig. 4.14 is obtained.

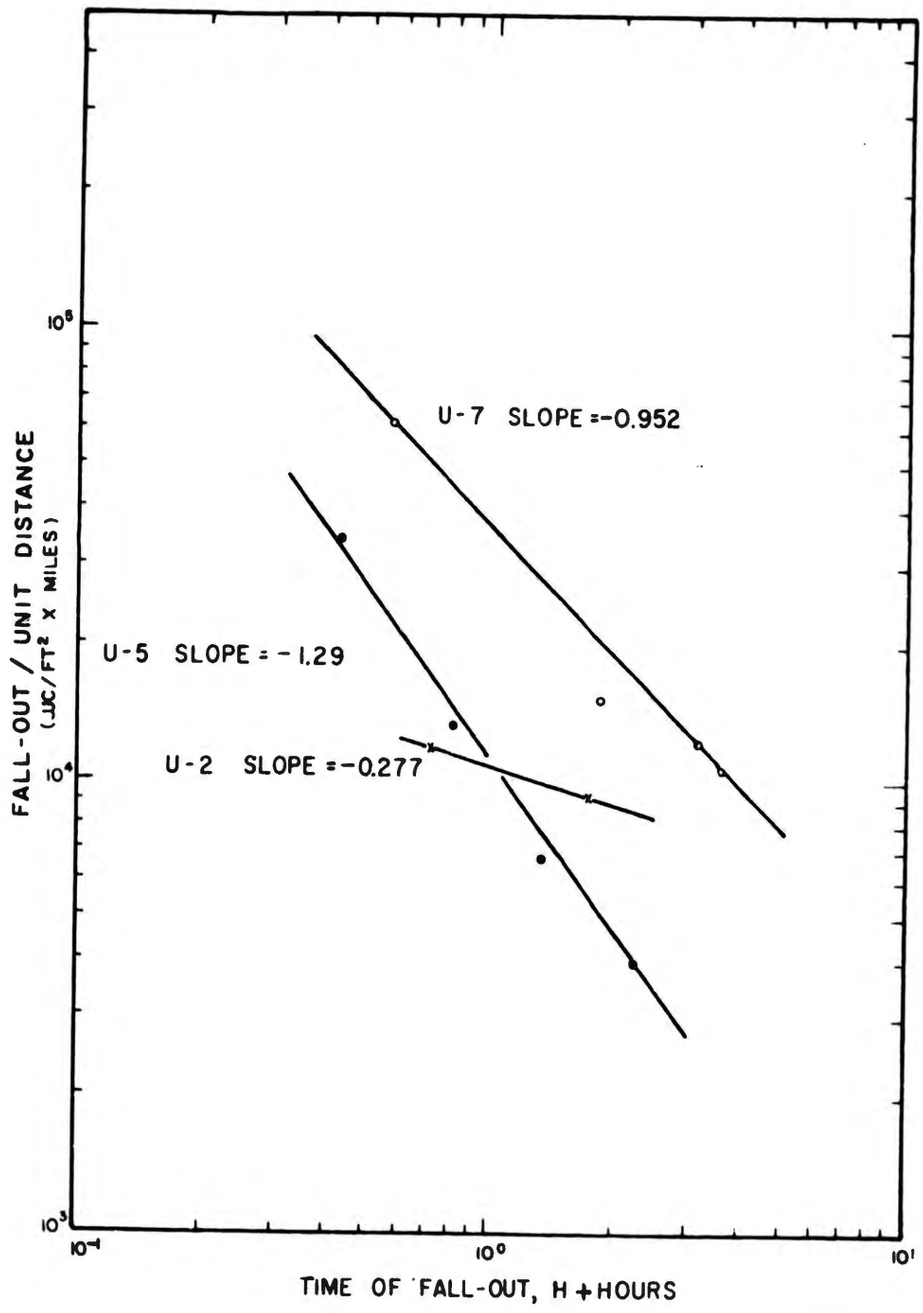

Fig. 4.14—Relation between total activity distributed along arcs and time of fall-out for Shots 2, 5, and 7. (Fall-out times measured for Shot 7 and estimated on the basis of observed winds for Shots 2 and 5.)

In each case the total activity along any arc decreases as the distance from Ground Zero to the arc is increased, and a straight line may be drawn through the plotted points. The slopes determined may be due to the particular detonation characteristics. If this is not the case, the data from Shot 7, which should be regarded with the most confidence since fall-out time was measured, indicate that the amount of activity falling per unit distance is inversely proportional to the fall-out time.

The divergence from a slope of –1 in the case of Shot 5 could be attributable to errors in estimation of wind velocity. That is, an increase or decrease in velocity after detonation would result in appreciable errors in fall-out time estimation. The data from Shot 2 are questionable because monitoring was limited to two roads, one of which did not closely approximate an arc. Therefore, based on Shots 5 and 7, the inverse relation between fall-out per unit distance and fall-out time (slope of –1) may be considered to be correct as a first approximation.

Since the fall-out per unit distance is directly proportional to the fall-out per unit time at a given velocity, the relation may therefore be expressed as

$$F = F_0 t^{-1} \tag{4.2}$$

where F = fall-out per unit time at time t
F_0 = fall-out per unit time at H+1 hr
t = time of fall-out, H+hr

and activities are expressed at a common time of H+12 hr.

4.4.5 Total Fall-out Activity as a Function of Kt Yield

It is logical to assume that under similar experimental conditions the total material deposited during any time interval, as well as at any time, should be a function of the kt yield. A comparison of Shot 5 and Shot 7 fall-out with respect to kt yield is presented in Table 4.10. The calculations are based on H+0.5 hr contaminations and Eq. 4.2 and are subject to the limitations of fall-out time estimation for Shot 5.

Table 4.10—FALL-OUT MATERIAL DEPOSITED AT H+1 HR AND TOTAL PRIMARY FALL-OUT AS A FUNCTION OF KT YIELD*

Shot	Yield, kt	Kt ratio	F_0, curies deposited per min †	Total primary fall-out from H+0.5 to H+5 hr, curies	Fall-out ratio
5	27.4	1:1.86	2.59×10^5‡	35.8×10^6	1:1.68
7	51.5		4.36×10^5	60.2×10^6	

*Activity values are corrected to H+12 hr.
†($\mu c/ft^2 \times$ miles) × wind velocity. Observed winds are assumed to be valid until H+1 hr.
‡Calculated value since fall-out time was not measured.

The similarity of the respective kt and fall-out ratios suggests that the total primary fall-out is approximately proportional to kt yield. Based on a total yield of 266 megacuries of beta activity at H+24 hr for a 20-kt bomb,[1] the total yields for Shots 5 and 7 would be 848 and 1590 megacuries beta at H+12 hr, respectively. The total fall-out from Shots 5 and 7 during the time interval of H+0.5 to H+5 hr therefore accounts for 4.22 and 3.79 per cent, respectively, of the total beta yield.

4.4.6 Expected Fall-out Distribution from a Tower Detonation As a Function of Kt Yield and Wind Velocities

The integrated dose at any distance from Ground Zero may be estimated using the empirical relations established in the preceding sections.

The validity of the predictions is dependent upon the validity of the following relations:

(a) The material deposited per unit time varies inversely as the time after detonation [$F = F_0 t^{-1}$ (Sec. 4.4.4)].

(b) The factor F_0 is a direct function of kt and has a value of 1.77×10^5 curies/min for a 20-kt bomb (Sec. 4.4.5).

(c) The material along any arc is distributed so that the average mr/hr is equal to one-third of the maximum mr/hr along that arc (Sec. 4.2.1).

(d) 1 mr/hr = ~10 $\mu c/ft^2$ (Sec. 4.2.2).

(e) Relations a to d are valid during the time interval of H+15 min to H+8 hr.

An expression of dose as a function of distance and wind velocity may be derived from Eq. 4.2 as follows:

$$\text{R/hr} \times \text{miles at H+12 hr} = F_0 t^{-1} \frac{1}{\text{velocity}} \tag{4.3}$$

$$\text{R/hr} \times \text{miles at fall-out time} = F_0 t^{-1} \frac{1}{\text{velocity}} \left(\frac{t}{12}\right)^{-1.2} \tag{4.4}$$

$$\text{Infinite dose, r} \times \text{miles} = 5t \left[F_0 t^{-1} \frac{1}{\text{velocity}} \left(\frac{t}{12}\right)^{-1.2} \right] \tag{4.5}$$

$$\text{24-hr integrated dose, r} \times \text{miles} = \text{infinite dose} \left[1 - \left(\frac{t}{24}\right)^{0.2} \right] \tag{4.6}$$

where r/hr × miles = fall-out per unit distance
F_0 = fall-out per unit time at H+1 hr
t = time of fall-out, H+hr

Figure 4.15 illustrates the dependence of integrated dose at any distance upon wind velocity. The values presented are for infinite and 24-hr exposures along arcs at various distances from Ground Zero. The division of total dosage along any arc (r × miles) by the width of the fall-out pattern yields the average dose at that distance. As indicated by relation c, this average approximates one-third the maximum.

The use of Fig. 4.15 in the estimation of primary fall-out distribution is illustrated by assuming a wind velocity of 40 mph with a 10° shear and a minimum fall-out width of 5 miles; the fall-out pattern at a distance of 40 miles would be approximately 12 miles wide. From Fig. 4.15, the total infinite dose for a nominal bomb would be 95 r × miles. The average infinite dose would therefore be 95/12 or 7.9 r and the maximum approximately 23.7 r.

Since 1 r/hr corresponds to 10^4 $\mu c/ft^2$ beta contamination, the contamination per unit area at any distance may be derived by dividing the infinite dose by $5t \times 10^{-4}$. Thus in the example just used, the maximum contamination would be 4.74×10^4 $\mu c/ft^2$ at H+1 hr.

4.4.7 Estimated Distribution of Radiostrontium in Fall-out Areas

The contribution of the long-lived isotopes to the gross fission product is important for the estimation of possible long-term hazards. One of the most important of these long-lived isotopes is Sr^{90}.

The following ratios based upon the Way-Wigner estimate of pile product composition[2] have been reported:

$$\frac{\text{Total strontium}}{\text{Total fission products}} \text{ at H+24 hr} = 0.0025 \tag{4.7}$$

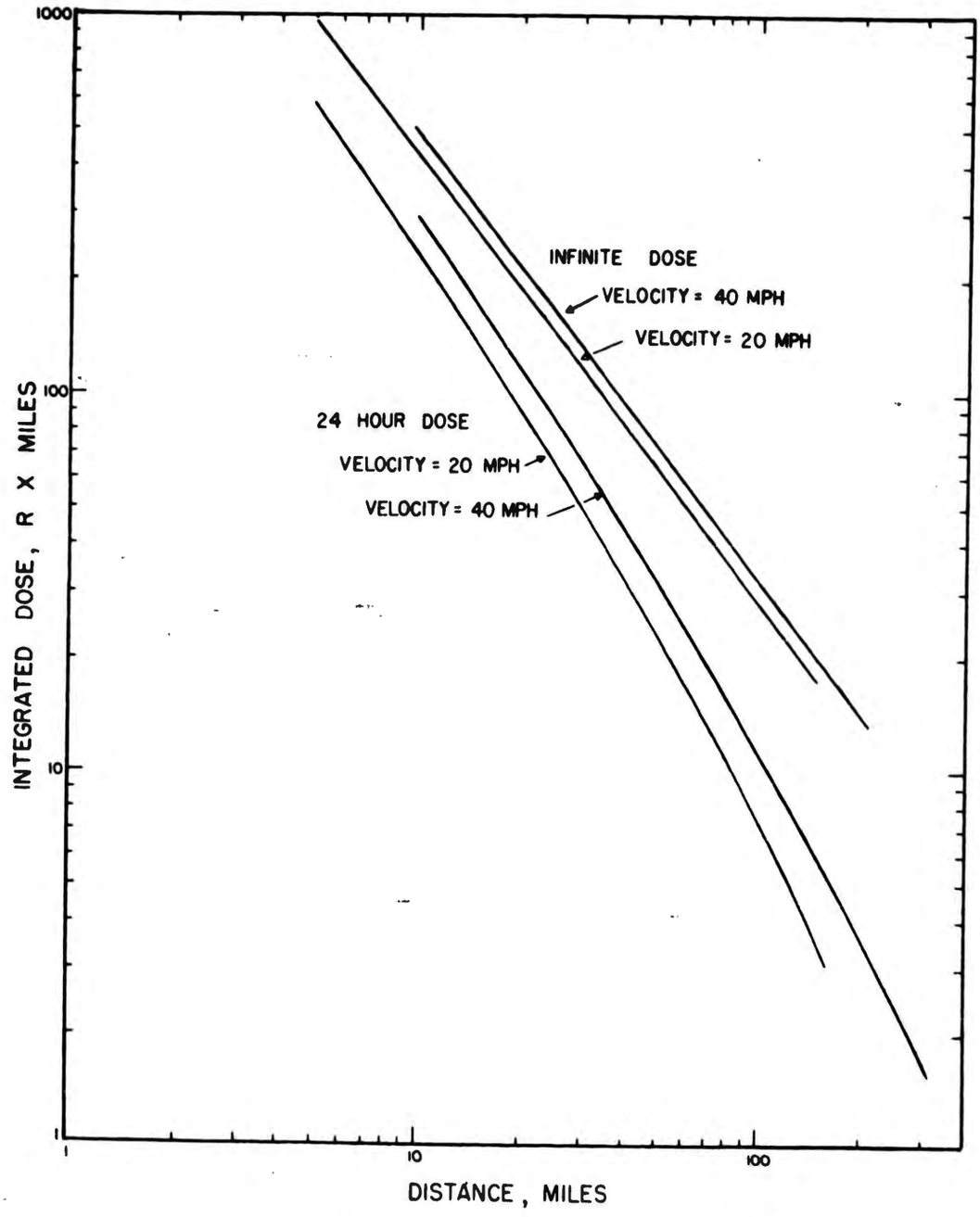

Fig. 4.15—Estimated infinite and 24-hr dose at various distances from Ground Zero on a nominal bomb detonation.

$$\frac{Sr^{90}}{Sr^{89}} \text{ at H+24 hr} = 0.0066 \qquad (4.8)$$

From these relations and the relation that 1 mr/hr corresponds to 10 $\mu c/ft^2$, it follows that the total strontium contamination per mr/hr at H+12 hr would be 0.0107 $\mu c/ft^2$, of which 0.00002 $\mu c/ft^2$ is attributable to Sr^{90}.

Thus the calculated total strontium contamination at Nye 1, where the dose rate was 1630 mr/hr at H+12 hr following Shot 7, was 17.5 $\mu c/ft^2$, of which 0.032 $\mu c/ft^2$ was Sr^{90}.

REFERENCES

1. Los Alamos Scientific Laboratory, "The Effects of Atomic Weapons," U. S. Government Printing Office, Washington, 1950.
2. M. Eisenbud and J. H. Harley, Progress Report Covering the Period from September 1953 to Jan. 4, 1954, New York Operations Office, AEC Report NYO-4571, January 1954.

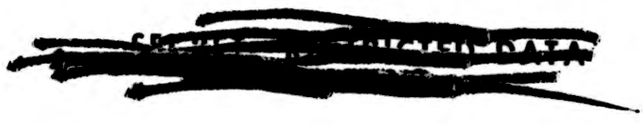

CHAPTER 5

CONCLUSION

5.1 SUMMARY AND CONCLUSIONS

Project 27.1 of the Civil Effects Test Group performed detailed studies of the distribution and the various characteristics of settled and airborne fall-out material. The purpose of these studies was to provide information basic to the proper evaluation of possible hazards due to fall-out. The project functioned during Shots 2, 3, 4, 5, and 7, of Operation Upshot-Knothole, at distances greater than 10 miles from the respective Ground Zeros.

5.1.1 Contamination Due to Primary Fall-out

Three detonations resulted in widespread distribution of moderate to high levels of radiation. Shot 2 produced a wide pattern of fall-out, and the area within which the infinite dose was greater than 25 r extended some 20 miles from Ground Zero. Shots 5 and 7 resulted in narrow primary fall-out patterns. Areas within which the infinite dose was greater than 125 r extended approximately 22 miles from Ground Zero for both detonations; areas of greater than 25 r infinite dose extended approximately 60 miles from Ground Zero. Shots 3 and 4, because of the small yield and the height of detonation, respectively, resulted in relatively low but not insignificant levels of contamination.

The maximum surface contamination at an established sampling station was detected following Shot 7 at a distance of 14.5 miles from Ground Zero. Field measurements at this location indicated that the dose rate, at H+12 hr, was 1630 mr/hr, and the surface contamination was 18,580 $\mu c/ft^2$ beta radiation determined by laboratory assay. Eighty-five per cent of the activity was associated with the 175- to 350-μ fractions of soil. The resulting infinite dose would be 176 r. The calculated Sr^{89-90} component would approximate 20 $\mu c/ft^2$ in this area.

5.1.2 Distribution of Primary Fall-out Material

The total primary fall-out material deposited within the time interval of H+0.5 to H+5.0 hr varied approximately as the kt yield. The total material distributed along any arc crossing the fall-out pattern varied inversely as the time of fall-out at that distance. Along each arc the average mr/hr was approximately equal to one-third of the maximum. A uniform contamination of 10 $\mu c/ft^2$ beta radiation corresponded to field measurements of approximately 1 mr/hr at 3 ft.

An inverse relation between median particle size and distance was indicated by individual samples taken along the midline of fall-out as well as by integrating the total material along each arc. Following Shot 5, the median diameters of the radioactive particles were 450 and 225 μ along arcs 17 and 51 miles, respectively, from Ground Zero. A significant variation in particle-size distribution occurred at individual locations along each arc.

5.1.3 Distribution of Airborne Radioactive Material

Detailed sampling of airborne material was successful for Shot 7 only. The maximum 2-hr concentration detected was approximately 10 $\mu c/m^3$ at a distance of 14.5 miles from Ground Zero. The corresponding 24-hr average concentration was 1.1 $\mu c/m^3$. The 24-hr average concentrations ranged from the above maximum to 0.005 $\mu c/m^3$ according to sampling location. No distinct correlation between surface and airborne contamination was observed. Analysis of the data suggests that both midline of fall-out and lateral stations received additional airborne material subsequent to the original contamination. Particle-size analysis of airborne material yielded inconclusive results.

5.1.4 Properties of the Collected Material

Microscopic examination of the collected particles indicated that they were generally spherical glassy beads which appeared to have been solidified in air. Solubilities of less than 1 per cent in water and approximately 2 per cent in 0.1N HCl were determined.

The activity per particle was approximately proportional to the surface area of particles greater than 150 μ and more nearly proportional to the volume for smaller particles.

The radioactive decay constant of the collected samples generally approximated -1.2, with variations attributable to sample thickness and instrumentation characteristics. The effective beta radiation energy varied between 0.4 and 0.6 Mev according to time during the first 4-month interval after detonation.

5.1.5 Mechanics of the Distribution of Primary Fall-out

Based upon the empirical relations observed, the distribution of primary fall-out with respect to distance from Ground Zero within the limits of H+0.5 to H+5 hr may as a first approximation be formulated as

$$F = F_0 t^{-1}$$

where F = fall-out per unit time at time t
F_0 = fall-out per unit time at H+1 hr
t = time of fall-out along the arc in H+hr

The fall-out per unit area and the resulting integrated dose would be determined by the wind velocity and shear.

By integrating the above expression, the total Shot 5 and Shot 7 fall-out material deposited during the time interval H+0.5 to H+5 hr was determined to be approximately 4 per cent of the total fission products produced.

It is concluded that the foregoing relations may be used to predict the fall-out pattern originating from a bomb detonated at 300 ft above the soil surface at NPG. Further, by the selection of proper conditions of wind, height of burst, and kt yield, contamination in a given area could be controlled.

5.2 RECOMMENDATIONS

It is recommended that future studies should include:

1. The expansion of the empirical treatment of the fall-out phenomenon. This should include a theoretical analysis and the performance of confirmatory investigations during subsequent test series, particularly to determine the time interval over which the observed relations are valid.

2. A thorough investigation of the influence of Ground Zero soil characteristics upon the fall-out-particle-size distribution. This should include a more detailed definition of the particle size–distance relation, extending the study to distances up to 200 miles from Ground

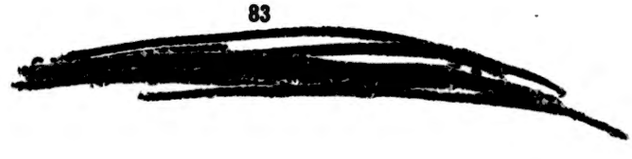

Zero in order to explore the possibility of certain areas being biologically more significant owing to the greater concentrations of small particles.

3. The close correlation of an air-sampling program with studies of biological availability in the environment contaminated by fall-out. This should include the improvement of existing air-sampling equipment and techniques and the use of equipment capable of sampling the gaseous and/or colloidal components of radioactive airborne material.

4. The performance of detailed meteorological investigations in conjunction with future primary fall-out and airborne studies to facilitate interpretation and to permit possible extrapolation of observations to areas other than NPG.

APPENDIX A

TABULATION OF SHOT 7 AIRBORNE CONCENTRATIONS

Sample interval, hr	Concentrations at stations along 20-mi arc, $\mu c/m^3 \times 10^{-3}$								
	EV-7	P-9.5	EV-8	EV-10	Nye 1	207	208	209	210
H to H+2	60.5	1.27	155	2080	9900	8.30	N.S.*	157	572
H+2 to H+4	248	43.8	98.5	130	2360	21.2	N.S.	41.9	157
H+4 to H+6	100	10.5	43.8	47.5	750	3.70	N.S.	19.1	36.8
H+6 to H+8	57.3	8.95	Nil	48.0	275	7.40	N.S.	91.3	125
H+8 to H+10	7.72	0.125	43.7	23.5	137	14.1	N.S.	1.96	39.0
H+10 to H+12	N.S.	Nil	9.35	4.04	45.8	2.27	N.S.	2.12	61.4
H+12 to H+14	N.S.	Nil	2.48	25.0	173	1.38	0.334	2.20	9.65
H+14 to H+16	5.43	Nil	0.340	4.88	84.3	0.933	0.607	0.618	0.667
H+16 to H+18	3.18	Nil	0.0985	2.76	5.95	0.232	1.49	2.43	4.00
H+18 to H+20	Nil	Nil	5.20	2.30	1.23	Nil	2.33	0.331	2.98
H+20 to H+22	Nil	Nil	0.0665	2.67	1.33	0.610	5.13	1.71	3.00
H+22 to H+24	Nil	Nil	Nil	Nil	4.60	Nil	0.285	1.16	0.345

Sample interval, hr	Concentrations at stations along 40-mi arc, $\mu c/m^3 \times 10^{-3}$											
	415	416	418	419	420	421	422	423	424	425	426	427
H to H+2	N.S.*	613	6.33	Nil	Nil	Nil	Nil	11.7	N.S.	4.16	10.7	3460
H+2 to H+4	N.S.	177	7.61	2.51	Nil	Nil	Nil	6.23	N.S.	7.68	76.4	4180
H+4 to H+6	N.S.	76.1	N.S.	N.S.	Nil	Nil	Nil	4.01	N.S.	7.01	847	845
H+6 to H+8	N.S.	8.08	N.S.	N.S.	Nil	Nil	Nil	10.6	N.S.	141	304	1260
H+8 to H+10	N.S.	N.S.	N.S.	N.S.	Nil	N.S.	147	9.61	N.S.	11.3	291	1090
H+10 to H+12	0.991	N.S.	N.S.	N.S.	33.5	N.S.	60.9	8.60	N.S.	N.S.	31.7	417
H+12 to H+14	Nil	0.146	4.15	31.8	3.86	3.73	22.2	2.50	11.3	24.0	61.0	101
H+14 to H+16	N.S.	N.S.	Nil	N.S.	10.5	2.67	85.4	1.87	0.324	Nil	12.8	9.30
H+16 to H+18	N.S.	N.S.	N.S.	N.S.	0.816	2.42	1.62	0.405	N.S.	Nil	9.19	4.65
H+18 to H+20	N.S.	N.S.	N.S.	N.S.	1.06	1.66	Nil	19.6	N.S.	Nil	30.9	4.96
H+20 to H+22	N.S.	N.S.	N.S.	N.S.	3.84	Nil	1.58	0.411	N.S.	0.349	11.3	4.06
H+22 to H+24	N.S.	N.S.	N.S.	N.S.	0.921	N.S.	1.97	0.345	N.S.	N.S.	3.99	7.16

Sample interval, hr	Concentrations at stations along 80-mi arc, $\mu c/m^3 \times 10^{-3}$					
	Caliente	818	823	ROX	824	825
H to H+2	Nil	Nil	21.2	67.7	43.6	6.29
H+2 to H+4	Nil	Nil	4.51	80.1	87.0	0.790
H+4 to H+6	Nil	86.1	1.58	44.7	737	0.548
H+6 to H+8	5.43	328	79.2	143	738	2.16
H+8 to H+10	13.9	89.5	111	10.1	51.8	0.294
H+10 to H+12	47.7	N.S.*	6.05	N.S.	40.8	N.S.
H+12 to H+14	87.7	42.9	0.590	25.8	17.2	Nil
H+14 to H+16	55.8	10.2	4.18	N.S.	8.0	Nil
H+16 to H+18	17.9	3.14	3.37	N.S.	4.38	N.S.
H+18 to H+20	6.02	3.74	2.06	N.S.	2.38	N.S.
H+20 to H+22	6.41	2.02	41.4	N.S.	3.21	N.S.
H+22 to H+24	4.10	1.01	2.88	N.S.	2.44	N.S.

* N.S., no sample collected due to equipment failure.

APPENDIX B

METEOROLOGY

By J. J. Fuquay

Hanford Engineer Works

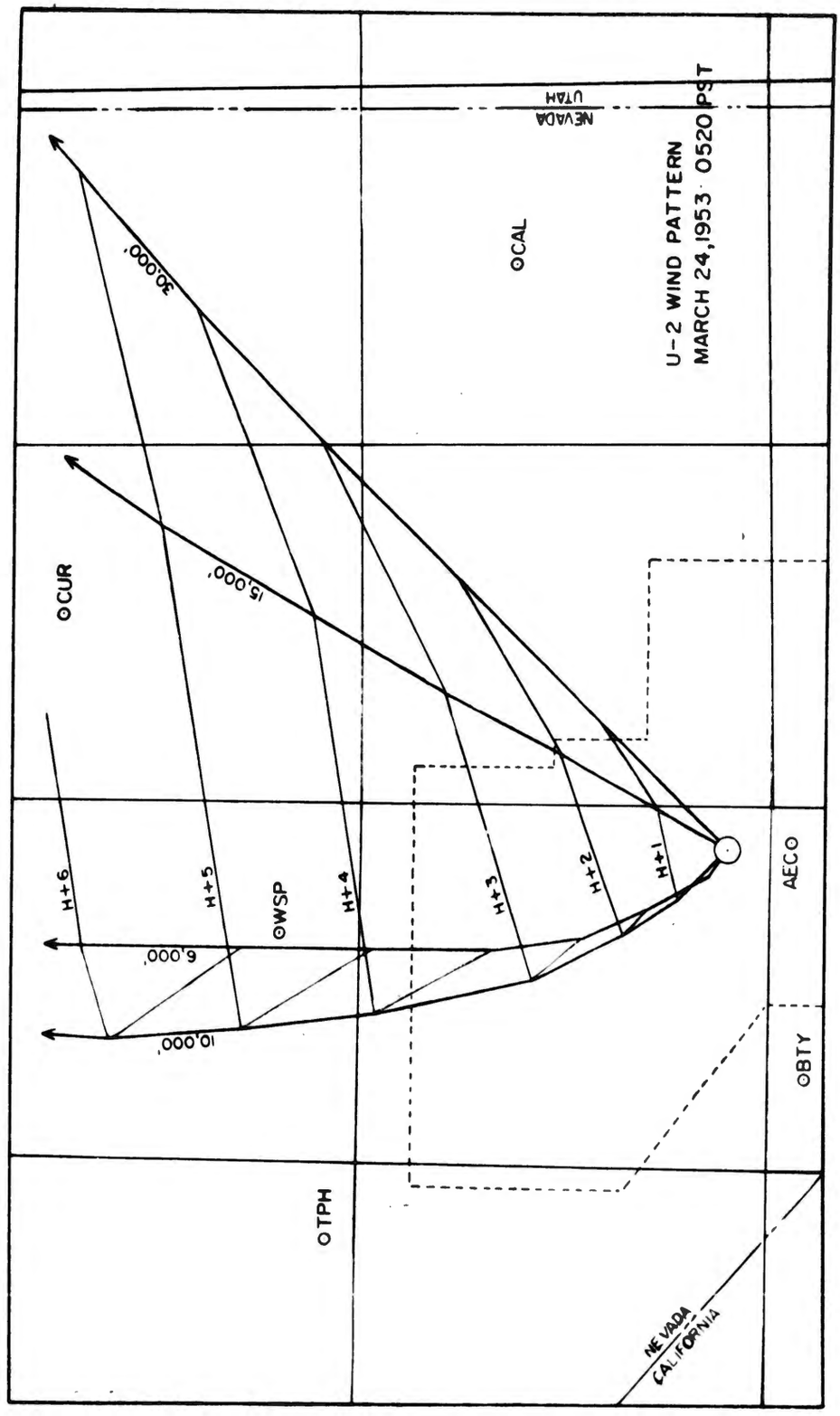

Fig. B.1—Shot 2 wind pattern, Mar. 24, 1953, 0520 PST.

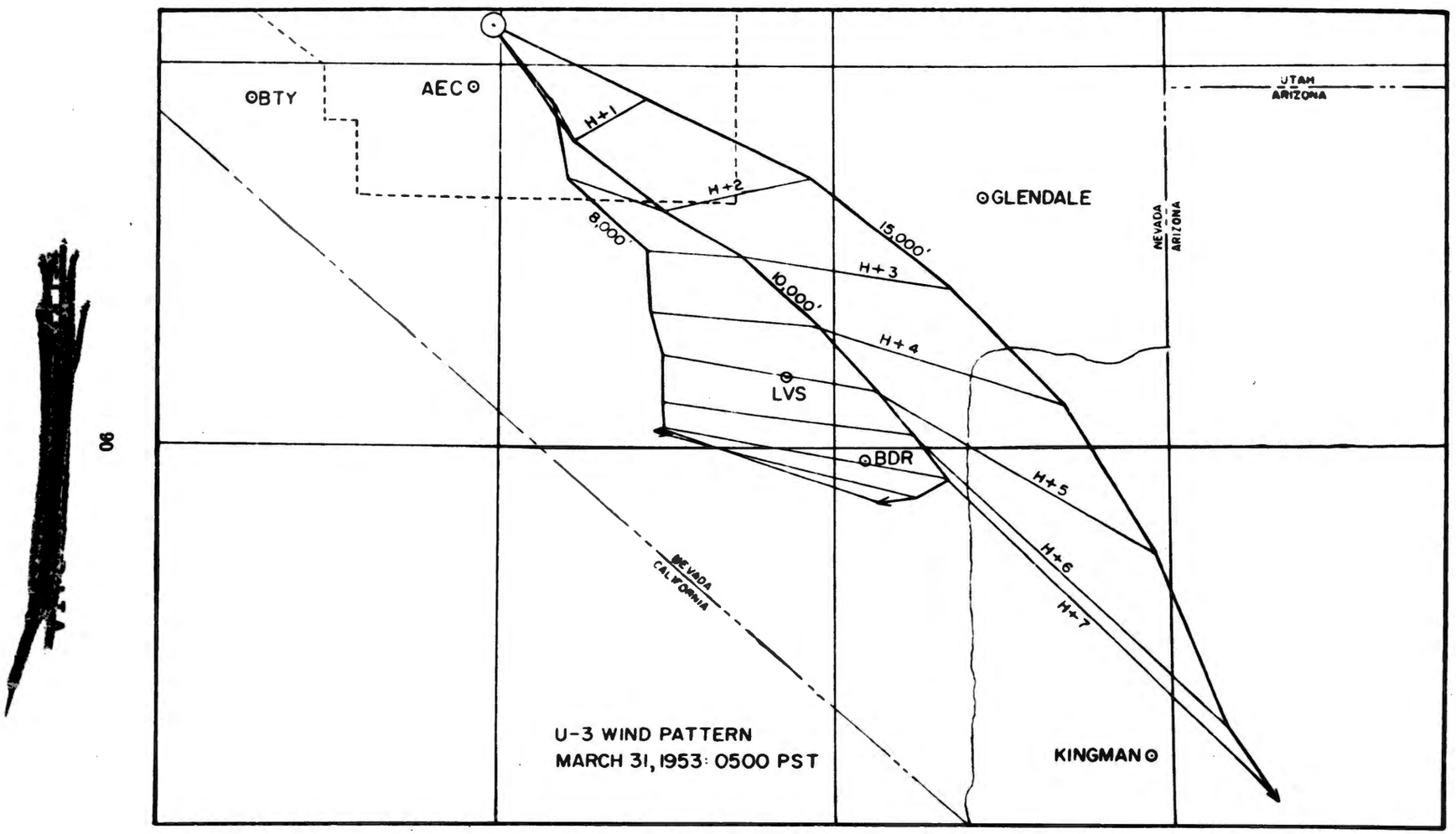

Fig. B.2—Shot 3 wind pattern, Mar. 31, 1953, 0500 PST.

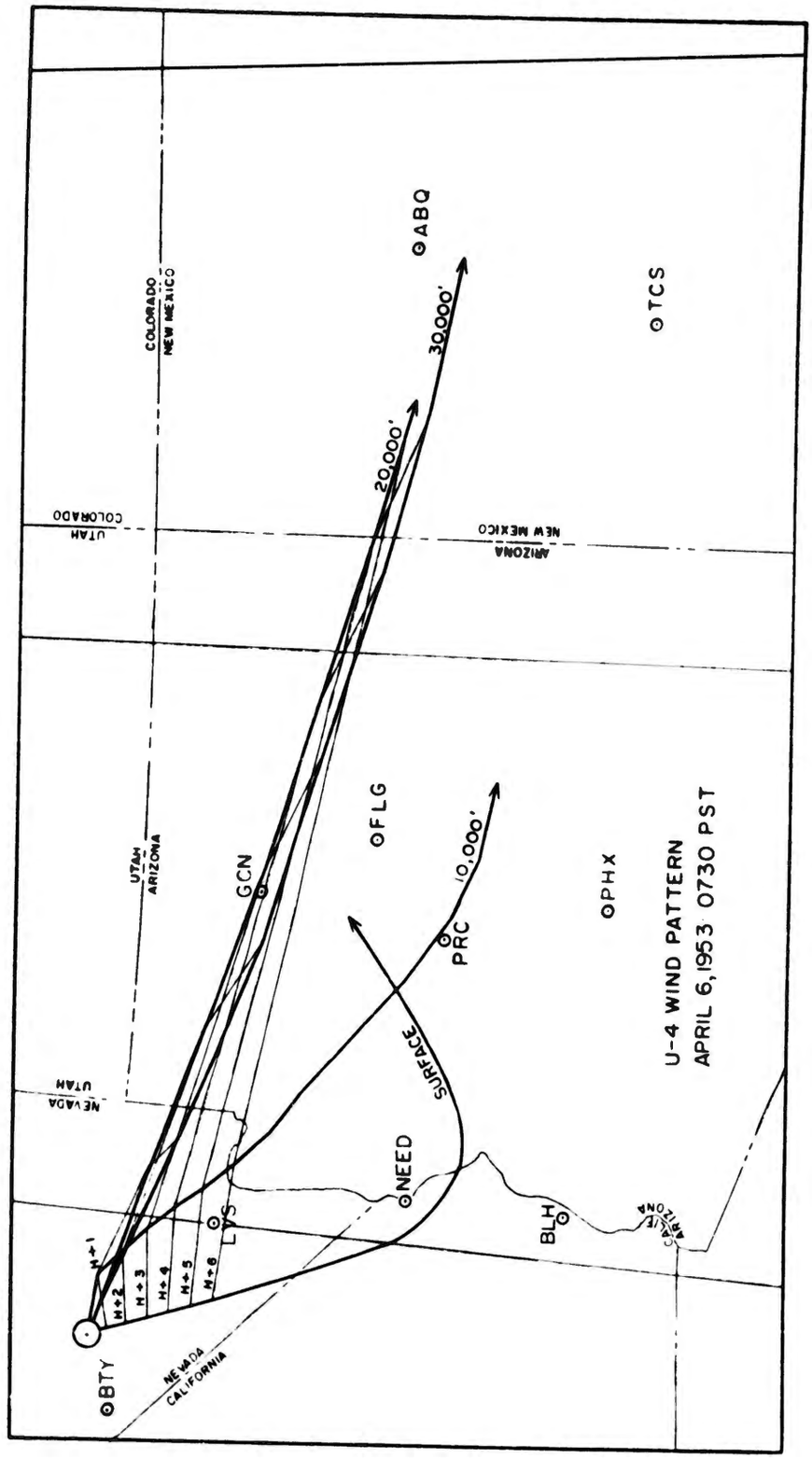

Fig. B.3—Shot 4 wind pattern, Apr. 6, 1953, 0730 PST.

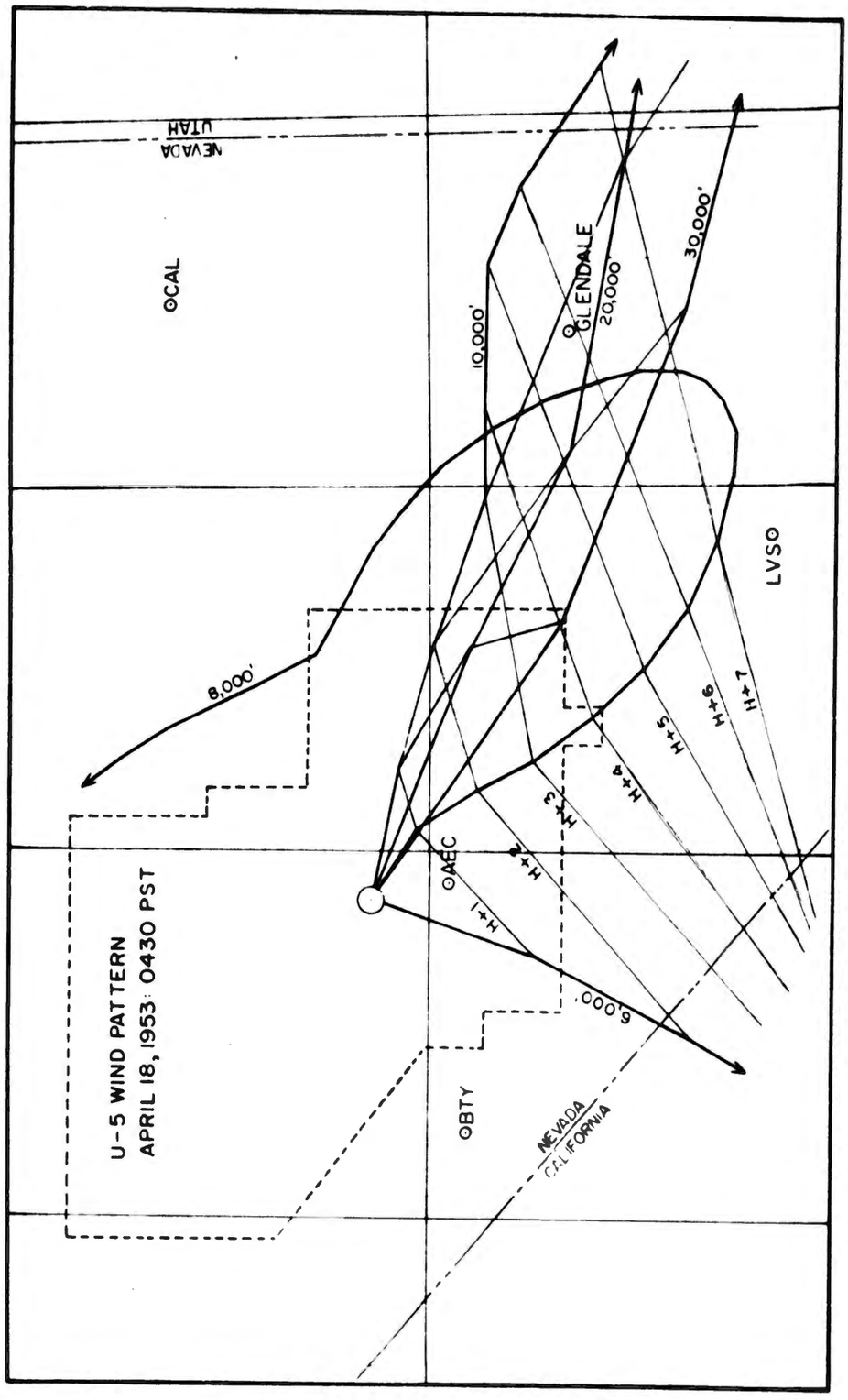

Fig. B.4—Shot 5 wind pattern, Apr. 18, 1953, 0430 PST.

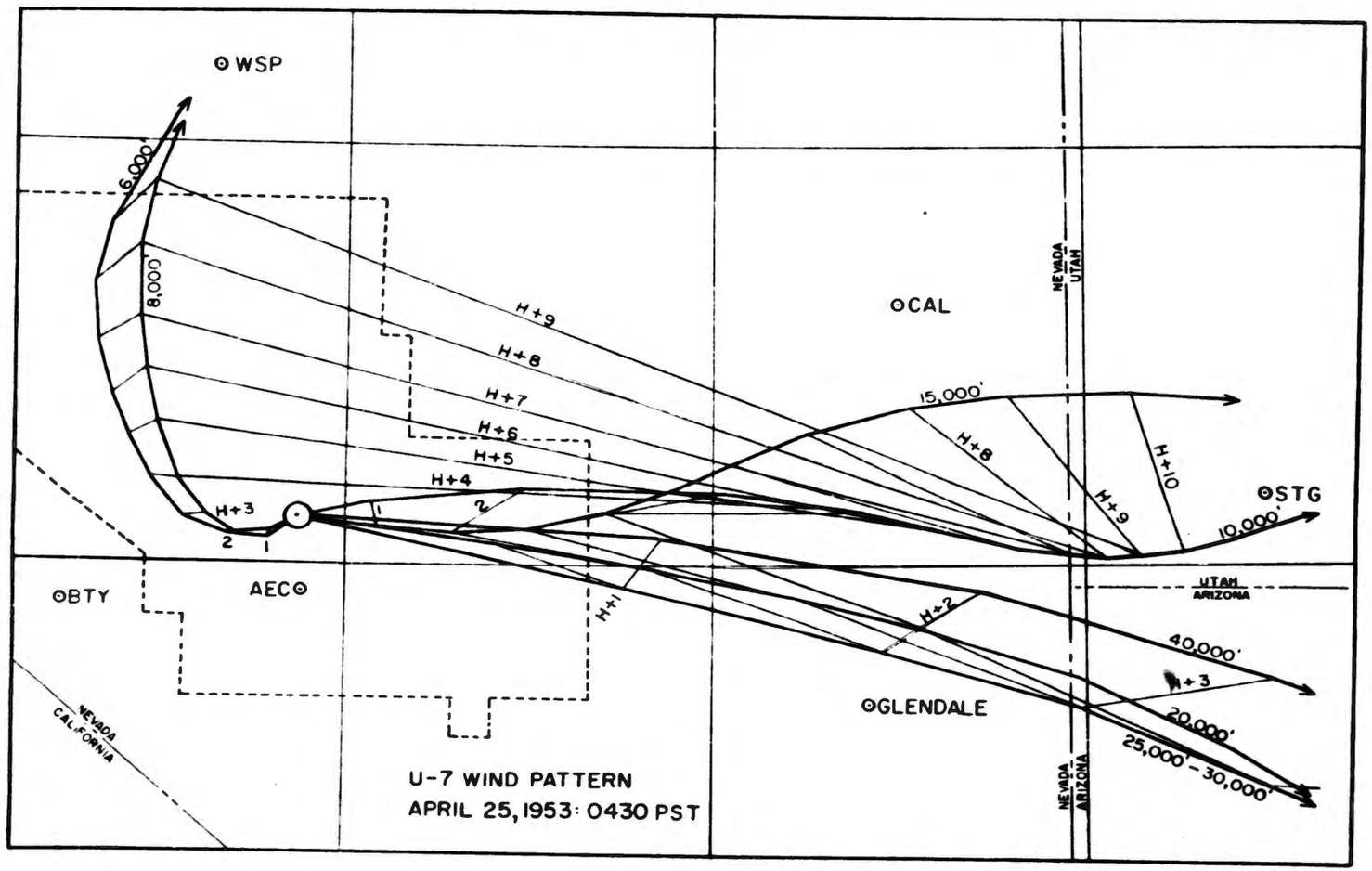

Fig. B.5—Shot 7 wind pattern, Apr. 25, 1953, 0430 PST.

APPENDIX C

EXAMPLE OF FALL-OUT PARTICLE TRAJECTORY (SHOT 2)

A. Calculation of Trajectory

Elevation, ft, MSL	Observed postshot winds*			Sum of vectors*				Resultant velocity†		
	Symbol	Direction, deg	Speed, knots	Symbol	Direction, deg	Speed, knots	Weight	Symbol	Direction, deg	Speed, mph
10,000	V_1	150	12	r_1	150	12	1/1	R_1	150	13.8
15,000	V_2	200	20	r_2	181	30	1/2	R_2	181	17.3
20,000	V_3	210	20	r_3	192	49	1/3	R_3	192	18.9
25,000	V_4	210	25	r_4	198	73	1/4	R_4	198	21.0
30,000	V_5	220	31	r_5	205	103	1/5	R_5	205	23.8
35,000	V_6	230‡	33‡	r_6	211	133	1/6	R_6	211	25.6
40,000	V_7	240	37‡	r_7	216	167	1/7	R_7	216	27.6

* See step B. † See step C. ‡ No observations available; values estimated.

B. VECTOR REPRESENTATION

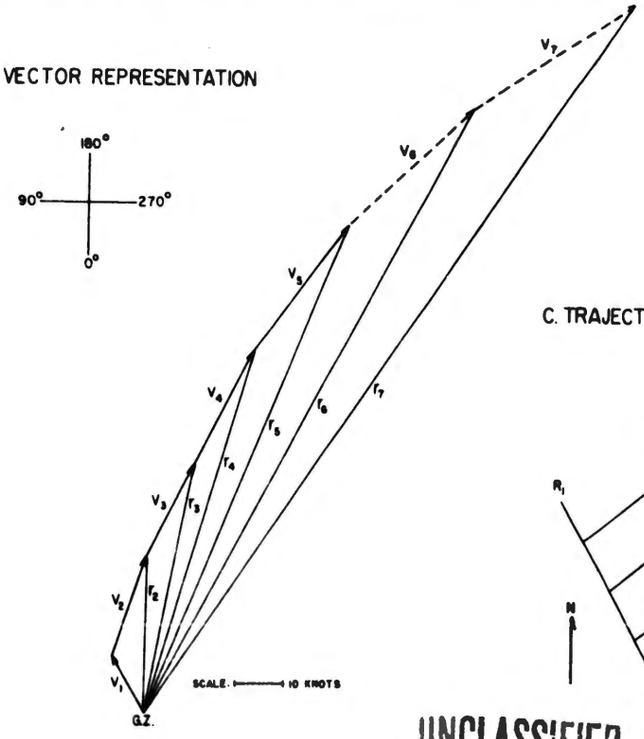

C. TRAJECTORY REPRESENTATION

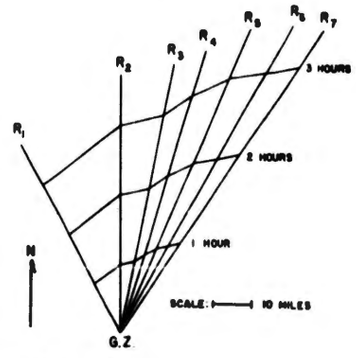

DISTRIBUTION

ARMY ACTIVITIES	Copy
Asst. Chief of Staff, G-1, D/A, Washington 25, D. C., ATTN: Human Relations and Research Board	1
Asst. Chief of Staff, G-3, D/A, Washington 25, D. C., ATTN: Dep. CofS, G-3 (RR&SW)	2
Asst. Chief of Staff, G-4, D/A, Washington 25, D. C.,	3
Chief of Ordnance, D/A, Washington 25, D. C., ATTN: ORDTX-AR	4
Chief Signal Officer, D/A, P&O Division, Washington 25, D. C., ATTN: SIGOP	5–7
The Surgeon General, D/A, Washington 25, D. C., ATTN: Chairman, Medical R&D Board	8
Chief Chemical Officer, D/A, Washington 25, D. C.	9–10
The Quartermaster General, CBR, Liaison Officer, Research and Development Div., D/A, Washington 25, D. C.	11–12
Chief of Engineers, D/A, Washington 25, D. C., ATTN: ENGNB	13–17
Chief of Transportation, Military Planning and Intelligence Div., Washington 25, D. C.	18
Chief, Army Field Forces, Ft. Monroe, Va.	19–22
President, Board #1, OCAFF, Ft. Bragg, N. C.	23
President, Board #3, OCAFF, Ft. Benning, Ga.	24
President, Board #4, OCAFF, Ft. Bliss, Tex.	25
Commanding General, First Army, Governor's Island, New York 4, N. Y.	26
Commanding General, Second Army, Ft. George G. Meade, Md.	27
Commanding General, Third Army, Ft. McPherson, Ga., ATTN: ACofS, G-3	28
Commanding General, Fourth Army, Ft. Sam Houston, Tex., ATTN: G-3 Section	29
Commanding General, Fifth Army, 1660 E. Hyde Park Blvd., Chicago 15, Ill.	30
Commanding General, Sixth Army, Presidio of San Francisco, Calif., ATTN: AMGCT-4	31
Commanding General, U. S. Army Caribbean, Ft. Amador, C. Z., ATTN: Cml. Off.	32
Commanding General, USARFANT & MDPR, Ft. Brooke, Puerto Rico	33
Commanding General, U. S. Forces Austria, APO 168, c/o PM, New York, N. Y., ATTN: ACofS, G-3	34
Commander-in-Chief, Far East Command, APO 500, c/o PM, San Francisco, Calif., ATTN: ACofS, J-3	35–36
Commanding General, U. S. Army Forces Far East (Main), APO 343, c/o PM, San Francisco, Calif., ATTN: ACofS, G-3	37
Commanding General, U. S. Army Alaska, APO 942, c/o PM, Seattle, Wash.	38
Commanding General, U. S. Army Europe, APO 403, c/o PM, New York, N. Y., ATTN: OPOT Div., Combat Dev. Br.	39–40
Commanding General, U. S. Army Pacific, APO 958, c/o PM, San Francisco, Calif., ATTN: Cml. Off.	41–42
Commandant, Command and General Staff College, Ft. Leavenworth, Kan., ATTN: ALLLS(AS)	43–44
Commandant, Army War College, Carlisle Barracks, Pa., ATTN: Library	45
Commandant, The Artillery School, Ft. Sill, Okla.	46
Commandant, The AA&GM Branch, The Artillery School, Ft. Bliss, Tex.	47
Commanding General, Medical Field Service School, Brooke Army Medical Center, Ft. Sam Houston, Tex.	48
Director, Special Weapons Development Office, Ft. Bliss, Tex., ATTN: Lt. Arthur Jaskierny	49
Commandant, Army Medical Service Graduate School, Walter Reed Army Medical Center, Washington 25, D. C.	50

Superintendent, U. S. Military Academy, West Point, N. Y., ATTN: Prof. of Ordnance	51
Commandant, Chemical Corps School, Chemical Corps Training Command, Ft. McClellan, Ala.	52
Commanding General, Research and Engineering Command, Army Chemical Center, Md., ATTN: Deputy for RW and Non-Toxic Material	53–54
Commanding General, Aberdeen Proving Ground, Md. (inner envelope), ATTN: RD Control Officer (for Director, Ballistic Research Laboratories)	55–56
Commanding General, The Engineer Center, Ft. Belvoir, Va., ATTN: Asst. Commandant, Engineer School	57–59
Commanding Officer, Engineer Research and Development Laboratory, Ft. Belvoir, Va., ATTN: Chief, Technical Intelligence Branch	60
Commanding Officer, Picatinny Arsenal, Dover, N. J., ATTN: ORDBB-TK	61
Commanding Officer, Frankford Arsenal, Philadelphia 37, Pa., ATTN: Mr. C. C. Fawcett	62
Commanding Officer, Army Medical Research Laboratory, Ft. Knox, Ky.	63
Commanding Officer, Chemical Corps Chemical and Radiological Laboratory, Army Chemical Center, Md., ATTN: Tech. Library	64–65
Commanding Officer, Transportation R&D Station, Ft. Eustis, Va.	66
Commanding General, The Transportation Center and Ft. Eustis, Ft. Eustis, Va., ATTN: Military Science & Tactics Board	67
Director, Technical Documents Center, Evans Signal Laboratory, Belmar, N. J.	68
Director, Waterways Experiment Station, PO Box 631, Vicksburg, Miss., ATTN: Library	69
Director, Armed Forces Institute of Pathology, 7th and Independence Avenue, S. W., Washington 25, D. C.	70
Director, Operations Research Office, Johns Hopkins University, 7100 Connecticut Ave., Chevy Chase, Md., ATTN: Library	71

NAVY ACTIVITIES

Chief of Naval Operations, D/N, Washington 25, D. C., ATTN: OP-36	72–73
Chief of Naval Operations, D/N, Washington 25, D. C., ATTN: OP-374(OEG)	74
Chief of Naval Operations, D/N, Washington 25, D. C., ATTN: OP-322V	75
Chief, Bureau of Medicine and Surgery, D/N, Washington 25, D. C., ATTN: Special Weapons Defense Div.	76–77
Chief, Bureau of Ordnance, D/N, Washington 25, D. C.	78
Chief of Naval Personnel, D/N, Washington 25, D. C.	79
Chief, Bureau of Ships, D/N, Washington 25, D. C., ATTN: Code 348	80–81
Chief, Bureau of Yards and Docks, D/N, Washington 25, D. C., ATTN: D-440	82
Chief, Bureau of Supplies and Accounts, D/N, Washington 25, D. C.	83
Chief, Bureau of Aeronautics, D/N, Washington 25, D. C.	84–85
Chief of Naval Research, Department of the Navy, Washington 25, D. C., ATTN: LT(jg) F. McKee, USN	86
Commander-in-Chief, U. S. Pacific Fleet, Fleet Post Office, San Francisco, Calif.	87
Commander-in-Chief, U. S. Atlantic Fleet, U. S. Naval Base, Norfolk 11, Va.	88
Commandant, U. S. Marine Corps, Washington 25, D. C., ATTN: Code A03H	89–92
President, U. S. Naval War College, Newport, R. I.	93
Superintendent, U. S. Naval Postgraduate School, Monterey, Calif.	94
Commanding Officer, U. S. Naval Schools Command, U. S. Naval Station, Treasure Island, San Francisco, Calif.	95
Commanding Officer, U. S. Fleet Training Center, Naval Base, Norfolk 11, Va., ATTN: Special Weapons School	96
Commanding Officer, U. S. Fleet Training Center, Naval Station, San Diego 36, Calif., ATTN: (SPWP School)	97–98
Commanding Officer, Air Development Squadron 5, VX-5, U. S. Naval Air Station, Moffett Field, Calif.	99
Commanding Officer, U. S. Naval Damage Control Training Center, Naval Base, Philadelphia 12, Pa., ATTN: ABC Defense Course	100
Commanding Officer, U. S. Naval Unit, Chemical Corps School, Army Chemical Training Center, Ft. McClellan, Ala.	101
Joint Landing Force Board, Marine Barracks, Camp Lejeune, N. C.	102
Commander, U. S. Naval Ordnance Laboratory, Silver Spring 19, Md., ATTN: EH	103
Commander, U. S. Naval Ordnance Laboratory, Silver Spring 19, Md., ATTN: R	104
Commander, U. S. Naval Ordnance Test Station, Inyokern, China Lake, Calif.	105

OTHER DEPARTMENT OF DEFENSE ACTIVITIES

ATOMIC ENERGY COMMISSION ACTIVITIES

AEC, Oak Ridge, Tenn., 9/2/51

UNCLASSIFIED